

This is to certify that the

dissertation entitled

Supramolecular Photoactive Assemblies

Based on Cyclodextrins

presented by

Zoe Pikramenou

has been accepted towards fulfillment of the requirements for

Ph.D. degree in Chemistry

Date 9124 1993

MSU is an Affirmative Action/Equal Opportunity Institution

O-12771



LIBRARY Michigan State University

PLACE IN RETURN BOX to remove this checkout from your record.
TO AVOID FINES return on or before date due.

DATE DUE	DATE DUE	DATE DUE
JUL 9 1 2005		
		pportunity Institution

MSU is An Affirmative Action/Equal Opportunity Institution cyclrolatedus.pm3-p.1

SUPRAMOLECULAR PHOTOACTIVE ASSEMBLIES BASED ON CYCLODEXTRINS

By

Zoe Pikramenou

A DISSERTATION

Submitted to

Michigan State University

in partial fulfillment of the requirements

for the degree of

DOCTOR OF PHILOSOPHY

Department of Chemistry

1993

ABSTRACT

SUPRAMOLECULAR PHOTOACTIVE ASSEMBLIES BASED ON CYCLODEXTRINS

By

Zoe Pikramenou

The synthesis of new supramolecular architectures bearing multiple recognition sites for substrate binding represents a central challenge to the study of photoinduced energy and electron transfer processes. Of the diverse molecular templates available for supramolecular design, cyclodextrins (CDs) not only provide a well-defined microenvironment for molecular recognition but are also well suited for functionalization with organic ligands. When the CD is modified with a secondary receptor site featuring a photoactive center, a supramolecular assembly is formed.

In our efforts to design structures in which luminescence is triggered by molecular recognition, we have synthesized assemblies featuring a cyclodextrin modified with a Ln^{3+} Caza crown ether (Ln = Eu, Tb) appended to the CD in a swing or a cradle conformation (β -CD \cup 1aza \supset Ln³⁺ and β -CD \cup 2aza \supset Ln³⁺, respectively). The modified

cyclodextrins are primarily characterized structurally by NMR techniques. The inclusion of a light-harvesting guest (LHG) in the cyclodextrin is heralded by light emission from the Ln³+ center. The enhancement of the lanthanide ion emission is attributed to an absorption-energy transferemission process from the aromatic donors in the cavity of cyclodextrin to the Ln³+ ion residing in the appended aza macrocycle. These architectures exemplify the antenna effect with the LHG playing the role of the antenna and energy transfer donor. The efficiency of the migration process from the LHG to the Ln³+ ion is intimately related to the structure of the supramolecular assembly as well as to the nature of the LHG. Association constants of the different guests, measured by the Benesi – Hildebrand method, reveal that the hydrophobic recognition of the guest by the CD is cooperative with its interaction to the metal ion. It is shown that specificity in binding coupled with shorter distances for energy transfer results in much brighter luminescence from the cyclodextrin supramolecule.

The development of cyclodextrins modified with appended crown ethers comprises a novel class of supramolecular systems. Practically, such spatially organized assemblies provide the framework for the development of luminescence-based sensors and materials.

to two very special people in my life,
my parents,
Irene and Stamatis

ACKNOWLEDGMENTS

My first days in MSU, the first year graduate students were advised how to choose a research director according to their scientific interests. I interviewed Professor Nocera and I was lucky to SEE THE LIGHT! I wish to express my gratitude to him that nourished my most important scientific steps. Dr. Nocera's guidance and enthusiasm supported my studies and educated me "how to do science".

Especially, I would like to thank Prof. Hollingsworth for introducing me to carbohydrate chromatography and molecular modeling and for kindly providing his chromatography set-up for my initial experiments. I always enjoyed insightful discussions with Prof. Jackson and his helpful suggestions for this thesis are gratefully acknowledged. I would also like to express my appreciation to Prof. Karabatsos for his concern and advice in key decisions throughout my studies. I also had the chance to work in a project with Prof. Kanatzidis that taught me a lot for an interesting field.

It was a joyful experience being in the Nocera group. Thanks to Janice, J. P., Mark, Adrian, Ann, Carolyn, Jim, Sara, Doug, Eric and the P-Chem. crew Jeff, Wanda, Yeh and Dan for providing a great environment for work! Older members are not to be forgotten, Jeonga, Colleen and Claudia provided their helpful insights my early years. I will not forget our stimulating scientific problem solving during coffee breaks or our

great group celebrations. Especially, I would like to thank Janice for always being a great supporting friend, Mark and Beatrice, Jeonga, J. P., Jeff, Carolyn, Ann and Ying for sharing many of my joys and problems.

The NMR group has been of great help and their patience for my overnight experiments is greatly appreciated. Special thanks to Kermit for working with me to find this one experiment for resolving my peaks. The Department of Chemistry that gave me the opportunity to study in USA and the Academy of Athens for a supporting fellowship are gratefully acknowledged. I would also like to thank to my undergraduate mentors in University of Athens, Profs. Koupparis, Kalokerinos and Mertis that encouraged and supported my interest for graduate studies.

I wish to thank the Tassiopoulos, Noceras, and Strangas families for giving me the feeling of home away from home and many friends, especially, Gennie, Sofia, Stacey, Trifon, Dea, George, Nikos and "the other" Zoe, that stood by me with understanding and concern. I am grateful to Mrs. Eleftheria for her love, encouragement and support. She was my guardian angel all these years and she shared every moment of my studies with me.

From the other side of the Atlantic, my friend Theodore and my grand-parents, Sotiris and Calliope, offered their supporting love and understanding through my graduate studies.

My deepest gratitude is for my parents, Irene and Stamatis, for being with me every step of the way with their infinite love, thoughts and faith in me. They taught me to be independent but they always have been by my side and supported my goals giving me strength. Thank you.

TABLE OF CONTENTS

		1	Page
LIS'	ТО	F TABLES	xi
LIS	ΤO	F FIGURES	xii
I.	IN	TRODUCTION	1
	A.	Perspective of Supramolecular Chemistry	1
		Compounds	7
		Cryptands, and Spherands 3. Basket–like Molecules	13 13
	B.	Supramolecular Photochemistry	27
		SupramoleculesEnergy Transduction in Nature and Biomimetic SystemsDevelopment of Photochemical Molecular Devices Based	30 33
		on Photoinduced Energy and Electron Motion	37 41
	C.	Cyclodextrin Supramolecules Designed to Perform AETE 1. Cyclodextrins as Receptors	49 52 58
ΤΤ	ΕX	PERIMENTAL	61

A. S	ynthesis
1.	General Procedures
2.	β-CDO-Ts
3.	β-CD∪ ¹ aza
4.	β-CD∪ ¹ triamine
5.	β-CD∪¹tetraamine
6.	β-CDO-SiPh ₂ (tert-Bu)
7.	Methylation of β-CDO-SiPh ₂ (tert-Bu)
8.	Eu^{3+} \subset aza $(NO_3)_3$
9.	β -CD \cup ¹ aza \supset Eu ³⁺ (NO ₃) ₃
10.	Tb ³⁺ \subset azaCl ₃ and β-CD∪ ¹ aza⊃Tb ³⁺ Cl ₃
11.	Eu^{3+} (triamine) ₂ (NO ₃) ₃
12.	$Eu^{3+}(tetraamine)_2(NO_3)_3$
13.	Reaction of Eu(NO ₃) ₃ with β -CD \cup ¹ triamine and β -CD \cup ¹
	tetraamine
14.	Biphenyl-4,4'-disulfonyl-A,D-capped β-CD
15.	Diiodo–β-CD
16.	β-CD∪²aza
17.	β -CD∪ ² aza⊃Eu ³⁺ (NO ₃) ₃
18.	β -CD \cup ¹ aza \supset Y ³⁺ (NO ₃) ₃ and β -CD \cup ¹ aza \supset Y ³⁺ (NO ₃) ₃
B. Ir	strumentation and Methods
1.	Chromatographic Procedures
	a. Flash Chromatography
	b. Molecular Exclusion Chromatography
	c. Thin Layer Chromatography (TLC)
2.	Nuclear Magnetic Resonance
3.	Infrared Spectroscopy
4.	Mass Spectrometry
5.	Molecular Modeling Studies
6.	Electronic Absorption Spectroscopy
7.	
- •	a. Energy Transfer Studies and Characterization
	b. Association Constant Studies
R	Time-Resolved Luminescence Spectroscopy

			Page
III.	SW	VING CYCLODEXTRINS	83
	A.	Synthesis and Characterization	83
		1. Background	83
		2. Results and Discussion	86
		a. β-CD∪ ¹ aza	86
		b. β -CD \cup^1 triamine and β -CD \cup^1 tetraamine	95
		c. Protection of OH Group by ClSiPh ₂ (tert-Bu) and	
		Methylation of β -CDO–SiPh ₂ (tert-Bu)	96
	B.	Luminescence Spectroscopy	106
		1. Background	106
		2. Results and Discussion	109
		a. β-CD∪¹aza⊃Eu³+	109
		b. β-CD∪¹aza⊃Tb³+	115
		c. Amine Complexes with Eu ³⁺	115
	C.	Inclusion Complexes of β -CD \cup ¹ aza \supset Eu ³⁺	120
		1. Background	120
		2. Results and Discussion	121
		a. Association of Guests	121
		b. AETE Studies for Various LHGs	123
		i. Benzene	123
		ii. Benzoic, Picolinic Acids	127
		iii. Other Guests	135
IV.	CR	ADLE CYCLODEXTRINS	145
	A.	Synthesis and Characterization	145
		1. Background	145
		2. Results and Discussion	147
	B.	Luminescence Spectroscopy	155
		1. Results and Discussion	155
	C.	Inclusion Complexes of β-CD∪²aza⊃Eu³+	156
		1. Results and Discussion	156
		a. Association of Guests	156
		b. AETE Studies for Various LHGs	158

		Page
V.	CONCLUDING REMARKS	167
	APPENDIX	177
	LIST OF REFERENCES	207

LIST OF TABLES

		Page
1.	Association constants (M $^{-1}$) of various light–harvesting guests with β -CD and β -CD \cup 1aza \supset Y $^{3+}hosts$	122
2.	Association constants (M^{-1}) of light–harvesting guests with β - $CD \cup {}^{2}aza \supset Y^{3+}$	157

LIST OF FIGURES

		Page
1.	Schematic representation of the formation of a supramolecule by the molecular recognition of individual components	4
2.	The development of chemistry from molecular to supramolecular	6
3.	(a) Crown ethers with different ring sizes. (b) Coronands containing heteroatoms and functional groups	9
4.	(a) Cryptands with different cavities and bridges. (b) Selective examples of spherands	11
5.	(a) Caged Fe(III) and Ru(II) complexes with high affinity ligands. (b) Schematic representation of different types of cage-like hosts	15
6.	Cage-type structures derived from (a) cyclophanes and (b) crown porphyrins	17
7.	(a) Macrotricyclic structures with different possible modifications and an example of linear recognition of the cationic pentyldiamine. (b) Channel and bouquet type	10
	molecules composed from macrocycles	19

		Page
8.	Spealands, bearing a rigid aromatic region, enhance the binding of the hydrophobic units of molecules as methyl amine	22
9.	Calixarenes can be synthesized with different sizes of cavities as a resemblance to crown ethers	24
10.	Cavitands, at the top, and a carcerand, lower, which can include different guests as shown	26
11.	Photophysical processes prompted by molecular recognition	29
12.	Schematic description of electron motion in energy and electron transfer	32
13.	A carotenoid – porphyrin – porphyrin – quinone tetrad	36
14.	Block diagrams that describe the function of molecular devices based on energy transfer	40
15.	The tetrametallic Os[(2,3-dpp)Ru(bpy) ₂] ₃ ⁸⁺ complex and a schematic energy level diagram that illustrates the antenna effect	43
16.	Structures of lanthanide complexes with cryptands and a schematic energy level diagram that demonstrates the AETE process in the bipyridine substituted Ln ³⁺ cryptate	45
17.	Simplified energy level diagram describing the relative energies between Tb ³⁺ or Eu ³⁺ and the LHC	48
18.	Representation of the exogenous LHC approach and a selective example of acid binding in $Eu^{3+} \subset 2.2.1$	51
19.	Block description of a new design for AETE, consisting of a receptor with two binding sites, for lanthanides and hydrophobic substrates	54

		Page
20.	Cyclodextrin cups of different size and the structure of β -CD	56
21.	Block diagram of the preparative scale liquid chromatography apparatus	73
22.	Emission spectra of 1,8 ANS with addition of pyridine as competitor for cyclodextrin binding	81
23.	The 500 MHz 1 H NMR spectrum of β -CD \cup 1 aza in d 6 -DMSO. The inset spectrum displays an expanded region showing the triplet peak at 2.51 ppm flanking the DMSO solvent resonance; the numbering of the carbons of the glucose subunit is also depicted in an inset. See text for assignments	90
24.	The 300 MHz two-dimensional $^1H^{-1}H$ COSY contour plot of β - CD \cup 1 aza	93
25.	The 300 MHz 1 H NMR spectrum of β -CD \cup 1triamine in D ₂ O/d ⁶ -acetone. Please note discontinuity in abscissa	98
26.	The 300 MHz 1H NMR spectrum of $\beta\text{-}CD\cup^1 tetraamine}$ in $D_2O/d^6\text{-}acetone$	100
27.	The 300 MHz 1 H NMR spectrum of β -CDO–SiPh ₂ (tert-Bu)in d ⁶ -DMSO. Residual DMF peaks appear at 2.7, 2.9 and 7.9 ppm	103
28.	The 300 MHz 1 H NMR spectrum of β - C D-(OMe) $_{12}$ (OSiPh $_2$ (tert-Bu))in d 6 -DMSO. Residual DMF peaks appear at 2.7, 2.9 and 7.9 ppm	105
29.	Partial energy level diagrams of Eu(III) and Tb(III) emphasizing the splitting of 4f ⁶ and 4f ⁸ configurations	108
30.	Excitation spectra of (a) Eu ³⁺ \subset aza and (b) β -CD \cup ¹ aza \supset Eu ³⁺ in CH ₃ CN monitored at λ_{em} = 616 nm	111
31.	Emission spectrum of Eu(NO ₃) ₃ in CH ₃ CN (λ_{exc} = 394 nm)	114

		Page
32.	Emission spectrum of TbCl ₃ in CH ₃ CN (λ_{exc} = 313 nm)	117
33.	Excitation spectrum of $Eu^{3+}(triamine)_2(NO_3)_3$ in CH ₃ CN monitored at λ_{em} = 616 nm, representative for the Eu(III) amine complexes	119
34.	Dependence of the emission intensity from D_2O solutions of $Eu^{3+} \subset aza$ and $\beta - CD \cup ^1 aza \supset Eu^{3+}$ upon addition of benzene ($\lambda_{exc} = 254$ nm). Concentrations of the lumophore are 2.5×10^{-4} M	125
35.	Relative emission intensity from D_2O solutions of β - $CD\cup^1$ aza $\supset Eu^{3+}$ upon addition of light harvesting guests (λ_{exc} = 254 nm for PcA, Bz and 280 nm for BzA). Please note abscissa discontinuity. Concentrations of the lumophore are 5.8×10^{-4} M for BzA and PcA and 2.5×10^{-4} M for Bz	129
36.	Dependence of the emission intensity from D_2O solutions of β - $CD\cup^1$ aza $\supset Tb^{3+}$ upon addition of benzoic acid ($\lambda_{exc}=280$ nm). Concentration of the lumophore is 5.4×10^{-4} M	132
37.	Excitation spectrum of β -CD \cup 1aza \supset Tb ³⁺ including benzoic acid monitored at λ_{em} = 546 nm	134
38.	Relative emission intensity from D_2O solutions of β - $CD\cup^1$ aza $\supset Eu^{3+}$ upon addition of pyridine ($\lambda_{exc}=313$ nm). Concentration of the lumophore is 3.0×10^{-4} M.	137
39.	Dependence of the emission intensity from D_2O solutions of β - $CD\cup^1$ aza $\supset Eu^{3+}$ upon addition of naphthoic acids as LHGs (λ_{exc} = 280 nm). Concentrations of the lumophore are 4.95×10^{-4} M	139
4 0.	Dependence of the emission intensity from D_2O solutions of $Eu(NO_3)_3$ upon addition of naphthoic acids as LHCs (λ_{exc} =	
	280 nm). Concentrations of the lumophore are 4.5×10^{-4} M	141

		Page
41.	Relative emission intensity from D_2O (\triangle) and 10% CH ₃ CN/ D_2O (\triangle) solutions of β -CD \cup ¹ aza \supset Eu ³⁺ upon addition of benzoic acid (λ_{exc} = 280 nm). Concentrations of the lumophore are 6.4×10^{-4} M	143
42.	The 500 MHz 1 H TOCSY spectrum of β -CD \cup 2 aza in D $_2$ O at 30°C. The mixing time was 120 ms. The HDO signal is suppressed by presaturation	151
43.	The 500 MHz $^1\text{H}-^{13}\text{C}$ HMQC spectrum of $\beta\text{-CD}\cup^2$ aza in $D_2\text{O}$	154
44.	Relative emission intensity from D_2O solutions of β - $CD\cup^2$ aza $\supset Eu^{3+}$ upon addition of light harvesting guests (λ_{exc} = 280 nm for BzA, PcA and 254 nm for Bz). Concentrations of the lumophore are 2.4×10^{-4} M for BzA and 2.6×10^{-4} M for PcA and Bz	160
4 5.	Comparison of the dependence of the emission intensity from D ₂ O solutions of β -C D \cup ² aza \supset Eu ³⁺ (cradle) and β -CD \cup ¹ aza \supset Eu ³⁺ (swing) upon addition of pyridine (λ_{exc} = 313 nm). Concentrations of the lumophores are 3.1×10^{-4} M	163
46.	Fluorescence of pyridine in D_2O solutions of β - $CD\cup^2$ aza $\supset Eu^{3+}$ (cradle) and β - $CD\cup^1$ aza $\supset Eu^{3+}$ (swing) ($\lambda_{exc} = 313$ nm)	166
47.	Examples of receptors with structural characteristics similar to crowned cyclodextrins	169
48	Conformations of the appended aza $\supset Eu^{3+}$ moiety in the swing CD (β -CD \cup 1aza $\supset Eu^{3+}$) in the presence of benzene and benzoic acid guests	172
4 9.	Comparison of pyridine residing in the swing and cradle CD	175
A1.	The 300 MHz 1 H NMR spectrum of β -CD in d^6 -DMSO	178
Δ2	The 75 MHz ¹³ C NMR spectrum of B-CD in d ⁶ -DMSO	180

		Page
A3.	The 500 MHz ^1H NMR spectrum of $\beta\text{-CDO-Ts}~$ in $d^6\text{-DMSO}~$.	182
A4.	The 75 MHz 13 C NMR spectrum of β -CDO–Ts in d 6 -DMSO	184
A5.	The 300 MHz ¹ H NMR spectrum of aza in d ⁶ -DMSO	186
A6.	The 75 MHz ¹³ C NMR spectrum of aza in d ⁶ -DMSO	188
A7.	The positive ion FABMS spectrum of β -CD \cup 1aza with glycerol as matrix. The molecular ion peak is shown at 1379.8 amu and the fragment corresponding to the matrix adduct with a loss of the azaCH ₂ — group is at 1105.7 amu. The peak at 1381.7 amu corresponds to an adduct of the matrix upon the fragmentation therefore it shows as a doublet comparing with the molecular ion peak. A higher fragment corresponds to a usual presence of sodium which tends to form complexes with carbohydrates.	190
A8.	The 500 MHz 1 H TOCSY spectrum of β -CD \cup 1 aza in D $_2$ O at 30°C. The mixing time was 120 ms. The HDO signal is suppressed by presaturation	192
A9.	The 75 MHz 13 C NMR spectrum of β -CD \cup 1 aza in d 6 -DMSO	194
A10.	The 300 MHz 1 H NMR spectrum of Eu $^{3+}$ Caza in d 3 -nitromethane	196
A11.	The 300 MHz ¹ H NMR spectrum of triamine in D ₂ O	198
A12.	The 75 MHz 13 C NMR spectrum of β -CDO–SiPh2(tert-Bu) in d 6 -DMSO	200
A13.	The 300 MHz 1 H NMR spectrum of biphenyl-4,4′-disulfonyl-A,D-capped β -CD in d^6 -DMSO	202
A14.	The 300 MHz 1 H NMR spectrum of diiodo- β -CD in d 6 -DMSO	204
A15.	The positive ion FABMS spectrum of protonated β -CD \cup ² aza with glycerol as matrix. The (M + 5H ⁺) is shown at 1367.2 amu	

	Page
and the fragment corresponding to the matrix adduct is shown	
at 1459.1 amu. The loss of the azaCH ₂ — group is at 1071 amu	
not shown at this scale. Higher fragments correspond to	
presence of sodium and water molecules	206

CHAPTER I

INTRODUCTION

A. Perspective of Supramolecular Chemistry

Most biological and biochemical processes involve intermolecular interactions between multi-component assemblies to produce characteristic function. The energetic and stereochemical features of these interactions are essential to this fundamental biochemical function. The desire to understand these delicate structure/energy/function relationships has inspired the relatively new field called supramolecular chemistry. Jean-Marie Lehn introduced the new area as "the chemistry beyond the molecule" [1]. Supramolecules have distinct characteristics that differentiate them from any "large molecule". They are formed from two or more molecular species that are juxtaposed entities of higher complexity organized by intermolecular forces (electrostatic forces, hydrogen bonding, van der Waals forces, etc.). The molecular components are subunits that exist independently, each having their own properties

which may be preserved or altered within the supramolecule. The complementarity of the individual components is a requirement for the preferential binding accompanying molecular recognition (Figure 1). The origin of molecular recognition is found in the classic "lock and key" concept of enzymes where the specificity between receptor and substrate is critical to function.

The above requirements for a supramolecule may be satisfied by adequately building the receptor with recognition sites not only for substrate binding but also for substrate induced reactivity yielding a supramolecular reagent or catalyst (Figure 2). These design features of recognition and reactivity within a supramolecular architecture are fundamental functions at the foundation of multiple–center catalysis, and thermally and photochemically induced multi–electron processes. In addition, these functions, coupled with the potential for organization by self-assembly, are the determinants for the development of supramolecular devices (Figure 2). An especially important emerging function of supramolecules is to exploit self-assembled systems for information storage and programming. Instead of storing all the information via a preorganized molecular receptor, it is stored in the different molecular components that may spontaneously aggregate into a supramolecular architecture by self-assembling.

Although many supramolecular studies are motivated by biological or biomimetic structure/function relationships, the emphasis in supramolecule design is definitely on abiotic, non-natural species that perform desired chemical, biological or physical functions. At this point

Figure 1. Schematic representation of the formation of a supramolecule by the molecular recognition of individual components.

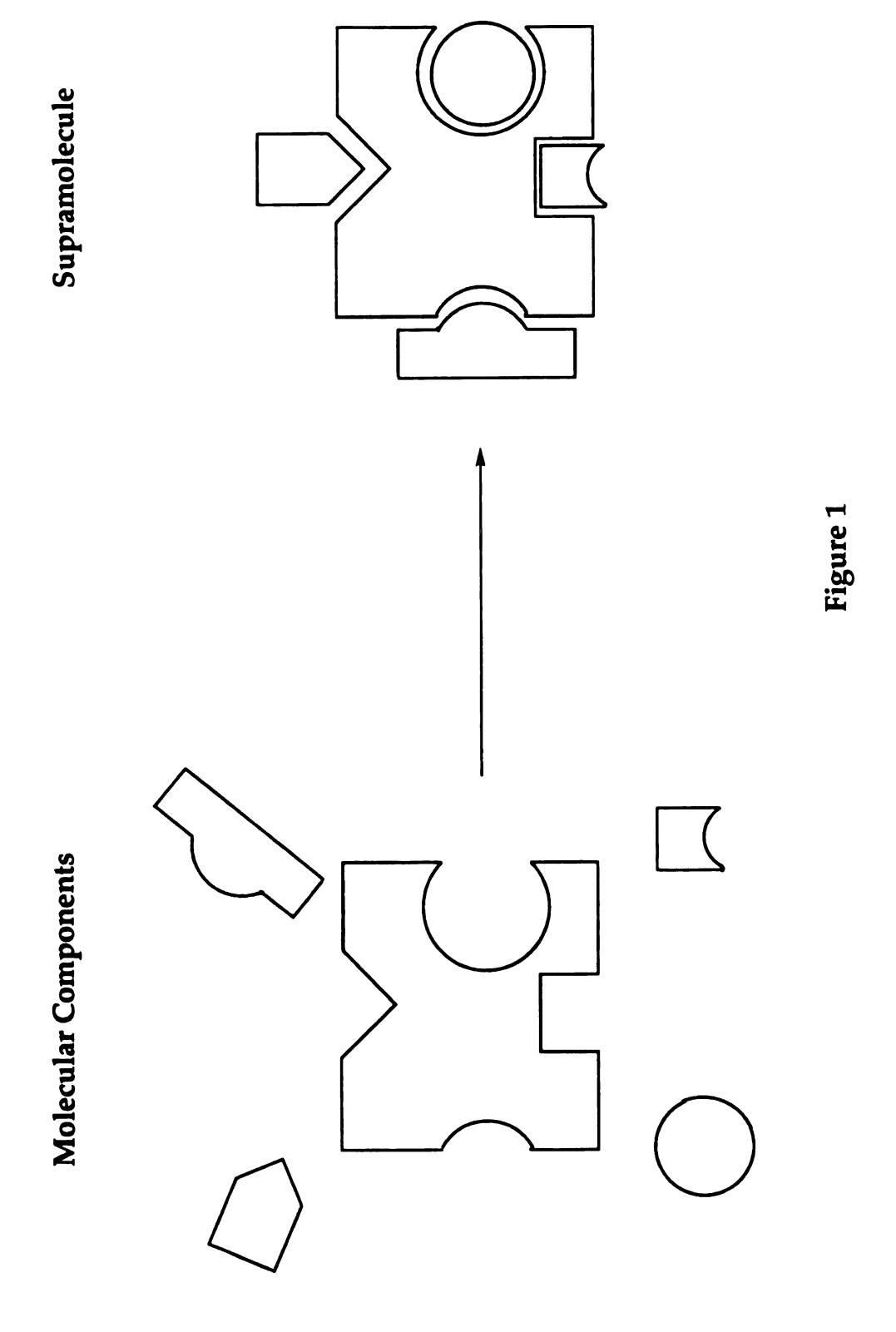


Figure 2. The development of chemistry from molecular to supramolecular.

MOLECULAR



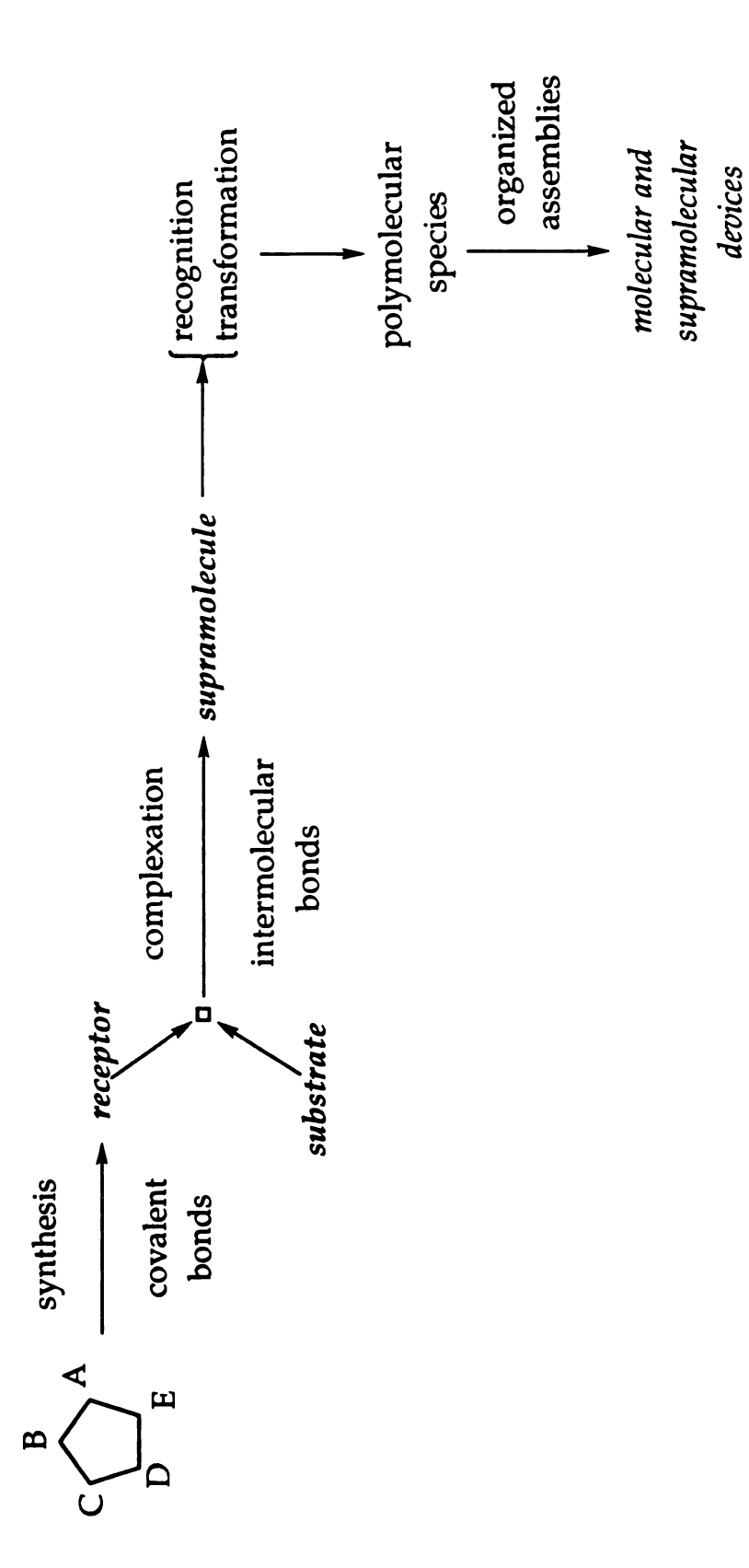


Figure 2

some of the different types of supramolecular systems will be highlighted [3]. An overview of the fundamental structural classes will reveal how the structural features may engender remarkable properties and lead to the design of supramolecular structures with desired function.

1. Fundamental Structures for Spherical Recognition: Crown Ethers, Cryptands, Spherands and Cage-Type Compounds

One of the early breakthroughs in supramolecular chemistry came with the development of crown ethers by Pedersen [4], cryptands by Lehn [5], and spherands by Cram [6]. These receptors have provided the skeletons for supramolecule construction and they have inspired a vast array of shapes and functions for supramolecular architectures. Crown ethers are macrocycles consisting of only ethyleneoxy units, which according to their number, yield different-sized cavities (Figure 3a). The coronands are formed when heteroatom containing units are included in the macrocycle (Figure 3b) [7]. The cryptands and spherands are spherical macropolycyclic structures with the latter being completely preorganized by rigid aromatic rings. Selective examples of these molecules are shown in Figure 4.

The polar cavities of these macrocycles strongly and selectively encapsulate cationic or anionic substrates. Thermodynamic and kinetic studies of substrate binding [8] have revealed clearly the effect of macrocycle organization. It has been found that crown ethers bind cations more strongly by a factor of thousands than do the relevant non-cyclic analogs (podands). Cryptands, spherands and cryptospherands

Figure 3. (a) Crown ethers with different ring sizes. (b) Coronands containing heteroatoms and functional groups.



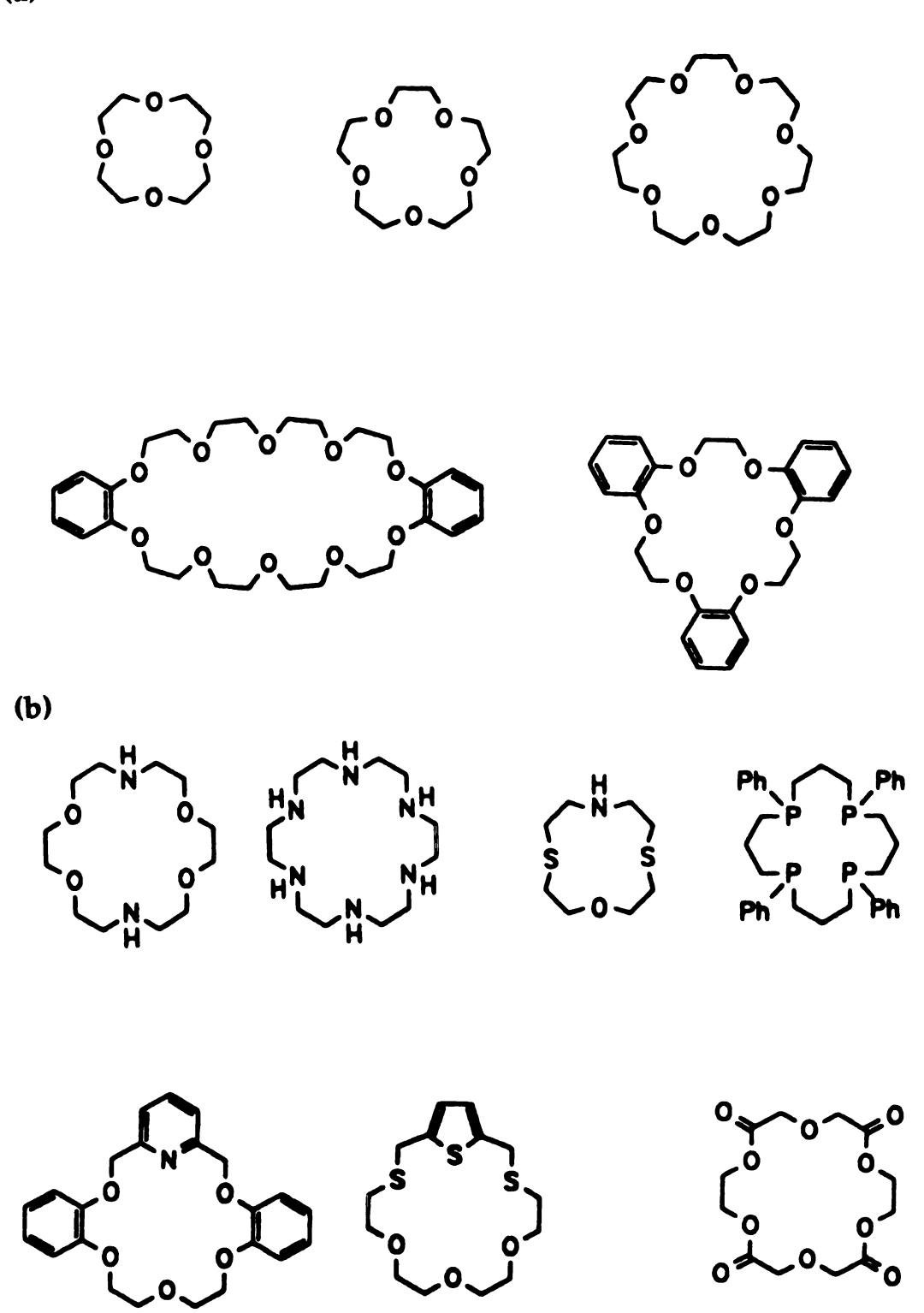
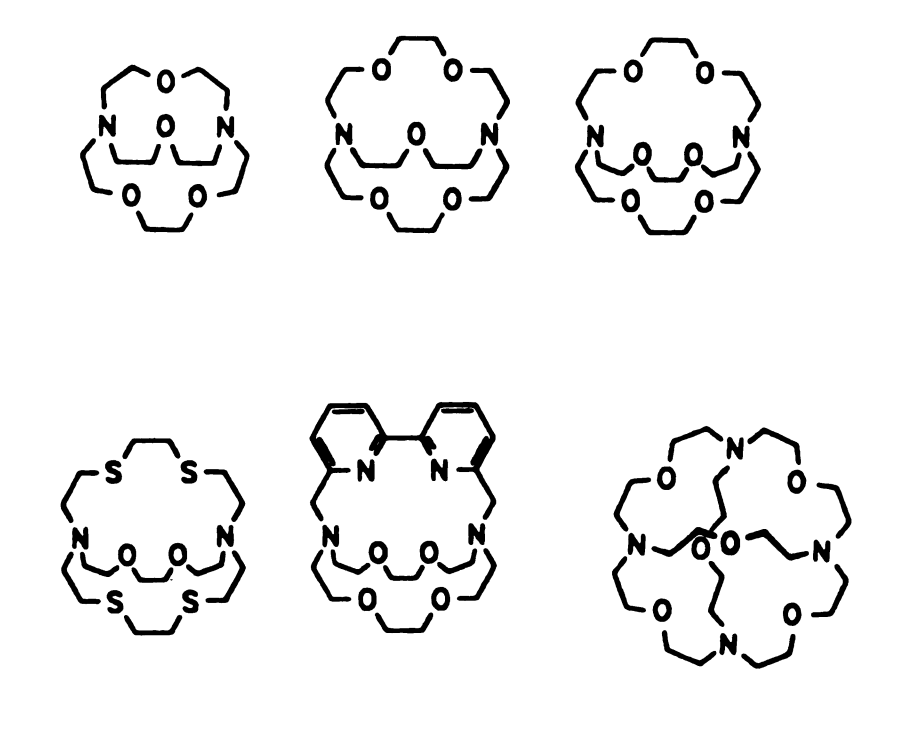


Figure 3

Figure 4. (a) Cryptands with different cavities and bridges. (b) Selective examples of spherands.





(b)

 $R = OCH_3$; OH

 $R = OCH_3$

Figure 4

consecutively form even more stable complexes with alkali, alkaline—earth and lanthanide ions, exhibiting at least four orders of magnitude higher binding constants than the relevant crowns. This enhancement, which demonstrates the importance of structural preorganization, is known as the macrocyclic or cryptate effect.

The binding properties of these macrocycles have led to a greater understanding of metal-ion binding in natural and unnatural materials. In the case of the former, the structure/function relationship of natural antibiotics, capable of binding alkali and alkaline earths, such as valinomycin [9] has evolved from cryptand studies. Biomimetic model crown ethers have been designed to incorporate the function of antibiotics for applications in cation transport through membranes and as models for enzymatic catalysis. Further practical applications for crown ether, cryptand, and spherand type molecules, are solubilization of salts, cation deactivation during chemical reactions or phase transfer catalysis by anion activation, and pH- or redox-switching [10]. Another outcome of the crown ether chemistry has been the development of crystalline materials with tailored optical, magnetic and electronic properties. In alkalides [11] and electrides [12], crown ethers and cryptands provide effective coordination to the alkali metal cation in order to stabilize its salt with the alkali metal anion or trapped electron, respectively.

Synthetic siderophore analogs [13] and cage-like compounds introduced mainly by Vögtle [3e] also have spherical shapes similar to crowns, cryptands and spherands. These systems are synthesized with a molecular-LEGO based strategy of donor groups and spacer. The result is

the design of cavities with high affinities for Fe(III), Ru(II) (Figure 5) or organic molecules to engender novel photophysical properties. Cyclophanes [14] and crown capped porphyrins [3] are other spherical receptors with cage—type structures. Figure 6 shows some of the many examples of these structures.

2. Super-Macropolycyclic Structures Based on Crowns, Cryptands, and Spherands

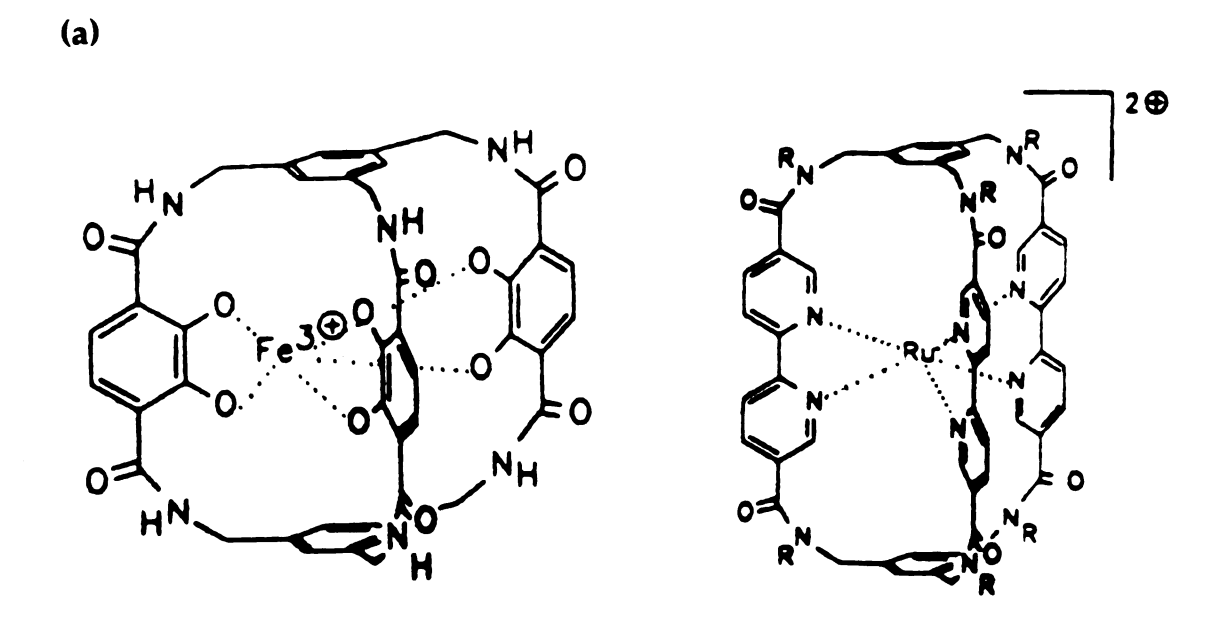
The introduction of multiple cavities, clefts, functional branches and bridges confers greater selectivity to the recognition process thereby allowing for the binding of more than one substrate or the multiple binding of a single polyfunctional substrate.

Cylindrical macrotricyclic ethers provide new topological features that enable the linear recognition of charged substrates as representatively shown in Figure 7a. Channel and bouquet shaped molecules (Figure 7b) have been useful in cation transport [15]. The topological control in design of other complicated supramolecules is demonstrated by different synthetic approaches invoking threading [16], Möbius strip catenation [17] and use of the template effects [18]. The charge transfer interaction between 4,4'-bipyridinium and crown ether building blocks have also led to the development of molecular knots, catenanes and rotaxanes [19].

3. Basket-like Molecules

Receptors shaped as baskets comprise the classes of spealands, calixarenes, cyclodextrins, and carcerands. Spealands [1] consist of a polar

Figure 5. (a) Caged Fe(III) and Ru(II) complexes with high affinity ligands. (b) Schematic representation of different types of cage-like hosts.



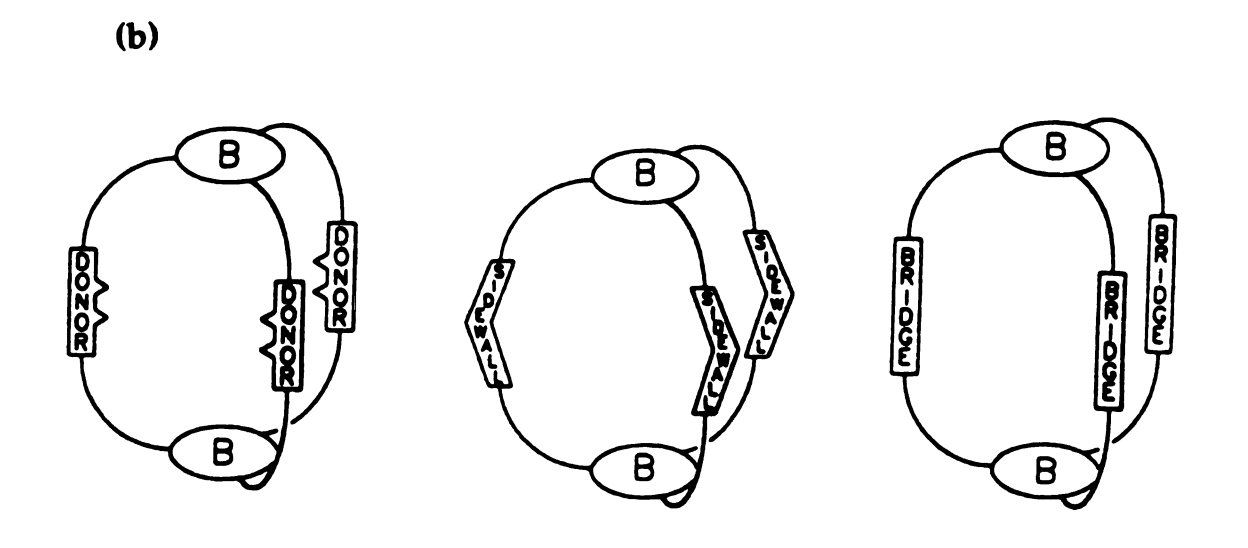
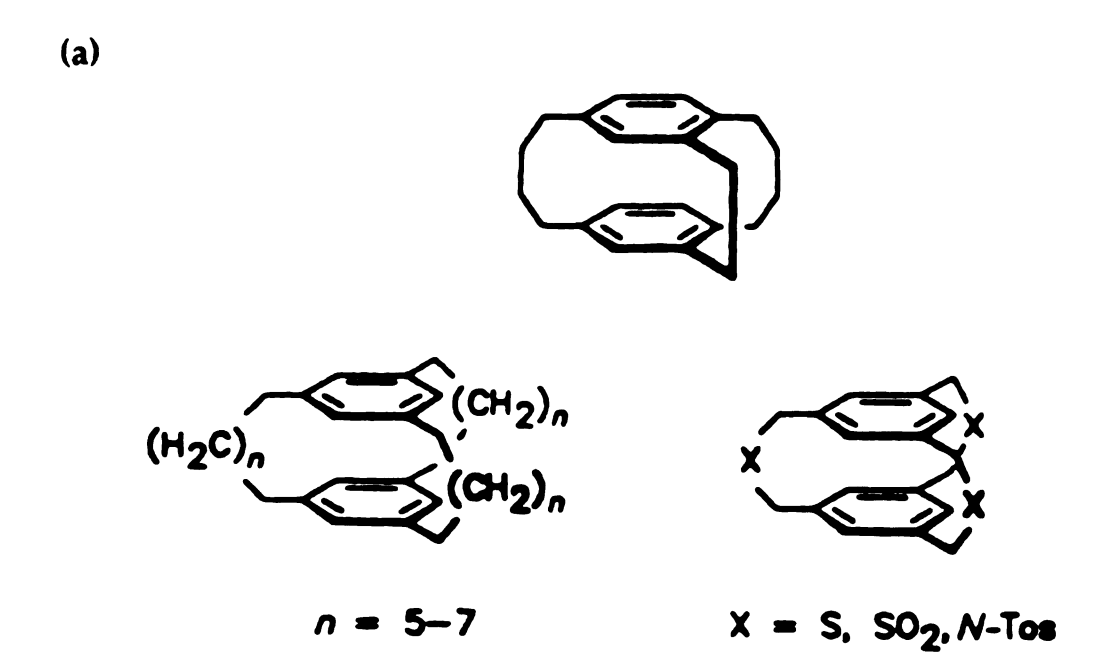


Figure 5

Figure 6. Cage-type structures derived from (a) cyclophanes and (b) crown porphyrins.



(b)

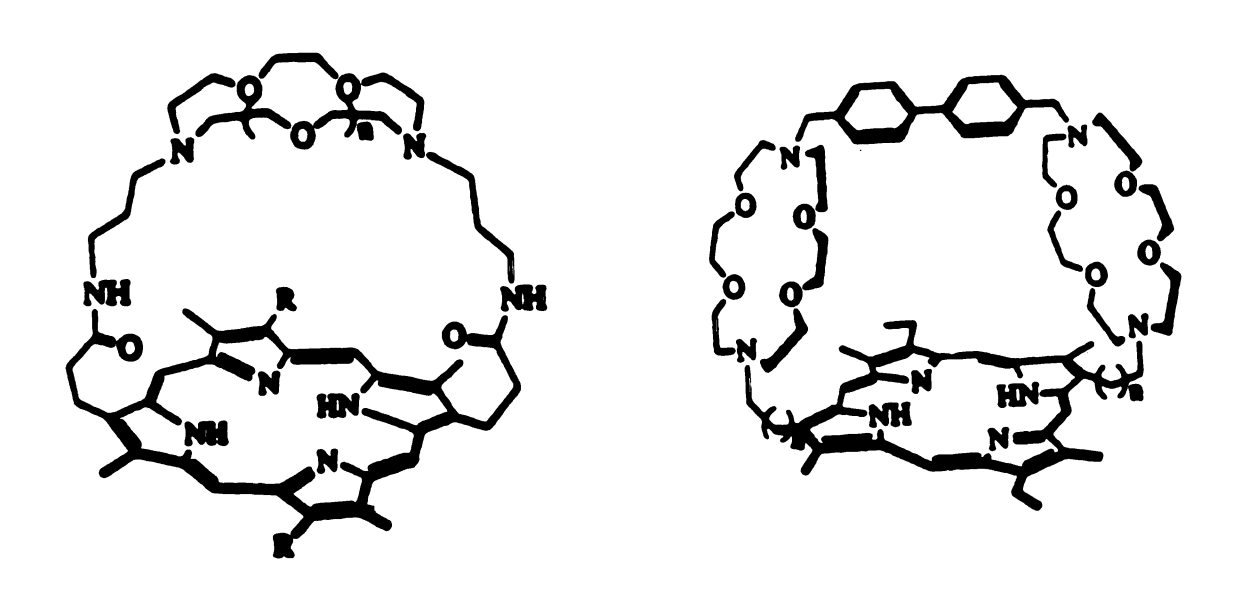


Figure 6

Figure 7. (a) Macrotricyclic structures with different possible modifications and an example of linear recognition of the cationic pentyldiamine. (b) Channel and bouquet type molecules composed from macrocycles.

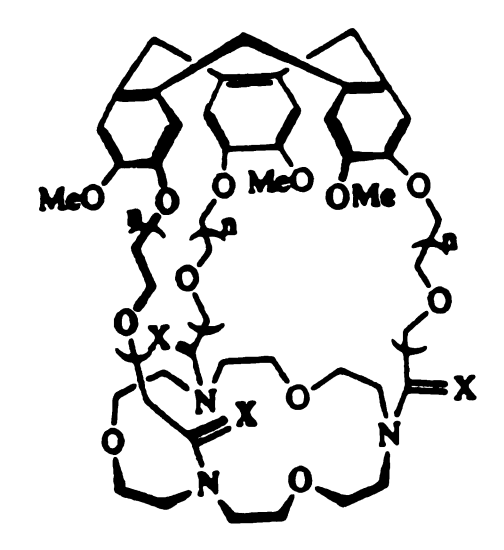
$$A = S, n = m = 1,$$

$G = C(0)CH_2OCH_2C(0)$

Figure 7

macrocycle attached with bridges to a rigid non-polar backbone (Figure 8). Characteristically, it is shown that the directional binding of a substrate with a hydrophobic moiety such as methyl ammonium cation, depicted in Figure 8, is enhanced compared to its binding to a flat macrocycle. Calixarenes [20] consist of phenolic rings connected via carbon atoms whose number varies, yielding different sized oligomers (Figure 9). Their name indicates the calix (= vase) shape, assuming the most stable, "cone" conformation. The various possible conformations of calixarenes affect the binding properties for both aromatics and ions. Most of the time, properly chosen derivatives interlock the structure in a rigid conformation. Calixarenes' substitution chemistry is rich resulting in numerous compounds functionalized in the lower or upper rim of the basket. Calixcrowns, a double cavity calixarene, and a recent double porphyrin double calixarene are representative examples [21, 22]. Cyclodextrins are naturally occurring carbohydrates with a rigid non-aromatic conical cavity whose chemistry and properties will be discussed extensively later in this chapter. The spherands have led to the development of compounds shaped like molecular vessels or cells, known as cavitands [6] and carcerands [23]. These biomimetic compounds feature enforced concave surfaces that are of large enough dimension to receive host molecules. Some representative compounds are illustrated in Figure 10.

Figure 8. Spealands, bearing a rigid aromatic region, enhance the binding of the hydrophobic units of molecules as methyl amine.



$$n = 0, X = H_2$$
 $n = 0, X = 0$
 $n = 1, X = H_2$ $n = 1, X = 0$

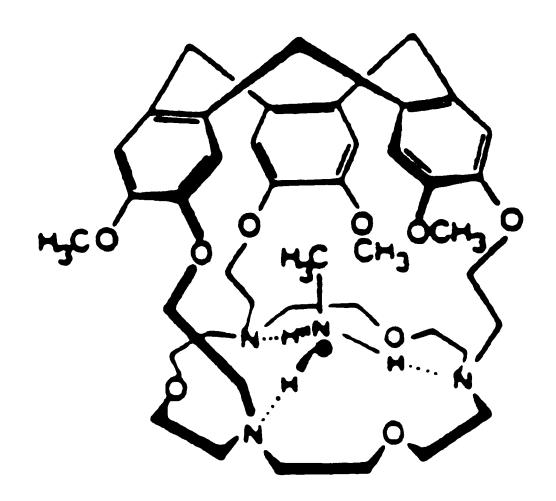
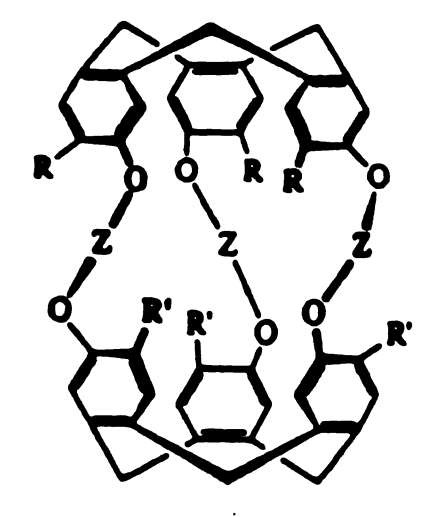


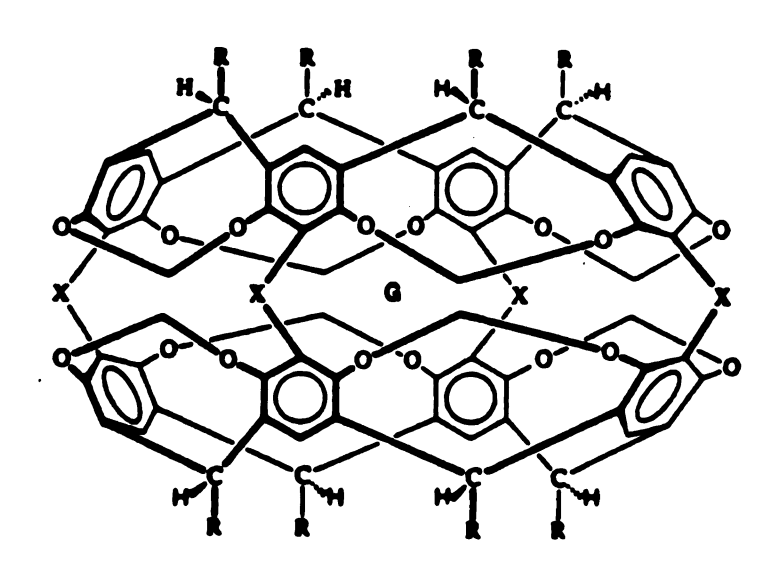
Figure 9. Calixarenes can be synthesized with different sizes of cavities as a resemblance to crown ethers.

Figure 9

Figure 10. Cavitands, at the top, and a carcerand, lower, which can include different guests as shown.



 $Z = (CH_2)_2$, $R = R' = OCH_3$



R - C.H,CH,CH,

X = 0CH20 G = (CH₂),50 G = (CH,),NC(O)CH,

 $G = (CH_3)_3NCHO$

Figure 10

B. Supramolecular Photochemistry

The function of the diverse supramolecule structures presented above has most extensively been exploited in an array of photochemical schemes. The field of supramolecular photochemistry [24] has been very attractive for many studies. On one hand, it gives the opportunity to study systems that perform photochemical processes that occur in living organisms, so that progress can be made towards the understanding of complex photobiological processes [25]. On the other hand, the design of artificial systems capable of performing useful light functions leads towards the development of photoactive devices [1]. The organizational architecture of a supramolecular system provides arrangements of photoactive subunits according to space, time or energy so that photochemical processes such as photoinduced energy migration, charge separation by electron transfer or selective photochemical reactions can be studied. In most cases, the event that triggers the processes is molecular recognition of a species to form the supramolecular structure, as shown pictorially in Figure 11. Energy and electron transfer processes will be described as well as examples of biomodel compounds. Focus will be given to the energy flow schemes in supramolecular species for the development of devices. Finally, the fundamentals of our design of supramolecular systems will be discussed.

1. Mechanisms of Photophysical Processes in Supramolecules

Energy and electron transfer processes are functions of the donor-

Figure 11. Photophysical processes prompted by molecular recognition.

acceptor distance, orientation, and environment. General unimolecular descriptions of the processes are,

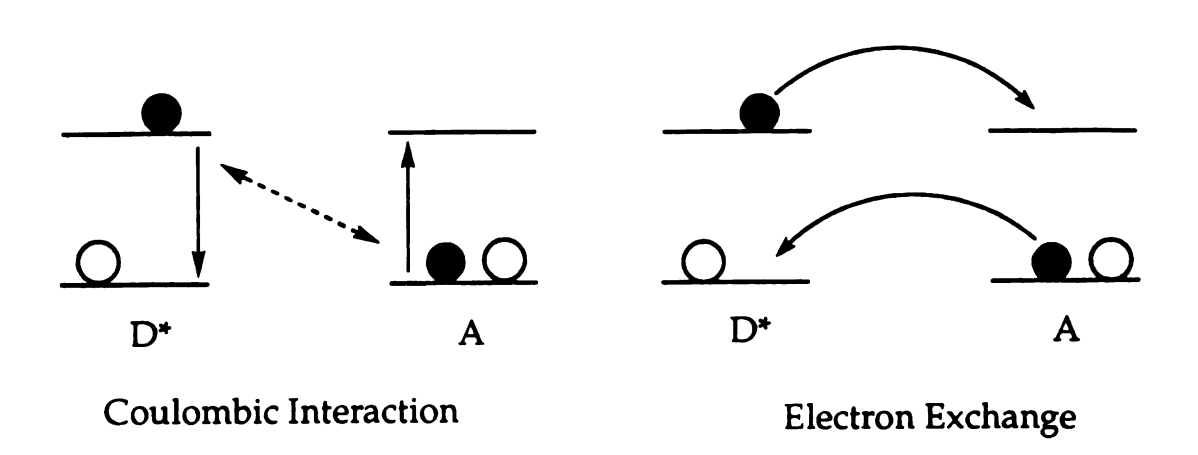
$$D - A \rightarrow D^* - A \rightarrow D - A^* \tag{1}$$

$$D - A \rightarrow D^* - A \rightarrow D^+ - A^- \tag{2}$$

Models for the respective orbital interactions in the two processes are shown in Figure 12. Energy transfer (eq 1) is described by two mechanisms: one involves a Coulombic interaction proposed by Förster [26] and the other an exchange interaction suggested by Dexter [27]. The Coulombic mechanism involves induction of dipole oscillation in the acceptor species (A) by the donor unit (D). The exchange resonance interaction occurs via overlap of electron clouds and requires physical contact between interacting partners. Consequently, the energy transfer rate constant exhibits a $1/r^6$ (for Förster mechanism) or $e^{-\alpha r}$ (for Dexter mechanism) distance dependence. Electron transfer is best described by the classical model that Marcus, Hush and Sutin developed [28]. In many ways, the electron transfer formalism is similar to that of exchange energy transfer. However, there are differences. The reorganizational barriers are larger for electron transfer than energy transfer since the solvent repolarization is more important in the former process where a permanent dipole is formed. Orbital overlap is important for both electron transfer and exchange energy transfer processes, but in the case of electron transfer only one electron is exchanged between acceptor and donor versus the two electron formalism of the exchange energy transfer case. This is

Figure 12. Schematic description of electron motion in energy and electron transfer.

Energy Transfer



Electron Transfer

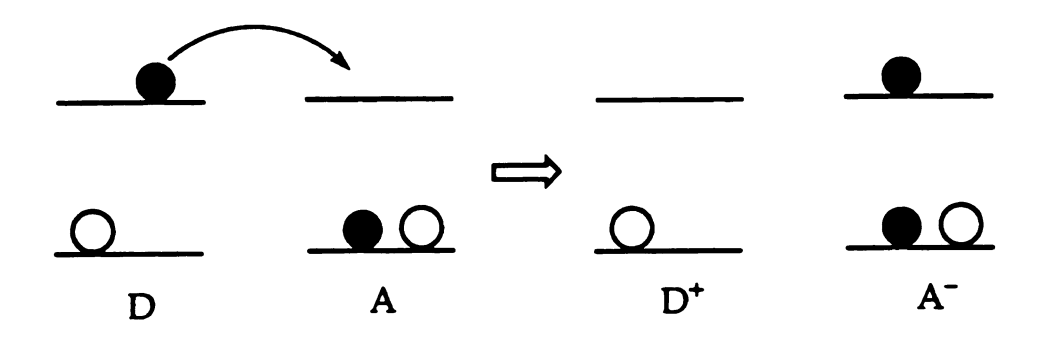


Figure 12

manifested in the exponential distance dependence of the electron transfer rate ($e^{-\beta r/2}$) versus that of energy transfer ($e^{-\alpha r}$). The studies of Closs and Miller [29] on selected organic donor–acceptor systems covalently linked with spacers, have elegantly elaborated these differences in the distance dependencies between energy and electron transfer processes.

2. Energy Transduction in Nature and Biomimetic Systems

Photosynthetic events are fascinating benchmarks for the study of energy transfer, electron transfer, or catalysis mechanisms. Photosynthesis is the natural process that converts solar energy into chemical energy, providing the fuel source for living processes. Light–sensitive biological systems have an architecture that permits directional motion of electrons and energy. Subunits consist of light–harvesting antennas that absorb one or more visible photons and transport the absorbed energy in a particular direction to a photoreaction center that converts the absorbed light to chemical potential. A catalytic site converts this potential to high–energy chemical products for long term storage.

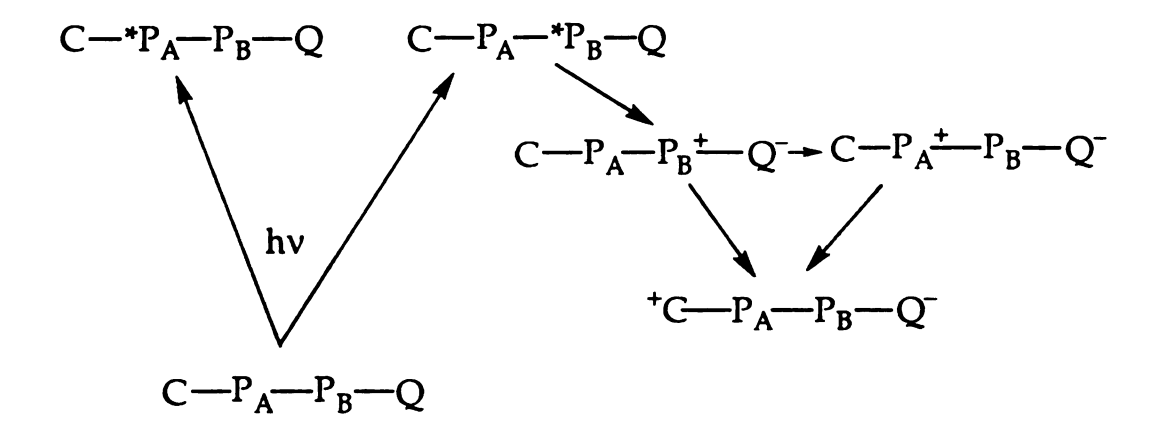
Indeed, the molecules that are involved in the energy and electron transfer process can be treated as a supramolecular assembly. The large organized light-harvesting assemblies responsible for efficiently collecting light are chlorophylls (Chl), bacteriochlorophylls (Bchl) and carotenoids. They play an antenna role by transferring energy to the reaction center where it is trapped rapidly and almost quantitatively [25]. From the electron transfer standpoint, the crystal structure of Huber shows that the primary electron transfer step occurs through the elegant supramolecular

assembly of a special porphyrin pair that ejects an electron to the nearby bacteriopheophytin [25]. The electron is then transferred to the primary quinone and from there to the secondary quinone. The latter three molecules comprise a supramolecular array that promotes a unidirectional charge separation. There is a vast literature concerned with studies on photoinduced electron and energy transfer in donor–acceptor systems. In particular, the design of supramolecular systems that are able to mimic stepwise energy and electron transfer have been very attractive.

Many biomimetic models for electron transfer have been developed. Biporphyrins linked with rigid spacers [30] or bichlorophylls [31] mimic the special pair of chlorophylls in green plants and photosynthetic bacteria where the first electron transfer step occurs. Moreover, many models that produce the photodriven charge separation have been synthesized. Studies on porphyrins (donors) linked with quinones (acceptors) [32] have investigated the effect of intervening spacer on the primary electron transfer process as well as the charge recombination step. Gust and Moore have developed and extensively studied polyad systems with linked porphyrins (P), polyenes or carotenoids (C) and quinones (Q) to explore sequential electron transfer steps that lead to charge separation (Figure 13) [33]. The scheme that shows the sequential electron transfer after light excitation of the porphyrin chromophores is shown below:

Figure 13. A carotenoid – porphyrin – porphyrin – quinone tetrad.

Figure 13



In addition to electron transfer studies, triplet–triplet energy transfer from the porphyrin moiety to carotenoid and singlet–singlet energy transfer from the carotenoid to the porphyrin have also been studied in appropriate chosen systems. Recently, a supramolecular array has been synthesized, combining quinone–substituted porphyrins linked by phenyl bridges, which exhibits light–harvesting, energy migration, trapping and photoinduced electron transfer [34].

3. Development of Photochemical Molecular Devices Based on Photoinduced Energy and Electron Motion.

Many artificial systems are developed not only for mechanistic purposes but also for potential device applications. Molecular devices may be defined as structurally organized and functionally integrated systems built into supramolecular architectures, and depending on the features of the components incorporated in the structure, devices may be photoactive, electroactive or ionoactive [1], [24], [35]. The receptors have potential to generate, process, transfer or store signals by making use of

the three dimensional structure and molecular recognition for substrate incorporation.

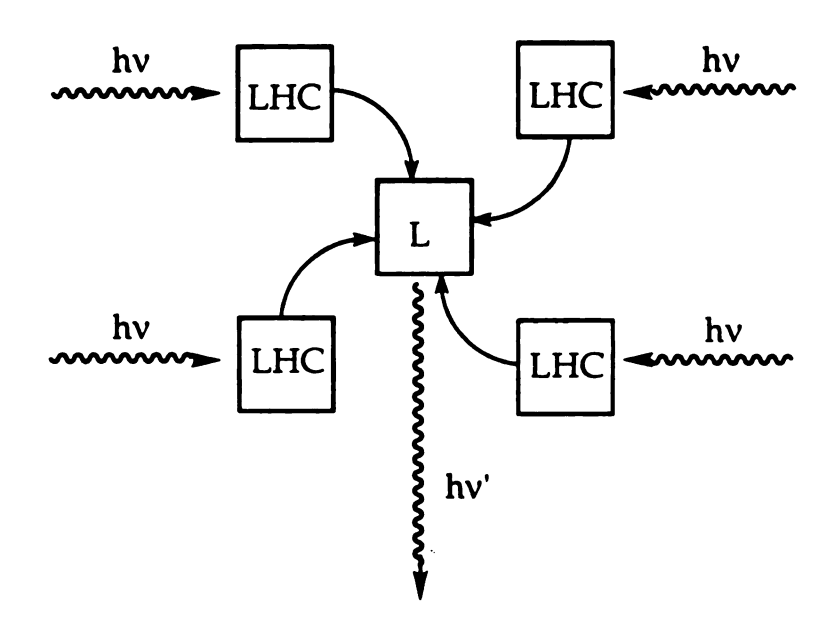
Energy transfer studies on model assemblies provide the framework for the design of light conversion schemes for the development of luminescent materials and sensors. Employing Balzani's block diagrams for supramolecular device operations [24], two designs of energy transfer devices important to this thesis – the remote photosensitization and the antenna effect – are illustrated in Figure 14.

Remote photosensitization refers to systems that transfer excitation energy from one component to the other; they are usually covalently linked rigid systems. In order to obtain energy migration from a donor to an acceptor over long distances, the design involves a sequence of energy transfer processes along a vectorial array of components. Polynuclear species containing M(bpy)_xⁿ⁺ units linked by cyano bridges and tri– or tetra– metallic systems bridged by polydentate ligands are well studied examples [36]. In the same context, polymers are important templates for arranging donor–acceptor subunits over extended distances. M. A. Fox and T. J. Meyer [37] have constructed polymers with organic backbones and organic or metal subunits as pendant groups encompassing donor, sensitization and acceptor function.

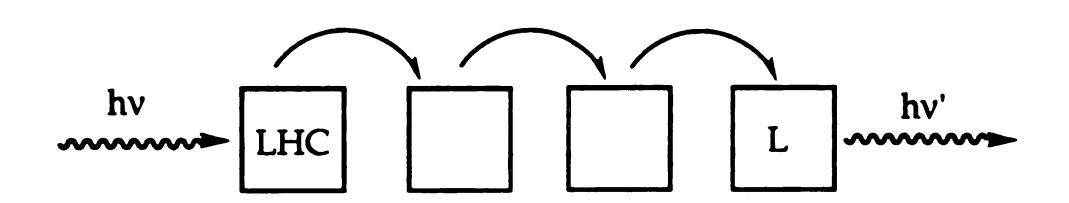
The antenna effect requires light–harvesting centers that absorb light efficiently and at the same time are able to convey energy to a common trap within the structure. The scheme effectively increases the absorption cross section of the trap by incorporating light harvesting centers about the trap. An illustrative example is the tetrametallic Os[(2,3–dpp)Ru(bpy)₂]₃⁸⁺

Figure 14. Block diagrams that describe the function of molecular devices based on energy transfer.

Antenna Effect



Remote Photosensitization



LHC = Light Harvesting Center L = Lumophore

Figure 14

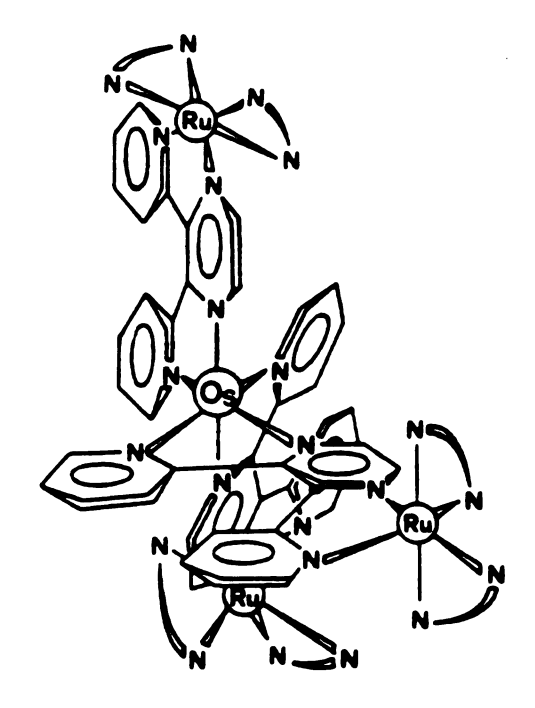
ruthenium chromophores, by excitation in the charge transfer bands (CT), is transferred to the "trap", the central osmium unit. Further development to cluster polynuclear arrays have been also reported [38].

4. Lanthanides as Photoactive Centers in Antenna Systems.

For the purpose of sensor development, the trap is a luminescent center. A convenient photoactive center is a luminescent ion as a lanthanide [39]. All of the Ln(III) ions with the exception of La(III) (4f⁰) and Lu(III) (4f¹⁴) are open shell paramagnetic species. Only four, Sm, Eu, Tb and Dy trivalent ions, are known to luminesce in solution. They exhibit narrow line luminescence, which has made them useful for lasing materials, immunoassays, and structural indicators of the metal binding sites in enzymes and proteins [40]. Two disadvantages of the Ln(III) ions are their low absorption coefficients (usually < 1 l•mol⁻¹•cm⁻¹) and their luminescence quenching by water molecules due to high energy O–H vibrations as efficient non-radiative traps.

These disadvantages are overcome when they are included in macrocyclic cryptand ligands, which are structural precursors to supramolecular assemblies [41]. Encapsulation of lanthanide ions in the cryptand cage, forming the Ln³+⊂2.2.1 cryptate (Figure 16), shields the ion from water molecules thereby increasing its luminescence [42]. When the arms of the cryptand are light–harvesting units such as bipyridine or phenanthroline, intense luminescence is observed owing to the efficient intramolecular energy transfer from the light–harvesting subunit to the

Figure 15. The tetrametallic $Os[(2,3-dpp)Ru(bpy)_2]_3^{8+}$ complex and a schematic energy level diagram that illustrates the antenna effect.



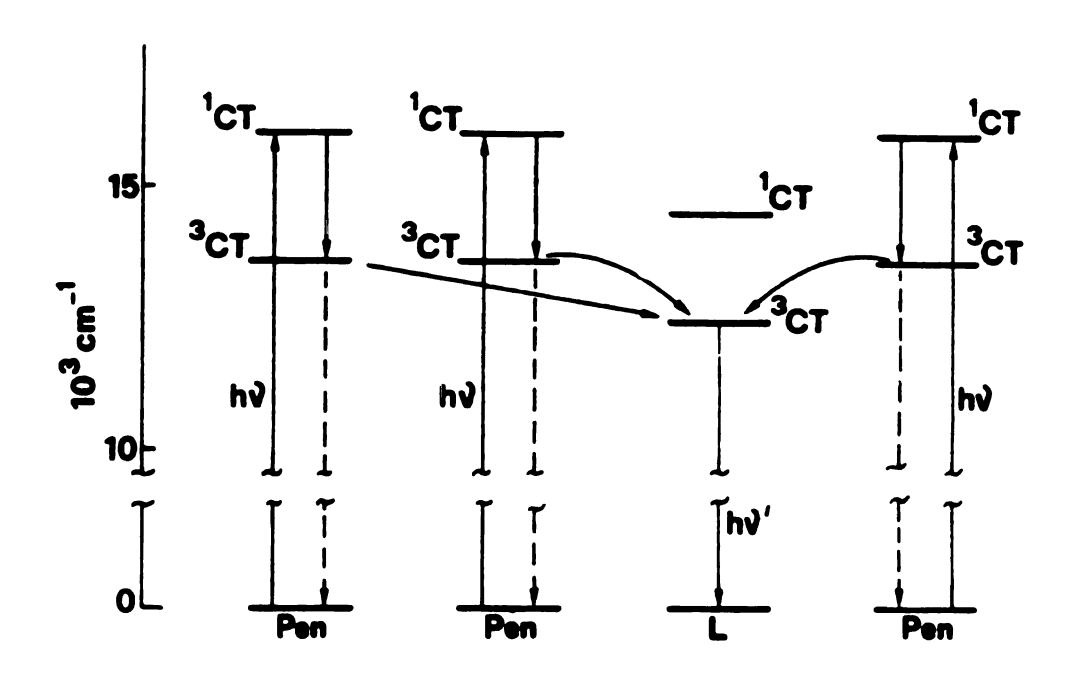
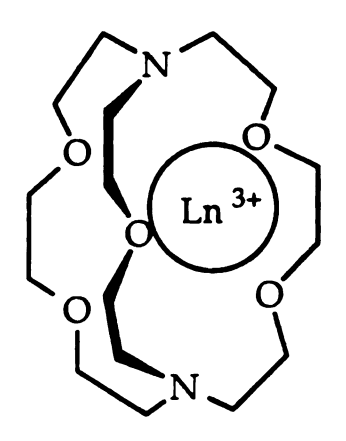


Figure 15

Figure 16. Structures of lanthanide complexes with cryptands and a schematic energy level diagram that demonstrates the AETE process in the bipyridine substituted ${\rm Ln^{3+}}$ cryptate.



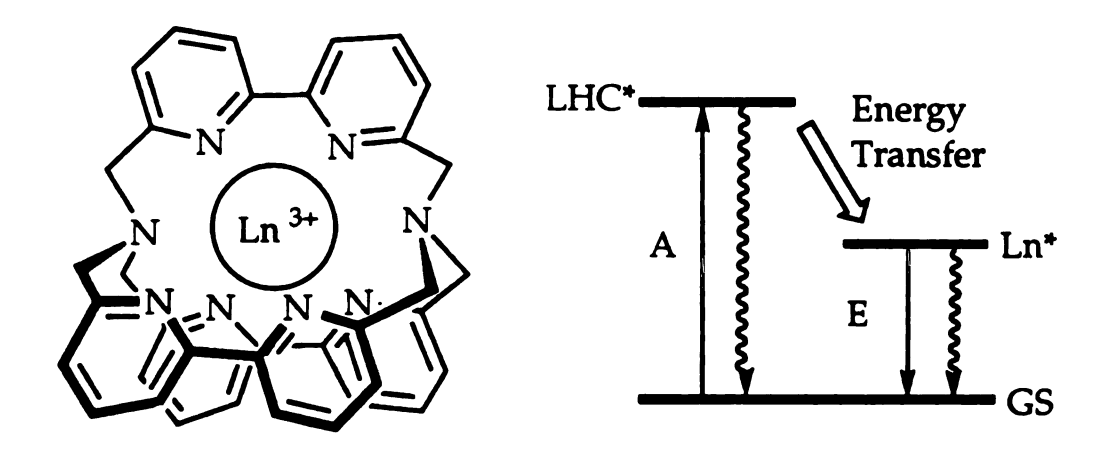


Figure 16

luminescent lanthanide ion [43]. Such light conversion processes have been described as absorption-energy transfer-emission (AETE). A simplified Jablonski diagram presented in Figure 16 describes the AETE process. Excitation of the light harvester to an energy level that is higher than the luminescent excited state of the lanthanide permits efficient energy transfer from light-harvesting center (LHC) to ion. The choice of the sensitizer with the proper energy gap is the crucial factor in establishing the antenna function. A simplified energy level diagram shown in Figure 17 demonstrates the energy requirements for the LHC compared with Eu(III) and Tb(III) energy levels. Ln³+Cbpy•bpy•bpy architectures exemplify the antenna effect with the bipyridine arms playing the role of the antenna and energy transfer donor.

Further elaboration has provided multiple bipyridine sites in an effort to improve the efficiency of light absorption, lanthanide encapsulation and consequently the luminescent properties [44]. Derivatized calixarenes have also used as receptors for lanthanide ions in an AETE photophysical mechanism [22]. In this case, the aromatic sheath of the calixarene is the antenna and the energy is channeled to the lanthanide bound to the appropriate functional groups on the calixarene rim. In a recent system, a calixarene was functionalized by amide groups as lanthanide binding sites and a phenacyl or diphenacylcarbonyl group as a sensitizer [22d]. It was shown that the presence of the sensitizer led to high emission quantum yields of the system. A limitation of the bipyridine or calixarene structures is that the systems are confined by the requirement that the light-harvesting aromatic moiety must be synthetically

Figure 17. Simplified energy level diagram describing the relative energies between ${\rm Tb}^{3+}$ or ${\rm Eu}^{3+}$ and the LHC.

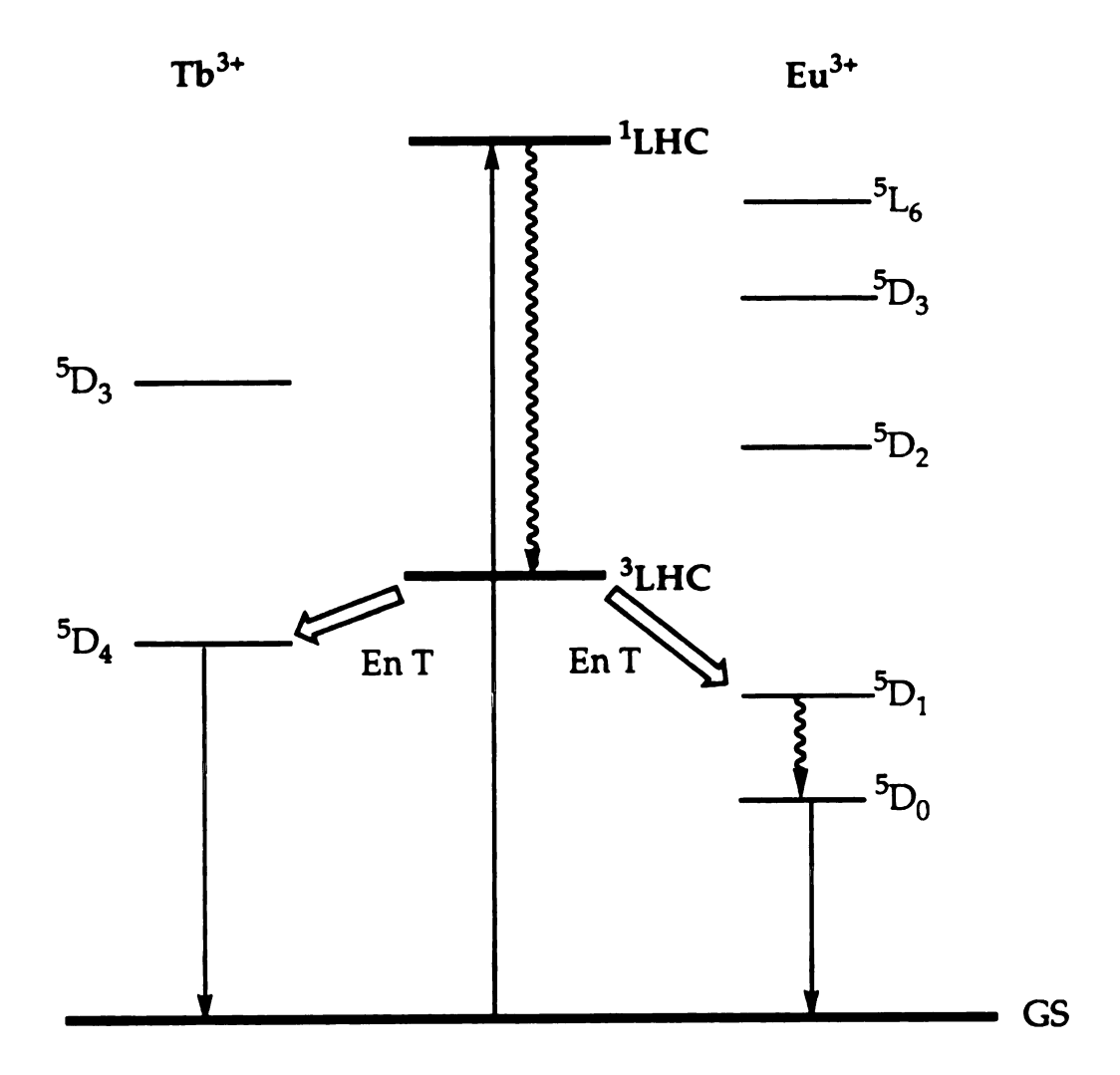


Figure 17

incorporated into the structure.

The AETE process can also be initiated by light-harvesters that are external to the supramolecular cage and capable of coordinating the lanthanide encapsulated in the cryptand structure. There are two available sites in the lanthanide coordination sphere after complexation in a cryptand cage that provide the opportunity for light-harvesters to bind the ion (Figure 18). For instance, the energy transduction steps in the AETE process of the acetylacetonate (as LHC) bound to Ln³+⊂2.2.1 cryptate are followed by picosecond laser spectroscopic techniques and the fast energy transfer from acetylacetonate moiety to the lanthanide is established [45a]. The AETE process is very sensitive to distance of the LHC from the luminescent ion and the shape of the LHC. The results of the AETE process with aromatic acids as antennas for lanthanides show that the most efficient energy transfer occurs when the light-absorbing benzene ring is near the Ln³⁺ center [45b]. As the number of methylene units between the carboxylate and the ring is increased the luminescence intensity decreases exponentially, as predicted by Dexter theory. In regard to shape selectivity the AETE is suppressed when a methyl group near the carboxylate functional group hinders approach of the aromatic acid to the lanthanide.

C. Cyclodextrin Supramolecules Designed to Perform AETE

In the above photophysical schemes, the light-harvester must be designed into the architecture or be capable of metal ion coordination. But

Figure 18. Representation of the exogenous LHC approach and a selective example of acid binding in $Eu^{3+} \subset 2.2.1$.

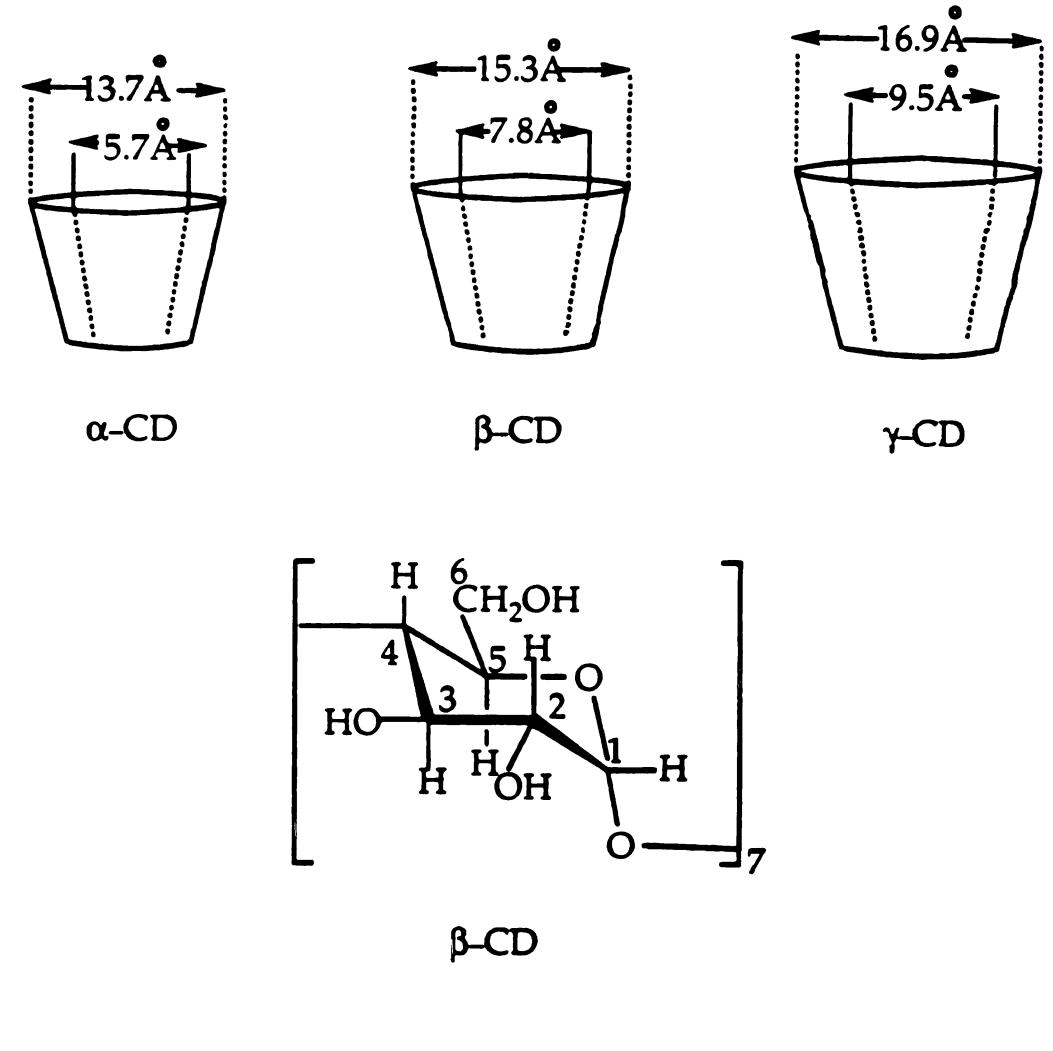
it is desirous in many applications, particularly in the design of optical sensing schemes, to initiate AETE with a non-coordinating light-harvester. The focus of this thesis is the design of a receptor capable of molecular recognition of a light-harvester to initiate AETE within a supramolecule. Figure 19 schematically illustrates our design. Supramolecular assemblies of this type are capable of juxtaposing a variety of energy donors to an acceptor without requiring donors to be directly bound to the photoactive lanthanide center thus providing the framework for the development of luminescence-based sensors and materials. Effectively, this design represents a substitution of one arm of a cryptand structure by a secondary receptor site that forms a new supramolecular assembly. Cryptand's arms have been substituted before with aromatic moieties [42d], [46] by taking advantage of the nitrogen reactive site on an aza crown ether to react with other functional groups in order to yield functionalized cryptands. A properly functionalized cyclodextrin can ideally play the role of the receptor in such a supramolecular approach.

1. Cyclodextrins as Receptors

Cyclodextrins (CD) are cyclic oligosaccharide molecules consisting of 6, 7 or 8 α (1-4) linked D-glucose units (α -, β -, and γ -CD, respectively) that are arranged in a torus to give a rigid conical structure with a hydrophobic cavity (Figure 20) [47]. The exterior of the molecule is relatively hydrophilic and CDs are soluble in water. Cyclodextrins provide an ordered medium capable of molecular organization since they form inclusion complexes with a variety of aliphatic and aromatic

Figure 19. Block description of a new design for AETE, consisting of a receptor with two binding sites, for lanthanides and hydrophobic substrates.

Figure 20. Cyclodextrin cups of different size and the structure of β -CD.



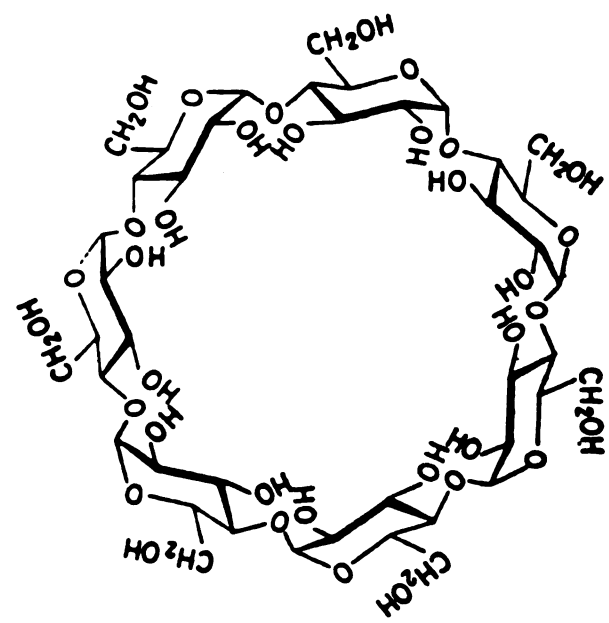


Figure 20

molecules by insertion of the appropriate size guest into their cavity [48]. The binding forces responsible for the inclusion of guests are due to hydrophobic interactions, van der Waals interactions, hydrogen bonding and stabilization due to the displacement of "high-energy" water from the cavity. The size of intramolecular cavity and therefore the complexation properties depends on the number of glucopyranose units forming the ring. Inclusion of luminescent probes in CDs modifies their photophysical behavior [49]. Such changes are usually attributed to an effect on the guest's radiative rate constant, a decrease in its rotational freedom, shielding from external quenchers or interaction with other molecules in the cavity. Characteristic examples are the fluorescence enhancement of the guests, shifts in their emission maxima, observation of room temperature phosphorescence [50] or intramolecular excimer formation [51]. These properties find many applications in the development of sensors [52]. Inorganic complexes bind to cyclodextrins that play the role of second sphere ligands, and their properties have been examined [53]. Attempts to study electron transfer processes and some examples with systems built for energy transfer have been reported [54].

Cyclodextrin derivatives have been widely studied particularly for the development of models in enzymatic catalysis [55]. The substrate is usually included in the cavity and reacts in the form of an inclusion complex. The aim is to mimic the ability of enzymes to bind certain substrates quickly and selectively, reversibly and non-covalently, and to catalyze possible reactions.

2. Crowned Cyclodextrins

The modification schemes of the CD [56] primarily rely on the differences in chemical reactivity between the primary and secondary hydroxyl groups on the glucose subunits, with the former exhibiting greater reactivity than the latter. This feature provides the foundation on which to build cyclodextrins functionalized with a juxtaposed recognition site external to the CD cup. To this end, the attachment of the macrocyclic ligand 1,4,10,13-tetraoxa-7,16-diazacyclooctadecane (an aza crown) on one site of a β -CD cup, first reported by Willner [57], inspired our studies to work on aza modified cyclodextrins.

We have developed the syntheses of aza cyclodextrins which we designate as β -CD \cup 1aza and β -CD \cup 2aza as described in Chapter II. We use the mathematical symbol \cup to indicate the covalent union of the cyclodextrin to the nitrogen of crown ether. A \cup 1 attachment is distinguished from a \cup 2 assembly in the number of nitrogens of the aza ligand that are joined to the cyclodextrin cup. In the first structure the aza crown has a swing conformation while in the latter it is rigidly situated at the base of the CD cup as a cradle. In these architectures, the conical cavity of the β -CD provides an ordered hydrophobic microenvironment capable of molecular recognition to form inclusion complexes with a variety of molecules, whereas the catenation of the aza ligand to the primary alcohol rim of the β -CD (i.e. attachment at the bottom of the CD cup) provides a receptor site for lanthanide ion binding. The successful incorporation of lanthanide ions in the aza site, as described in Chapter II, gave us the desirable supramolecular assemblies for photophysical studies. Within the

same context, more swing CDs were synthesized as described in Chapter II with different appended arms or modifications on the cup that would result in improvement of their photophysical properties.

Chapters III and IV describe the characterization and properties of the swing and cradle assemblies, respectively. Complete characterization of the compounds came mainly from Nuclear Magnetic Resonance (NMR) spectroscopy. NMR spectra of the precursors are included in the Appendix. Detailed analysis is presented for each of the compounds. The inclusion chemistry of different guests was elucidated by the determination of the association constants. The ion in the appended macrocycle not only affects the polarity of the whole assembly but also induces cooperative binding of the guests that bear functional groups. We also establish AETE photophysics for the supramolecular assemblies with the demonstration of energy transfer from the light harvesting guests (LHG) included in the cup of the CD to the Eu³⁺ or Tb³⁺ ion residing in the aza macrocycle. The antenna units (LHGs) were chosen for their ability to be incorporated in the CD cup. Since the inclusion chemistry of cyclodextrins is so rich this was not a limitation in our studies as will be shown. Bright luminescence from the lanthanides is triggered by the binding of the LHG; thus the compounds are potential luminescent sensors of aromatic moieties. Investigations on the nature of the LHG, its association constant with cups, and the distance dependence on the energy transfer studies will be discussed.

Chapter V reports a comparison on the energy transfer studies of the swing and cradle CD architectures with the different guests along with final remarks on the development of this class of receptors, the crowned cyclodextrins, that contributes to the design of photoactive supramolecular structures towards new polymolecular devices.

CHAPTER II

EXPERIMENTAL

A. Synthesis

1. General Procedures. Syntheses of all compounds were performed using Schlenk-line techniques with emphasis on excluding trace water from reaction mixtures. All chemicals were reagent grade. The solvents were deoxygenated, dried, and freshly distilled prior to use according to standard methods [58]. The syntheses of the modified β -CDs required especially dry pyridine, N,N-dimethylformamide and acetonitrile. In order to obtain pure, dry pyridine a special purification procedure was followed. Pyridine was refluxed over potassium hydroxide (KOH) for a week, distilled, and collected over barium oxide, where the final distillation prior to its use took place. The starting materials were purchased from Aldrich: β -CD was recrystallized from water and dried at 100 °C under a high vacuum manifold (10⁻⁶ Torr); 1,4,10,13 tetraoxa-7,16-diazacyclooctadecane (indicated as aza) and triethylene tetraamine, which was provided as a hydrate (indicated as tetraamine), were dried prior to

use; *p*-toluenesulfonyl chloride, *tert*-butylchlorodiphenyl silane, biphenyl-4,4'-disulfonyl chloride, imidazole, sodium hydride and diethylene triamine (indicated as triamine) and finely powdered potassium iodide 99.9% were used as received; methyl iodide was distilled over Cu wire under argon. Once isolated, all the products were dried under high vacuum unless otherwise noted.

- 2. β -CDO-Ts. Monotosylation at the primary face of β -CD to yield mono(6-O-p-tosyl) β -CD (β -CDO-Ts) was accomplished with the methodologies elaborated by Matsui [59]. A solution of p-toluenesulfonyl chloride (0.9 g, 4.7×10^{-3} moles) in 7.5 ml of dry pyridine was added to a solution of β -CD (7.38 g, 6.50×10^{-3} moles) in 75 ml of dry pyridine cooled below 5 °C. After stirring overnight at room temperature, the mixture was evaporated under vacuum at 40 °C to dryness. Diethyl ether was added, and the precipitate was collected and recrystallized from water to yield pure mono(6-O-p-tosyl)- β -CD (yield 35%). The product, which was recrystallized from water and dried, was characterized by 1 H and 13 C NMR, FTIR, and positive ion FABMS. It absorbs at λ_{max} = 258 nm (in H₂O with 1% MeOH).
- 3. β -CD \cup ¹aza. The synthesis of β -CD \cup ¹aza from β -CDO-Ts was accomplished by employing the procedures of Willner [57]. Reaction of mono(6-O-p-tosyl) β -CD (0.63 g, 0.49×10⁻³ moles) with excess aza crown ether (1.6 g, 6.10×10⁻³ moles) in 260 ml of dry DMF at 80 °C leads to a mixture of compounds, which are separated by flash chromatography over

silica gel or by gel filtration chromatography over Licrogel or Sephadex LH–20 as described later in this Chapter. The fragments were collected and identified by TLC. Although the tosylate is readily substituted by aza, as described by Willner and co-workers, our chromatographic separation scheme is essential to obtaining compound free of tosylated impurities. The substitution of β –CD tosylate by aza produces p-toluenesulfonic acid. We have evidence (from ¹H NMR spectra, *vide infra*) that the acid reacts with the aza substituted CD to form the tosylate salt of the protonated β -CD \cup 1aza supramolecule. Pure β -CD \cup 1aza can be recovered upon dissolution of the proposed β -CD \cup 1aza tosylate salt in basic aqueous solution with subsequent precipitation by tetrachloroethylene (yield 30%, mp = 260 °C). β -CD \cup 1aza was further characterized by ¹³C NMR, FABMS, and ¹H NMR COSY. The aza absorbs weakly at 300 nm.

4. β -CD \cup 1 triamine. The triamine and tetraamine monosubstituted CDs were first reported by Tabushi [60]. But a modification of the procedure by Matsui [61] for the ethylene diamine CD gave us the best results for a general procedure for the substitution of β -CDO-Ts by amines. A solution of 1.0 g of β -CDO-Ts in 50 ml of degassed diethylene triamine which is also the solvent for the reaction) was heated at 50 °C for 6 h, concentrated to 2 ml, and the residue was passed through a silica gel column in a flash chromatography set-up. The eluent was 0.5 N NH₄OH. Treatment of the pure compound with basic aqueous solution, and precipitation with tetrachloroethylene to eliminate the tosylated salt, afforded the substituted triamine cyclodextrin. It was characterized by

NMR and IR.

- 5. β -CD \cup ¹tetraamine. The same procedure as for β -CD \cup ¹triamine gave the tosylate salt of β -CD \cup ¹tetraamine, characterized by NMR. The tetrachloroethylene treatment is not sufficient, in this case to completely remove the salt.
- 6. β-CDO-SiPh₂(tert-Bu). A solution of 74 μl of (tert-Bu)Ph₂SiCl in 7 ml of DMF was added in portions, during a period of 30 min, to a solution of 0.3 g of β-CD and 39.6 mg of imidazole in 40 ml of DMF which was cooled at 0 °C. The mixture was left at room temperature for 48 h and then heated at 60 °C for an hour to assure complete reaction. The solvent was distilled off under vacuum and the residue was washed with water and dried. The imidazole and the unreacted (tert-Bu)Ph₂SiCl were removed by this procedure. TLC confirmed the existence of one compound that was proved to be monosubstituted CD by NMR. The same procedure using pyridine as a solvent and no imidazole failed to give the desirable product.
- 7. **Methylation of** β -CDO-SiPh₂(*tert*-Bu). The popular procedure of Szejtli [62] for methylation of cyclodextrins was applied to methylate β -CDO-SiPh₂(*tert*-Bu). A solution of 175 mg of β -CDO-SiPh₂(*tert*-Bu) in DMF was cooled at 0 °C before the addition of 12 mg of sodium hydride. The mixture was stirred at room temperature for 30 min. The jelly-like, dark yellow mixture was cooled again to 0 °C and 1.1 ml of freshly

methyl iodide was added over a period of 30 min. The solution was left at room temperature for 48 h because these conditions are more dilute than the reported ones. After 48 h the excess sodium hydride was decomposed by the addition of methanol at 0 °C. The mixture was poured into crushed ice with stirring. Extraction with chloroform gives a white precipitate in the aqueous layer; the organic layer was washed with water to neutral pHs and concentrated in vacuum. The residue was crystallized from chloroform/light petroleum and then from cyclohexane. NMR shows partial methylation of the hydroxyl groups.

8. $Eu^{3+} \subset aza$ (NO₃)₃. The $Eu^{3+} \subset aza$ complex was synthesized for comparative photophysical studies to β -CD \cup ¹aza $\supset Eu^{3+}$. Two methods have been employed.

The procedure of Desraux [63] requires strictly anhydrous conditions to prevent the hydrolysis of the Ln³⁺ ions since aza is a strong base. An anhydrous acetonitrile solution of Eu(NO₃)₃ (4.28 g in 50 ml, 0.2 M) was obtained by refluxing the solution for 24 h through a Soxelet extractor packed with activated molecular sieves. This solution (0.5 mmoles, 2 ml) was added to neat macrocycle at 1:1 ratio (0.13 g aza in 10 ml CH₃CN). After refluxing for 1 hr and reducing the volume, the solid was collected by suction filtration (yield 80%).

A second procedure is similar as the one followed for the preparation of lanthanide cryptates described by Pruett [64] but the conditions were drier in our case. A solution of Eu(NO₃)₃•5H₂O (0.343 mmoles) in 40 ml CH₃CN and 10 ml trimethylorthoformate (TMOF, acts as

drying agent) was refluxed overnight. A solution of aza (0.343 mmoles) in 15 ml CH₃CN was added and the reaction was left refluxing for 20 h. After cooling, the solution volume was reduced and diethyl ether was added to facilitate further precipitation. The solid was quickly filtrated in air and dried.

- 9. β -CD \cup 1aza \supset Eu³⁺(NO₃)₃. The complex was prepared following the procedures described for the preparation of Eu³⁺ \subset aza. Because β -CD \cup 1aza exhibits low solubility in cold acetonitrile, the reaction was performed in lower concentrations and longer times (two days refluxing after the β -CD \cup 1aza addition in the Eu(NO₃)₃ salt) or it was dissolved in warm acetonitrile.
- 10. $\mathsf{Tb^{3+}} \subset \mathsf{azaCl_3}$ and $\beta\text{-CD} \cup ^1 \mathsf{aza} \supset \mathsf{Tb^{3+}Cl_3}$. The second procedure as described in Section A. 3. was followed for both complexes.
- 11. Eu³⁺(triamine)₂(NO₃)₃. The complex was prepared according to a procedure that Forsberg reported for ethylenediamine chelates with trivalent lanthanides [65]. A solution of 0.496 g of Eu(NO₃)₃•5H₂O in 135 ml of acetonitrile and 34 ml of trimethyl orthoformate was refluxed overnight. This method is very efficient in providing anhydrous Ln³⁺ solutions. Neat amine (1 ml, 8 times molar excess over the lanthanide salt) was added, to produce initially a clear solution but in short time it turned cloudy and precipitation of the complex occurred. The reaction was completed in 12 h. The complex, which is highly moisture sensitive, was

vacuum filtrated and stored under argon. Elemental analysis proved the stoichiometry of the complex.

- 12. Eu³⁺(tetraamine)₂(NO₃)₃. The same procedure used for the triamine complex was followed. The reaction solution turned cloudy after the course of 6 or 8 h; thus it was left refluxing for 3 days. Again, elemental analysis elucidated the stoichiometry of the complex.
- 13. Reaction of Eu(NO₃)₃ with β -CDU¹triamine and β -CDU¹tetraamine. Two procedures were followed. The first one was the same as for the amine complexes referred above. The reactions took place over 3 to 5 days to assure completion. The procedure was plagued by the low solubility of the amines in acetonitrile, especially for the tetraamine case. Another procedure relied on the partially protonation of the amines with trifluoroacetic acid (for example 3 equiv of triamine/1 equiv of acid) and then the reaction was allowed to proceed as described above. This method gives a light yellow solid that might indicate partially oxidation of the amine.
- 14. Biphenyl-4,4'-disulfonyl-A,D-capped β -CD. As elaborated by Tabushi [66], reaction of the β -CD with biphenyl-4,4'-disulfonyl chloride yields a cyclodextrin rigidly capped with the biphenyl sulfonate spanning the (A, D) glucosyl subunits. To a solution of 6.56 g of dry β -CD in 175 ml of dry pyridine at 50 °C, 1.74 g of biphenyl-4,4'-disulfonyl chloride was added in four portions during 1 h while being stirred. After 3 h the

pyridine was removed under vacuum at a temperature no more than 40 °C. The biphenyl-4,4'-disulfonyl chloride sublimes at low temperatures under vacuum. The waxy residue (7.8 g), separated in portions, was dissolved in the minimum amount of water and the solution was added dropwise into a solution of CH₃CN/H₂O 5.5:1 v/v. Most of the oligomeric products and unreacted β-CD were precipitated. The filtrate was concentrated and introduced to the Sephadex LH-20 column, since in our hands TLC shows that the oligomeric products cannot be completely removed by the CH₃CN method and there is also some amount of byproduct, the A, C isomer. The pure A, D isomer was isolated in the second chromatographic fraction collection (yield 17%). characterized by NMR, and IR spectroscopies. Further attempts to change the reaction conditions (more dilute solutions of the reactants, smaller ratio of β -CD: biphenyl-4,4'-disulfonyl chloride, shorter reaction time) in order to eliminate the oligomeric products gave lower yields for the pure A, D product. It absorbs at UV λ_{max} = 260 nm (in H₂O with 1% MeOH).

15. Diiodo-β-CD. The method followed is similar as the one reported for the A, C isomer [67]. 75 mg of biphenyl-4,4'-disulfonyl-A,D-capped β-CD were dissolved in 10 ml of dry DMF and 0.27 g of KI were added. The reaction solution was kept at 80 °C under argon for 2 h with stirring. Higher temperature is not recommended as a yellow color indicates iodine formation. The solution was dried under vacuum at 30 °C and then dissolved in a minimum amount of water, kept at 0 °C, and a couple drops of tetrachloroethylene were added under vigorous stirring.

This procedure eliminates the bisulfonate salt formed during the reaction. The precipitate was collected and dried under vacuum in a desiccator (yield 85%). It was characterized by NMR spectroscopy.

- 16. β -CD \cup^2 aza. The diiodo- β -CD (0.06 g) was reacted in dry dimethyl formamide (DMF) with a ten-fold molar excess of the aza crown ether at 55 °C under argon. After 24 h, the DMF was distilled off under reduced pressure. The residue dissolved in a small amount of DMF was introduced on a Sephadex LH-20 for preparative scale liquid chromatography in order to afford the pure compound (yield 40%). At this step, there are no aromatic acids because they were eliminated in the diiodo-CD treatment with tetrachloroethylene. Characterization was employed by FABMS, NMR.
- 17. β -CD \cup ²aza \supset Eu³⁺(NO₃)₃. The same procedure described for β -CD \cup ¹aza \supset Eu³⁺(NO₃)₃ was employed.
- 18. β -CD \cup ¹aza \supset Y³⁺(NO₃)₃ and β -CD \cup ¹aza \supset Y³⁺(NO₃)₃. These complexes were made analogous to the europium analogs, and used for association constant studies.

B. Instrumentation and Methods

1. Chromatographic Procedures

a. Flash Chromatography. Rapid chromatographic technique

(retention time 10-20 min) [68] was used initially for the separation of β-CDU¹aza from the reactants. The apparatus that we used was similar to the one previously described [68] with a 40 mm (o.d.) column and a homebuilt flow controller. Argon was used as the driving gas to produce flow rates ranging from 1–2 in/min. Silica gel 60 (Merck) with pore size 230–400 mesh was used as the packing material and gives the best resolution for the conditions of rapid flash chromatography. A low viscosity solvent system consisting of AcOEt/*i*-PrOH/H₂O = 10:13:7 was used for eluent. Even flash chromatography is ideal for separations of compounds with ΔR_f > 0.1 units (as measured from analytical TLC) the use of silica gel for separation of cyclodextrins is disadvantageous because of adsorption of modified CDs on the silica gel due to polar interactions.

b. Molecular Exclusion Chromatography. This type of chromatography is widely used for carbohydrate separations [69]. The stationary phase is a gel with bead sizes to ensure that solutes applied to the column will have a differential distribution between the liquid outside and inside the beads. The small molecules penetrate the gel particles, getting retarded and eluted later than large molecules, which will move only in the interstitial volume (in the liquid surrounding the gel beads). Therefore, the important factors for separation are both the molecular volume of the solute and the distribution of pore sizes available in the gel particles.

Initially, we used Licrogel as the stationary phase and $nPrOH/H_2O/Acetone = 1:1:2$ as the eluent system in the liquid chromatography set-up. In order to change the eluent system to solvents

in which CDs are more soluble, we selected Sephadex LH–20 as the column packing material and DMF/ $H_2O=1:1$ as the eluent solvent system. Sephadex LH–20 is a lipophilic derivative of Sephadex G–25, a polydextran, obtained by alkylation of most of its hydroxyl groups hence having both hydrophilic and hydrophobic properties. It has a dry bead diameter of 25 to 100 μ m, it is stable in a wide range of pH (2–10), and swells in water and organic solvents. Its exclusion limit is at a molecular weight of approximately 4,000 [70].

A home-built apparatus whose representative block diagram is shown in Figure 21 was used for separations. The gel was left to swell overnight in degassed eluent, and then poured into the column. The column was washed with solvent overnight. The eluent system was degassed under vacuum obtained by suction filtration while the flask was immersed in a sonicator (Bransonic Ultrasonic cleaner, Model 3200-4) in order to remove the dissolved air. The flow was maintained by siphoning solvent from the reservoir into the column, the rate being governed by the hydrostatic pressure, developed from the difference in levels of liquid in the reservoir and column outlet. The column is resistant to organic solvents and has the dimensions 2.5×80 cm (Spectrum Medical Industries). Silicon tubing, which is inert to organic solvents, was chosen with 1/32 in internal diameter, in order to develop pump pressure according with the specifications suggested from the manufacturer of the multistatic pump (Buchler Instruments). The multistatic pump forwards the liquid after the column to the detector (Linear Instruments Model 200). The double beam, variable wavelength detector is equipped with a semi-preparative flow

Figure 21. Block diagram of the preparative scale liquid chromatography apparatus.

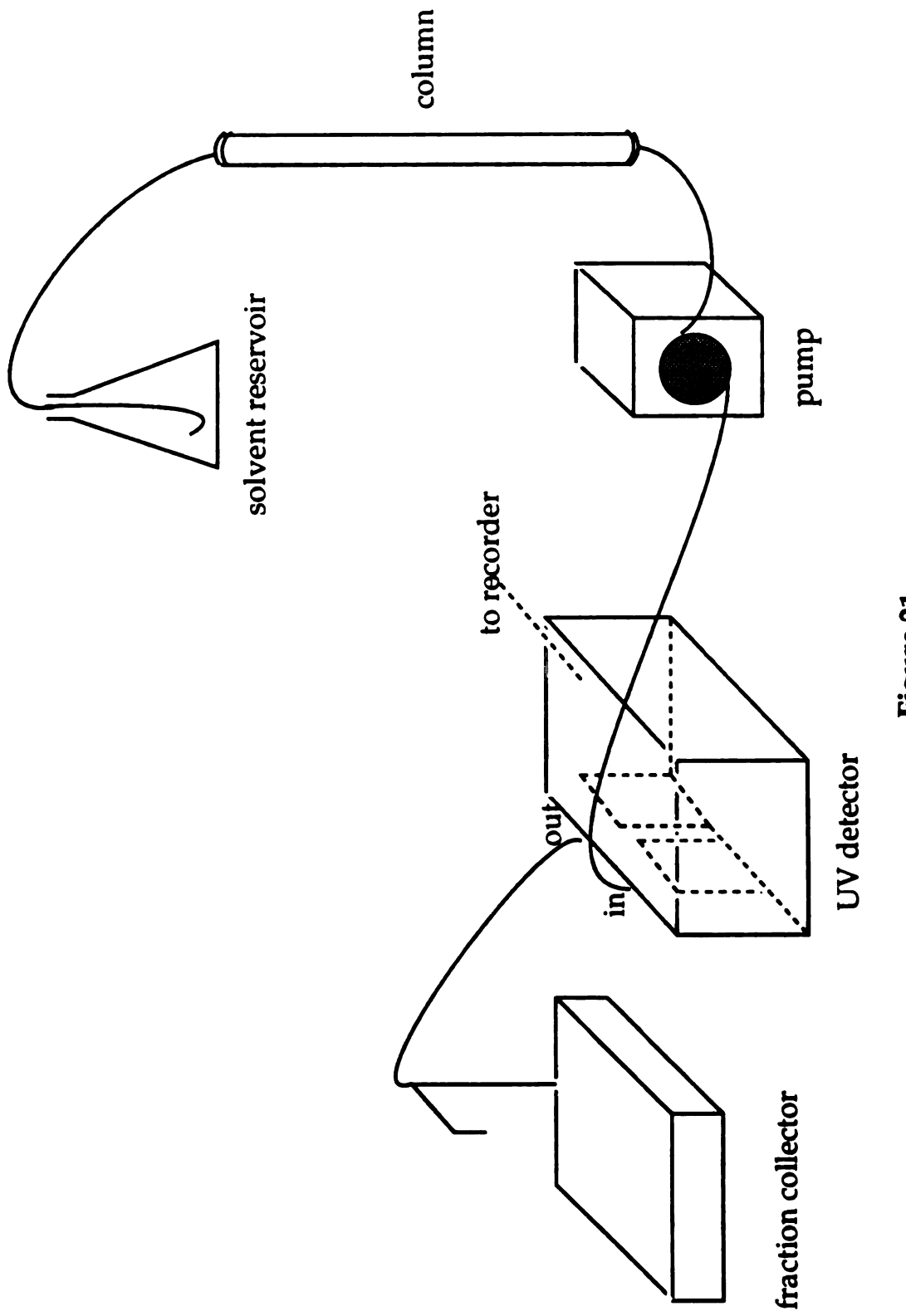


Figure 21

cell (Linear Instruments Model 9550–0101), a deuterium lamp for UV detection in the range 190–380 nm, and photodiodes for sample and reference detection. For the aza modified CDs, detection wavelengths were 300 nm and for the disulfonyl CD, it was 280 nm. The signal is directed to an HP integrator, which is only used as recorder for this application. The samples were collected with an automated fraction collector (Spectrum Medical Industries) that changes test tubes when a preset volume has been collected. The absorbance of the eluate is displayed on the recorder and can be correlated with the time and the number of tubes collected.

c. Thin Layer Chromatography (TLC). The detection of modified CDs was confirmed by analytical TLC. Aluminum sheets coated with silica gel 60 F254 (EM Separations) were used. The developing solvent systems were ethyl acetate: isopropanol: water 10:13:7 for the tosyl and aza modified CDs and n-propanol:ethyl acetate:water:ammonia 5:3:3:1 for the disulfonyl and diiodo CDs. Cyclodextrins were characterized by dark blue–green spots appearing when AcOH/anisaldehyde/ $H_2SO_4/MeOH = 45:2:22:430$ was used as the detection solution.

2. Nuclear Magnetic Resonance

¹H NMR spectra were recorded on a VXR-500 and a Gemini 300, at 500 and 300 MHz, respectively, while the ¹³C NMR spectra were recorded on a Gemini 300 spectrometer at 75 MHz. The two-dimensional experiments were performed on the VXR-500 instrument. Basic pulse

sequences for the ¹H-¹H Correlated Spectroscopy (COSY), ¹H-¹³C Heteronuclear Multiple Quantum Coherence (HMQC) and ¹H-¹H Total Correlation Spectroscopy (TOCSY) experiments, gave desirable sensitivity and resolution. For the HMQC and TOCSY experiments the 500 MHz VXR instrument, was equipped with an inverse detection probe. Deuterated dimethylsulfoxide (d⁶-DMSO, 99.9%), which was employed most commonly as solvent for the modified CDs, was purchased from Isotech and was used after drying over molecular sieves. Deuterium oxide (D₂O, 99.9%) from Cambridge Isotope Labs was also used as solvent in some cases.

3. Infrared Spectroscopy

Infrared spectra were recorded on a Nicolet 740 FT-IR spectrometer. Solid KBr pellets were prepared.

4. Mass Spectrometry

Positive ion fast atom bombardment mass spectrometry (FABMS) was performed on a Jeol HX 110 double focusing mass spectrometer housed at the National Institutes of Health/Michigan State University Mass Spectrometry Facility. Triethanolamine and glycerol were used as matrices.

5. Molecular Modeling Studies

The energy minimized conformation of the supramolecular assembly was determined on a Silicon Graphics IRIS 40-70GTX computer

by using a DREIDING force field [71] as implemented by BioGraph software (BioDesign Inc.) in the carbohydrate mode. Because lanthanide ions are not included in the software package, a hypothetical calcium cation with 3+ charge was selected for the minimization.

6. Electronic Absorption Spectroscopy

Electronic absorption spectra were recorded on a Varian 2300 UV- Vis- NIR spectrometer. All the compounds were stable in air.

7. Steady State Luminescence Spectroscopy

a. Energy Transfer Studies and Characterization. Steady state emission and excitation spectra were obtained by using a spectrometer designed and constructed at Michigan State University [72]. For excitation spectra, the source was a 150 W Xe lamp, and the $^5D_0 \rightarrow ^7F_2$ emission for Eu³⁺ was monitored at 616 nm with R1104 Hammamatsu photomultiplier tube as the detector; emission spectra were recorded by exciting at 313 and 394 nm with a Xe/Hg lamp. Both emission and excitation spectra were recorded at 23 \pm 1 $^{\circ}$ C and were corrected for instrument response functions.

Characterization by emission and excitation spectroscopy was performed in acetonitrile (spectroscopic grade, Burdick & Jackson). The energy transfer experiments required deuterium oxide (D_2O , 99.9%, Cambridge Isotope Labs) for solvent since water quenches lanthanide luminescence as it was discussed in Chapter I.

Lanthanide complexes of the free aza crown ether hydrolyze in aqueous solutions because the aza crown is very basic; the complexes tend to form hydroxides in strongly basic aqueous solution, which form immediately precipitates. In order to eliminate hydrolysis, the experiments were carried out in D₂O acidified solutions. Microliter quantities of an acidified solution of D₂O/DCl were added to the solid lanthanide salt and subsequently the appropriate volume of D₂O was added. The pH was stabilized to values around 5.5 units and hydrolysis was circumvented. The concentration of the lumophore was held constant $(3\times10^{-4} \text{ or } 6\times10^{-4} \text{ M})$, and the light harvesting guest (LHG) was added. The areas of the two strongest luminescence peaks for the lanthanides were integrated ($\lambda_{max} = 593$, 616 nm for Eu³⁺ and $\lambda_{max} = 495$, 546 nm for Tb³⁺). The ratio of the integrated luminescence area after addition of LHG to the initial (no LHG) luminescence area provides the relative emission intensity as a function of LHG concentration. The LHG solutions were made in D₂O, unless otherwise noted. Benzene was added neat in microliter quantities so that there was no need for volume corrections. In the cases of the acids the concentrations were corrected for volume additions higher than 50 µl. The pH of the added LHG solution was adjusted as the same way as for the lumophore. The acidic/anionic form of the acid plays the role of the buffer for the solutions of the acids.

b. Association Constant Studies. For association constant studies, a Perkin Elmer LS-5 luminescence spectrometer was used because of the better response of its emission monochromator in the UV region than the home-built instrument. Excitation light ($\lambda_{\rm exc}$ = 375 nm) from a 10

W Xe lamp was selected by a f/3 Monk–Gillieson monochromator. The luminescence of the sample was directed through the monochromator to a side-on photomultiplier ($\lambda_{em} = 400$ –600 nm). The slit widths for the emission and excitation monochromators were 5 mm. The spectra were corrected for the instrument response. A Zenith data station was used for collection of data which were then analyzed using Kaleidagraph software on a Macintosh computer.

Association constants were determined by the competitive binding technique and the data treatment was based on the Benesi - Hilderbrand method [73]. As referred in Chapter I, the introduction of aromatic guests in CDs affects their fluorescent properties due to the change from a hydrophilic to a hydrophobic environment. However, the changes in the fluorescence intensity are more pronounced for certain fluorescent probes originating from their intrinsic characteristics. Thus, we chose the competitive binding technique [74] using a strong fluorescent probe in order to accurately calculate the association constants of benzene, pyridine, benzoic, picolinic and naphthoic acids. Anilinonapthalene sulfonates is a class of compounds whose fluorescent properties are strongly affected by binding in CDs [75]. The competitor was 1-anilinonaphthalene-8-sulfonic acid (1,8 ANS). The concentrations of modified CD and ANS are chosen such that most of the ANS is bound to the CD cup. Addition of the guest in µl quantities displaces ANS from the CD cup thus decreasing its fluorescence. The concentrations were $\sim 10^{-5}$ M ANS and $\sim 6 \times 10^{-5}$ M modified CD. It is important to note that these experiments were performed with the yttrium modified CDs so that there will not be any loss

of ANS fluorescence intensity by possible energy transfer processes from ANS to europium or terbium ions. In addition, all the solutions were made up in a buffer from acetic acid/sodium acetate in high purity water. An example of the changes in the ANS fluorescence upon addition of another guest is shown in Figure 22.

The Benesi–Hildebrand method was applied for the calculation of the association constant. Below is shown a typical case where an excess of cyclodextrin is added to a solution of fluorescent guest, the equilibrium described by eq 1,

$$G + CD \longrightarrow G \cdot CD \quad [CD]_t >> [G \cdot CD]$$
 (1)

The equilibrium constant for the above conditions is

$$K_{G \cdot CD} = \frac{[G \cdot CD]}{[G] \times [CD]} \cong \frac{[G \cdot CD]}{([G]_{t} - [G \cdot CD]) \times [CD]_{t}}$$
(2)

where
$$[CD] \cong [CD]_t$$
 (3)

and finally expressed as a function of [CD]_t by eq 4, as follows,

$$\frac{1}{[G^{\bullet}CD]} = \frac{1}{[G]_t} + \frac{1}{K \times [G]_t \times [CD]_t}$$
(4)

Given that,

 $F_{tot} = F_G + F_{G^*CD} = Q_{1^X}[G] + Q_{2^X}[G^*CD] = Q_{1^X}([G]_{t^-}[G^*CD]) + Q_{2^X}[G^*CD]$ where F = fluorescence intensity, Q = relevant quantum yield, the final expression for the observed ΔF as a function of the complex concentration is given by eq 5 below

$$\Delta F_{\text{obs}} = F_{\text{t}} - F_{\text{G} \cdot \text{CD}} (Q_2 - Q_1) \times [\text{G} \cdot \text{CD}]$$
 (5)

The observed change in fluorescence intensity ΔF_{obs} is proportional to the concentration of complex formed [G•CD], which in turn is correlated to

Figure 22. Emission spectra of 1,8 ANS with addition of pyridine as competitor for cyclodextrin binding.

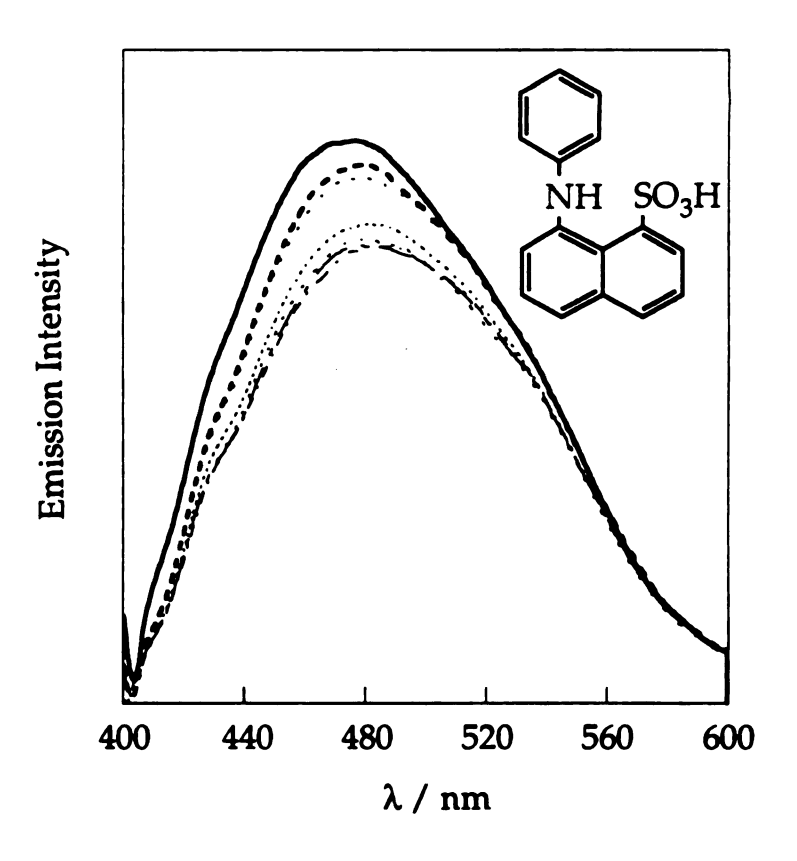


Figure 22

the association constant. A plot $1/\Delta F_{obs}$ versus $1/[CD]_t$ gives a straight line where intercept/slope will give $K_{G \bullet CD}$. The same principle was applied for the competitive binding technique. The only modification is keeping the guest whose association constant will be calculated in excess concentration; the competitor guest displaces ANS from the formed ANS•CD complex and the drop of the emission intensity of ANS is monitored as the concentration of guest increases.

8. Time–Resolved Luminescence Spectroscopy. A Nd:YAG pulsed laser system (λ_{exc} = 266 nm, fwhm = 8 ns) [76] was employed for lifetime measurements. The time–resolved response of luminescence was measured at the selected emission maximum of the most intense band for the lanthanides ($\lambda_{Eu(III)}$ = 616 nm and $\lambda_{Tb(III)}$ = 546 nm) with an R924 photomultiplier tube.

CHAPTER III

SWING CYCLODEXTRINS

A. Synthesis and Characterization

1. Background

Of the diverse molecular templates available for supramolecule design, cyclodextrins are well suited for functionalization with groups varying from alkyl chains to complex arms and macrocyclic receptors [56, 77]. A modification step, crucial for CD reactivity, is the selective monosubstitution of the primary rim which is highly dependent on reaction conditions. Derivatization requires the reaction to terminate after one of the primary hydroxyl groups has been substituted and before any of the secondary hydroxyl groups is modified. Although the synthetic schemes for modification are typical for carbohydrates, the purification and characterization of the products differ among reports in literature. A characteristic example is the tosylation of the primary hydroxyl groups to yield a key intermediate in cyclodextrin substitution chemistry. Various

synthetic procedures yield different numbers of substituents on the rim of the cup [59, 78]. Unfortunately, when the first procedures were reported, 2D–NMR spectroscopy, a main tool for the identification of the different derivatives, was not well developed. The similarity between the CD building blocks, the glucose units, engenders spectral complexity and overlap that can only be unraveled with high–field spectrometers and modern two–dimensional techniques to prove connectivities between protons [79]. Stoddart has elucidated cases of overmethylation of CD, which were not apparent with the conventional NMR techniques [80]. Consequently, many carbohydrate techniques for CD modification have been re-investigated in recent years.

Our interest in designing new photoactive supramolecular structures based on cyclodextrins led us to the synthesis of monofunctionalized CDs bearing a second recognition side for lanthanide ions. The flexible conformation of the resulting structure inspired the name of swing CDs. We have elaborated single substitution of monotosylated β -CD by the aza crown ether, triamine and tetraamine branches, and protection of one hydroxyl group with a new silyl-derived reagent for the subsequent methylation of the hydroxyl groups. In our work we have focused on the purification and detailed identification of each CD derivative by 2D-NMR since small impurities can drastically affect further luminescence properties.

Tosylated cyclodextrins have been used as precursors in aza crown functionalization since tosylate is a good leaving group for nucleophilic attack by substrates. The procedure by Matsui [59] (see Experimental

Section) gave in our hands the cleanest preparative method for the monosubstituted tosylate. The monosubstituted aza crown CD (designated as β -CD \cup 1aza) was obtained by elaborating Willner's procedure followed with new purification procedures developed to give the control of the photophysical properties needed in our studies.

The amine functionalization followed reports from different groups [60, 78b, 81]. The lanthanide ions were then coordinated to the swing amines or aza crown assemblies to yield new photoluminescent supramolecules. Considering Tabushi's results on flexibly capped amine cyclodextrins with Cu²⁺, Mg²⁺ and Zn²⁺ that exhibited high association towards anions with hydrophobic moieties [60], we expected similar behavior for the lanthanide cyclodextrins.

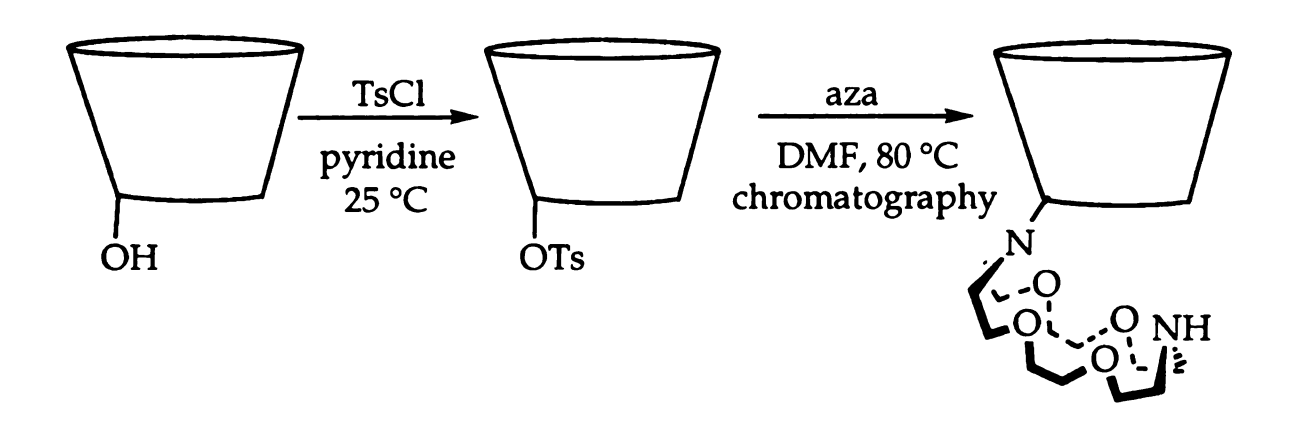
Photophysical studies of the lanthanide modified aza and amine CDs indicated that the OH environment of the CD rim quenches the lanthanide emission. Protection and subsequent methylation methodologies were developed to afford methylated swing CDs where the absence of hydroxyl groups on the primary side would enhance the lanthanide luminescence quantum yields. The methylation of cyclodextrins also facilitates the handling of these compounds by increasing their solubility in low boiling solvents such as chloroform and dichloromethane, as opposed to the usual higher boiling aprotic solvents such as dimethyl sulfoxide and dimethyl formamide. For purposes of producing monosubstituted swing CDs, we needed to protect one of the OH groups on the primary side and methylate the remaining OH functionalities. Most literature approaches employ trityl protection.

However trityl chloride is usually obtained in low purity and the procedure for mono-, di-, or tri- tritylation requires tedious chromatographic follow-ups [82]. For these reasons, silyl groups have recently become popular protecting functionalities for the hydroxyl groups in cyclodextrins. Specifically, chlorodimethylthexyl silane protects either just the seven primary hydroxyl groups or both the primary and secondary seven OH groups [83]. An earlier procedure used *tert*-butyldimethylsilyl chloride to functionalize either one or seven of the primary OH groups but the removal of the protecting group was not discussed [84]. Both procedures give high purity compounds and eliminate the need for chromatography. *Tert*-butyldiphenylsilyl chloride, used in the protection of non cyclic carbohydrates, proves to provide an excellent protecting group with greater stability towards acidic hydrogenolysis than the corresponding silyl and trityl ethers [85]. The (tert-Bu)SiPh₂ ethers have the advantage of permitting selective removal of trityl and acetal groups existing in the structure without being displaced. Finally, the tertbutyldiphenylsilyl group can be cleaved by treatment with tetra-n-butyl ammonium fluoride in THF or hydrolyzed in methanolic solution by HCl to regenerate the parent alcohol. For the advantages mentioned above we employed tert-butyldiphenylsilyl chloride for protection. A clean monosubstituted derivative of β -CD was obtained.

2. Results and Discussion

a. β -CD \cup ¹aza. The preparation of β -CD \cup ¹aza is accomplished by the reaction sequence shown below. We have found that proper function

of the supramolecular assembly as a photophysical template requires the careful separation and isolation of each intermediate as described in Chapter II.

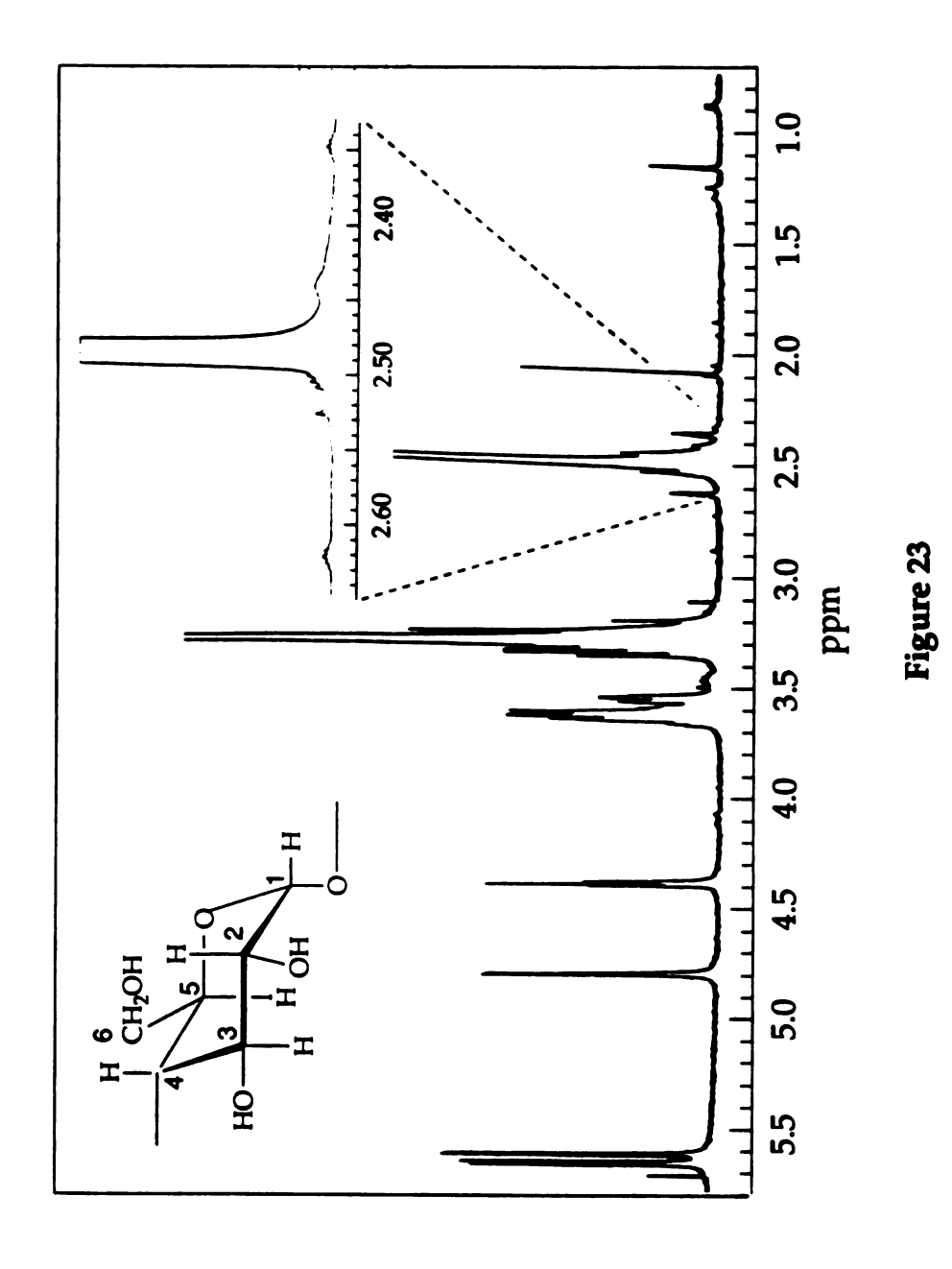


NMR spectroscopy was our main tool for the characterization [86]. The 1 H and 13 C NMR spectra of β -CD, β -CDO-Ts, and aza crown are shown in Appendix (Figures A1–A6). Extremely dry β -CD, β -CDO-Ts, β -CDU- 1 aza are established by the observation of a well-resolved triplet (δ = 4.42 ppm) and two doublets (δ = 5.64 and 5.68 ppm) for the primary and secondary hydroxyl proton resonances, respectively, in DMSO [87]. The presence of interfering trace solvents at the very least obscures these proton splittings and more usually causes the complete disappearance of the hydroxyl resonances. Furthermore, in the case of β -CDO-Ts, the high purity synthesis of the monotosylated compound is confirmed by observation of a 4:7 ratio of the aromatic protons of the tosylate to the anomeric H₁ signal of the cyclodextrin [88].

The monotosylate is substituted by aza to yield β -CD \cup ¹aza, but pure compound was obtained only when chromatography was employed.

Evidence of the product comes from the FABMS spectrum, which shows the molecular ion cluster at 1380 amu with a profile in accordance with the appropriate simulated isotope distribution (Figure A7). The loss of the aza-CH₂ in the FABMS is observed with a fragment centered at 1105 amu. Figure 23 shows the ¹H NMR spectrum of purified β-CD \cup ¹aza. The peaks at 4.8, 3.7-3.5, and 3.4-3.2 ppm have previously been assigned to the H₁, $H_{3.5,6.6}$, and $H_{2.4}$ proton resonances, respectively, of the glucopyranose ring (see insert for numbering scheme) [88]. A signature of the substitution is the appearance of the methylene protons of the aza attached to oxygens at 3.50 and 3.45 ppm (singlet and triplet), which can be observed only with the high resolution conditions of a 500 MHz instrument; at lower fields these resonances are obscured by the strong $H_{3.5.6.6}$ resonances of the glucose subunits of the cyclodextrin. The methylene protons a- to nitrogen are expected to shift upfield compared to their resonance in free aza (2.63 ppm) because of the conversion of the secondary amine to a tertiary amine upon reaction with the cyclodextrin. Consistent with this expectation is the appearance of a triplet at 2.51 ppm flanking the DMSO solvent peak (see inset of Figure 23). In addition, the $H_{6,6}$ resonance of the CD is expected to shift upfield upon substitution of the primary hydroxyl of the glucopyranose with nitrogen of the aza macrocycle. Obscured by the DMSO solvent peak, a resonance at 2.50 ppm is observed for D₂O solutions of the modified CD, which we tentatively assign to the $H_{6.6}$ resonance. These assignments are supported

Figure 23. The 500 MHz 1 H NMR spectrum of β-CD \cup 1aza in d⁶-DMSO. The inset spectrum displays an expanded region showing the triplet peak at 2.51 ppm flanking the DMSO solvent resonance; the numbering of the carbons of the glucose subunit is also depicted in an inset. See text for assignments.



by the two-dimensional ${}^{1}H^{-1}H$ COSY contour plot of β-CD \cup 1 aza (Figure 24). The coupling between H_{1} — H_{2} , H_{5} — H_{6} , H_{2} — H_{3} , H_{4} — H_{5} and H_{3} — H_{4} connectivities are easily distinguished from the cross-peak correlations. In addition, the triplet peak at 2.51 ppm displays a cross peak with the 3.5 ppm diagonal peak, which is expected from the coupling between the protons of the aza ligand. Further evidence for the swing came from total correlation spectroscopy (TOCSY) (Figure A8), which is ideal for carbohydrates since the magnetization transmission paths through bond and the coupling schemes are distinguishable. For the swing CD, the TOCSY spectrum is reported for comparison with the cradle compound (see Chapter IV).

Evidence for substitution at C_6 is supported by 13 C NMR. β - CD \cup 1aza (Figure A9) shows an upfield shift of one C_6 from 60 ppm for β - CD to 55 ppm for the aza substituted compound. This upfield shift is similar to that observed for primary hydroxyl substitution by alkylamines [78b, 88].

Although the tosylate is readily substituted by aza, as described by Willner and co-workers, our chromatographic separation scheme is essential to obtaining compound free of tosylated impurities. In addition to pure β -CD \cup 1aza, a substituted β -CD is isolated with a downfield shift of the aza methylene triplet resonance at 3.0 ppm. However this resonance is always accompanied by resonances from the phenyl ring of tosylate. In that the substitution of β -CD tosylate by aza produces p-toluenesulfonic acid, we believe that the fraction displaying the 2.8 ppm resonance is the tosylate salt of the protonated β -CD \cup 1aza supramolecule. In support of

Figure 24. The 300 MHz two-dimensional $^{1}H^{-1}H$ COSY contour plot of β -CD \cup 1 aza.

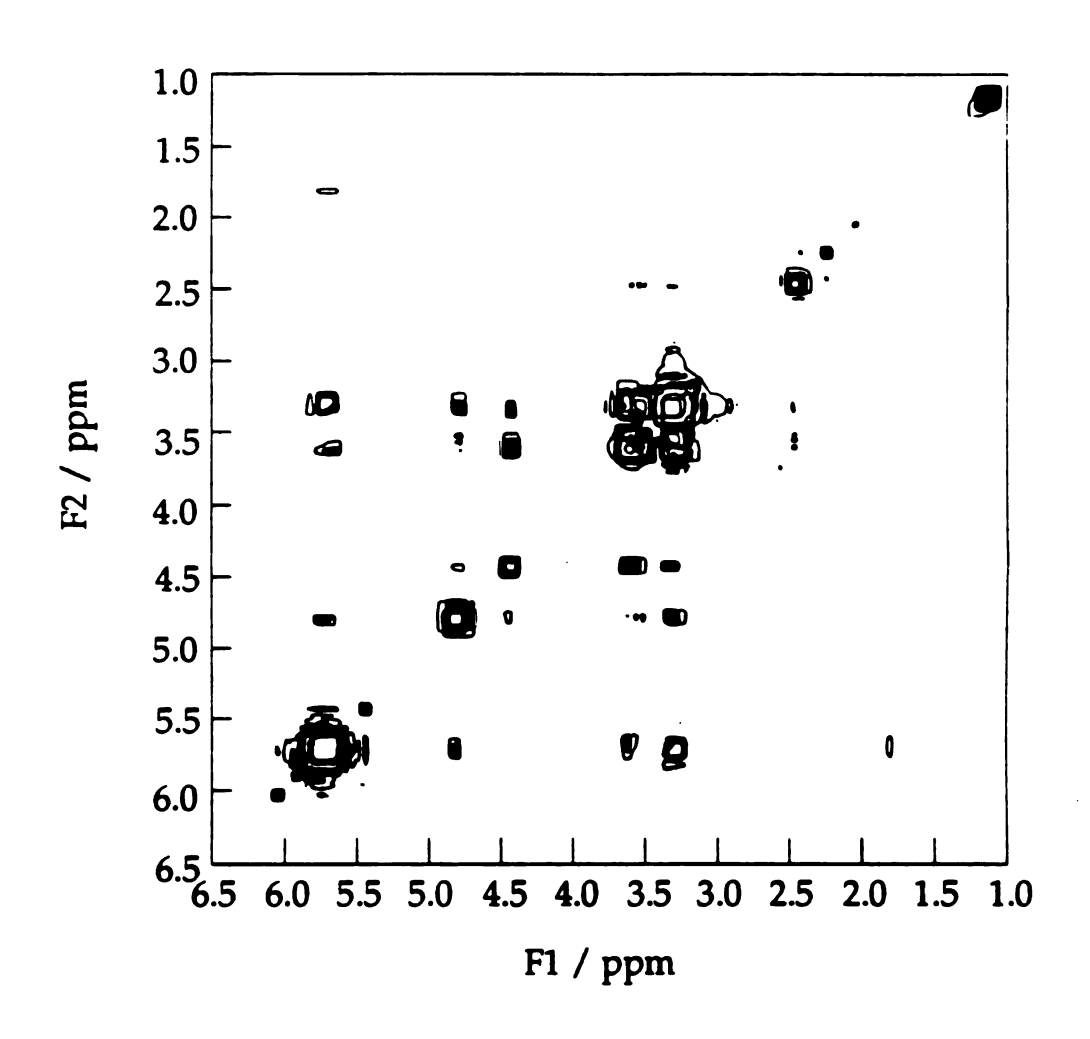
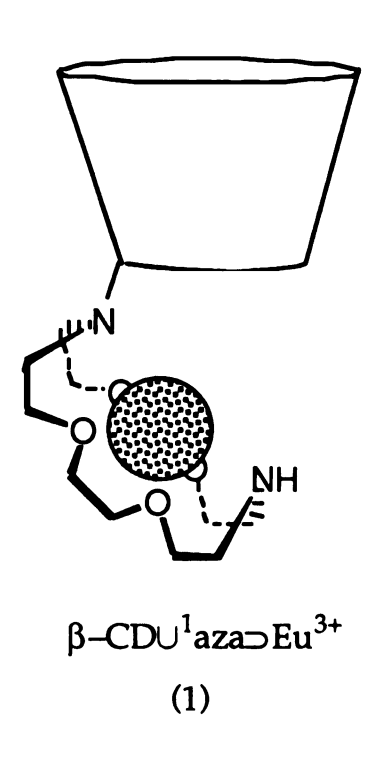


Figure 24

this contention are the following two observations: a downfield shift of the aza methylene resonances ($\delta = 2.6$ ppm to $\delta = 3.0$ ppm) occurs with protonation of the native aza amine by p-toluenesulfonic acid; and pure β -CD \cup 1aza can be recovered upon dissolution of the proposed β -CD \cup 1aza tosylate salt in basic aqueous solution with subsequent precipitation by tetrachloroethylene.

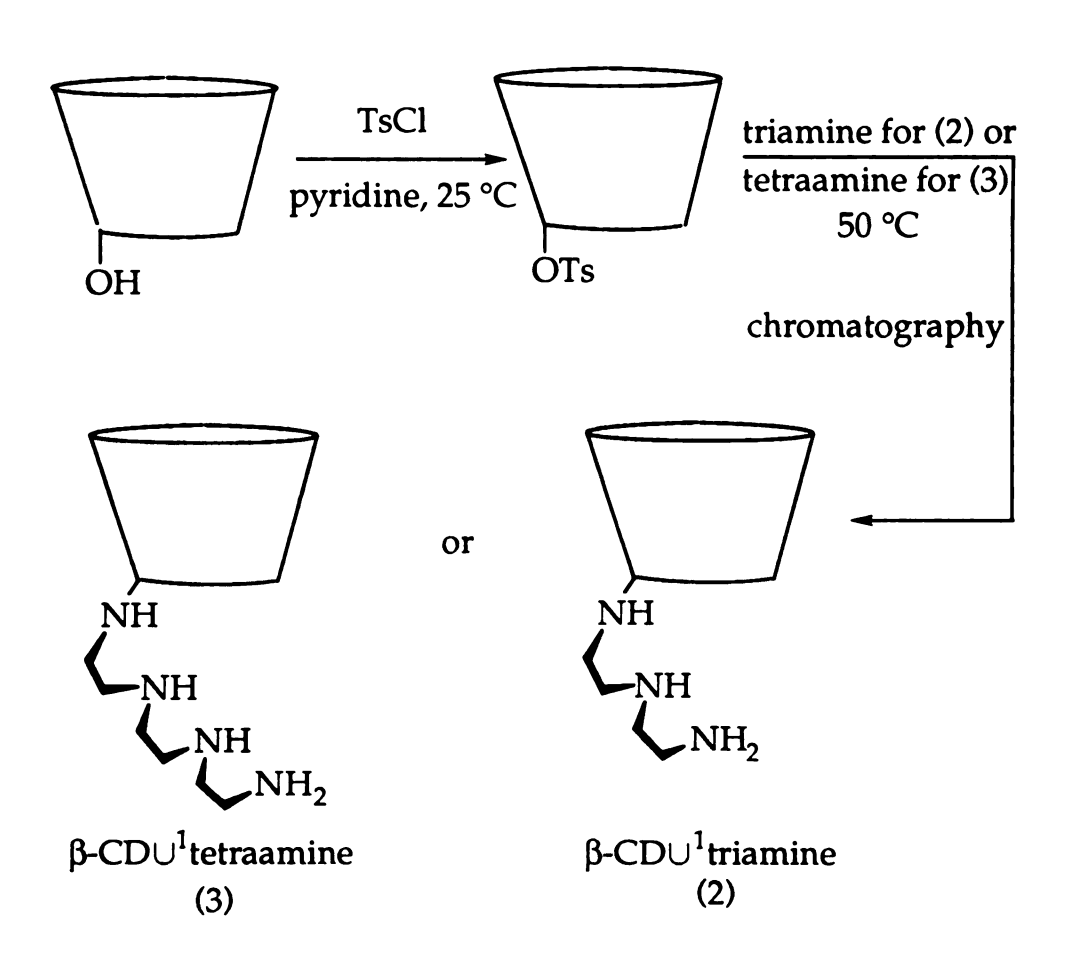
The introduction of Eu³⁺ and Tb³⁺ into the aza receptor site of β -CD proceeds with the methodologies established for the preparation of lanthanide ions encapsulated by crown and aza polycyclic ligands [41, 63].



Although residency of the lanthanide ion in the aza straps is established by the large and obvious paramagnetic shifts of the aza and β –CD proton resonances, the quantitative assignment of many of these resonances was frustrated by signal broadening coupled with the limited solubility of the compound such that only modest concentrations were attained for NMR

characterization. We were able to obtain good ${}^{1}H$ signals only for a very concentrated solution of $Eu^{3+} \subset aza$ in deuteurated nitromethane; the wide window spread spectrum is shown in Figure A10. Luminescence spectroscopy provides sufficient spectral sensitivity to monitor the incorporation of Eu^{3+} into the aza crown ether strap of β -CD \cup 1 aza, as will be discussed later in this Chapter.

b. β -CD \cup ¹triamine and β -CD \cup ¹tetraamine. We found the most effective substitution of tosylated CD by amines to proceed by Matsui's description. The synthetic scheme is shown below:



The isolated CDs were characterized by 1H NMR. Figure 25 shows the 300 MHz 1H NMR spectrum of β -CD \cup 1triamine in D $_2$ O/ d 6 -acetone. The CD proton manifold spans 3.4 to 4.2 ppm and only the anomeric protons distinctly appear at 5.1 ppm. Although the amine protons absorb in the region 2.8–3.3 ppm, their resonances are perturbed by the neat ligand (Figure A11). The difference in splitting in the overlapping region of the triamine CD compared with the β -CD can not be identified. Along with the ligand peaks, 1H phenyl resonances are also observed at 7.4 ppm and 7.7 ppm and methyl protons absorb at 2.2 and 2.3 ppm for the tosylate. As described for β -CD \cup 1aza, it is possible to isolate the tosylate salts of the amines. In the triamine case, the mono- or di- tosylate salt of the amine substituted CD is isolated. As observed in the β -CD \cup 1aza case an upfield shift of the amine methylenes (3.2 to 3.0 ppm) is found. Purification with tetrachloroethylene diminishes the tosylate peaks in the NMR, but the signal to noise ratio is small due to the lower solubility of the compound.

Similar results are obtained for β -CD \cup 1tetraamine. The ¹H NMR spectrum, shown in Figure 26, is characterized by amine methylene protons at 3.4–3.6 ppm. These resonances are accompanied by tosylate salt peaks. Coordination of Eu³⁺ to the amine swing was confirmed by excitation spectroscopy.

c. Protection of OH Group by ClSiPh₂(tert-Bu) and Methylation of the β -CDO-SiPh₂(tert-Bu). The monosubstitution of β -CD with tert-butyldiphenylsilyl chloride was successful using DMF as a solvent and

Figure 25. The 300 MHz 1H NMR spectrum of β -CD \cup 1triamine in D₂O/d⁶-acetone. Please note discontinuity in abscissa.

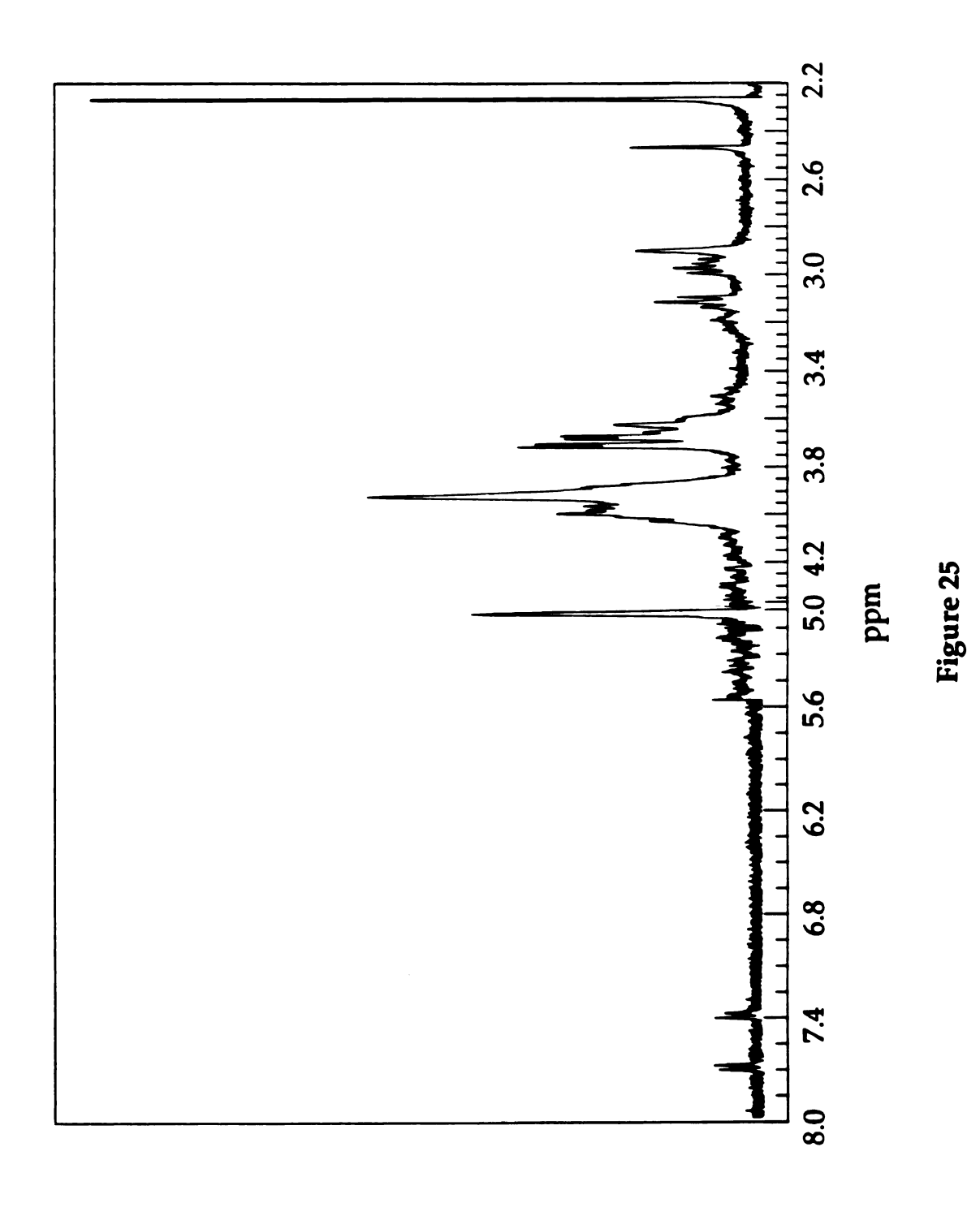
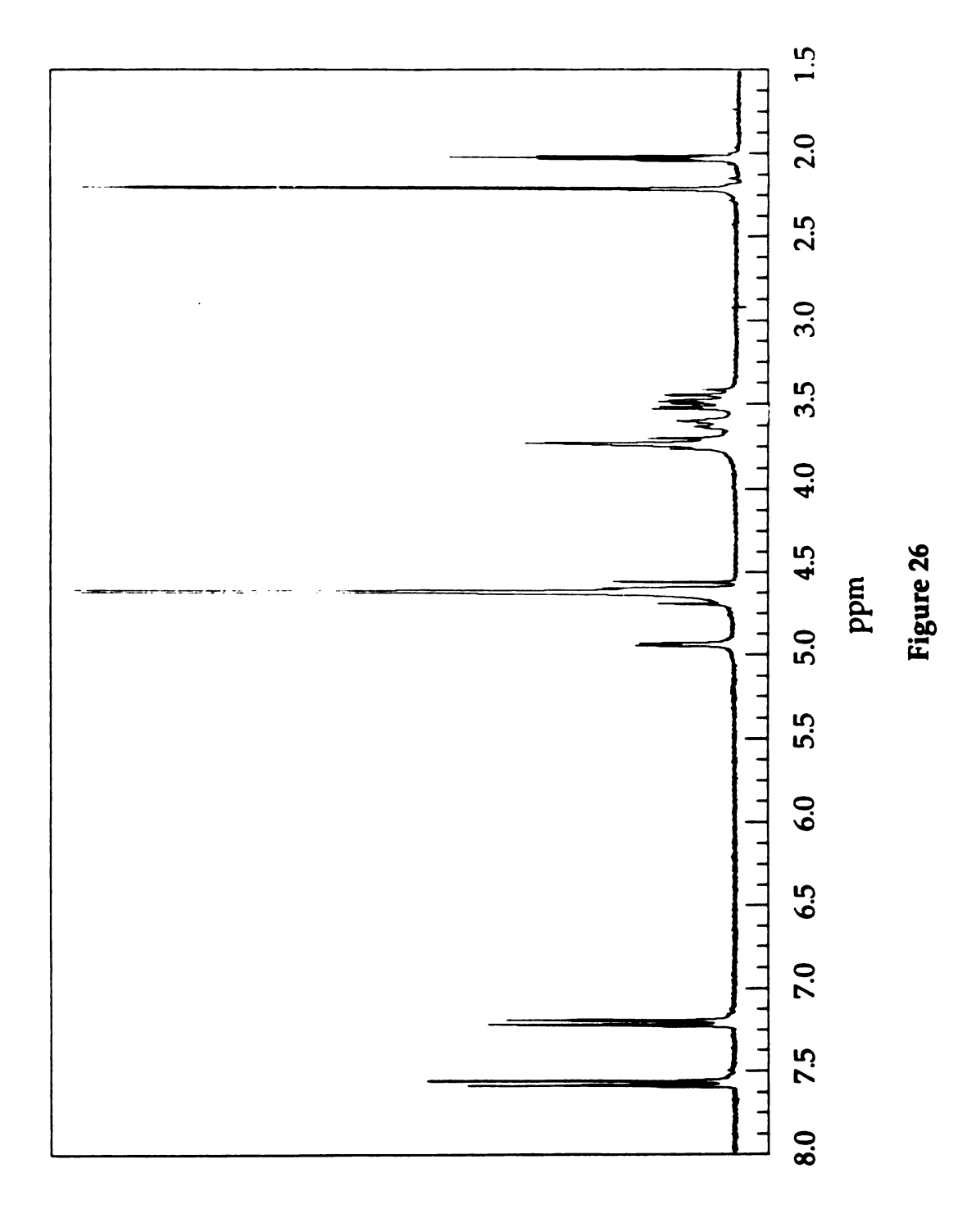


Figure 26. The 300 MHz 1H NMR spectrum of $\beta\text{-}CD\cup^1 tetraamine in <math display="inline">D_2O/d^6\text{-}acetone.$



imidazole as a catalyst. The 300 MHz 1 H NMR spectrum (Figure 27) of β -CD–SiPh₂(tert-Bu) shows the characteristic absorptions of the phenyl protons at 7.2–7.8 ppm and the methyl groups at 0.9–1.0 ppm. The cyclodextrin anomeric protons are split as in the monotosylated CD case. Their total integrated intensity compares with the intensity of the unreacted primary hydroxyl groups (7:6), confirming monosubstitution of one primary hydroxyl group. The 13 C NMR spectrum (Figure A12) shows CD peaks occur at 60, 72–74, 81, 102 ppm and the silyl chloride peaks at 28 and 128–136 ppm. The upfield shift of the C₆ of the CD is consistent with substitution. From these results we conclude that the cyclodextrin monoprotected by *tert*-butyldiphenyl silyl group (4), shown below, is a clean and reproducible intermediate.

The methylation is incomplete as determined by ¹H NMR (Figure 28). Specifically, four secondary hydroxyl groups at 5.8 ppm and four primary hydroxyl groups at 4.5 ppm indicate that methylation was unsuccessful.

Figure 27. The 300 MHz 1 H NMR spectrum of β-CDO–SiPh₂(tert-Bu)in d⁶-DMSO. Residual DMF peaks appear at 2.7, 2.9 and 7.9 ppm.

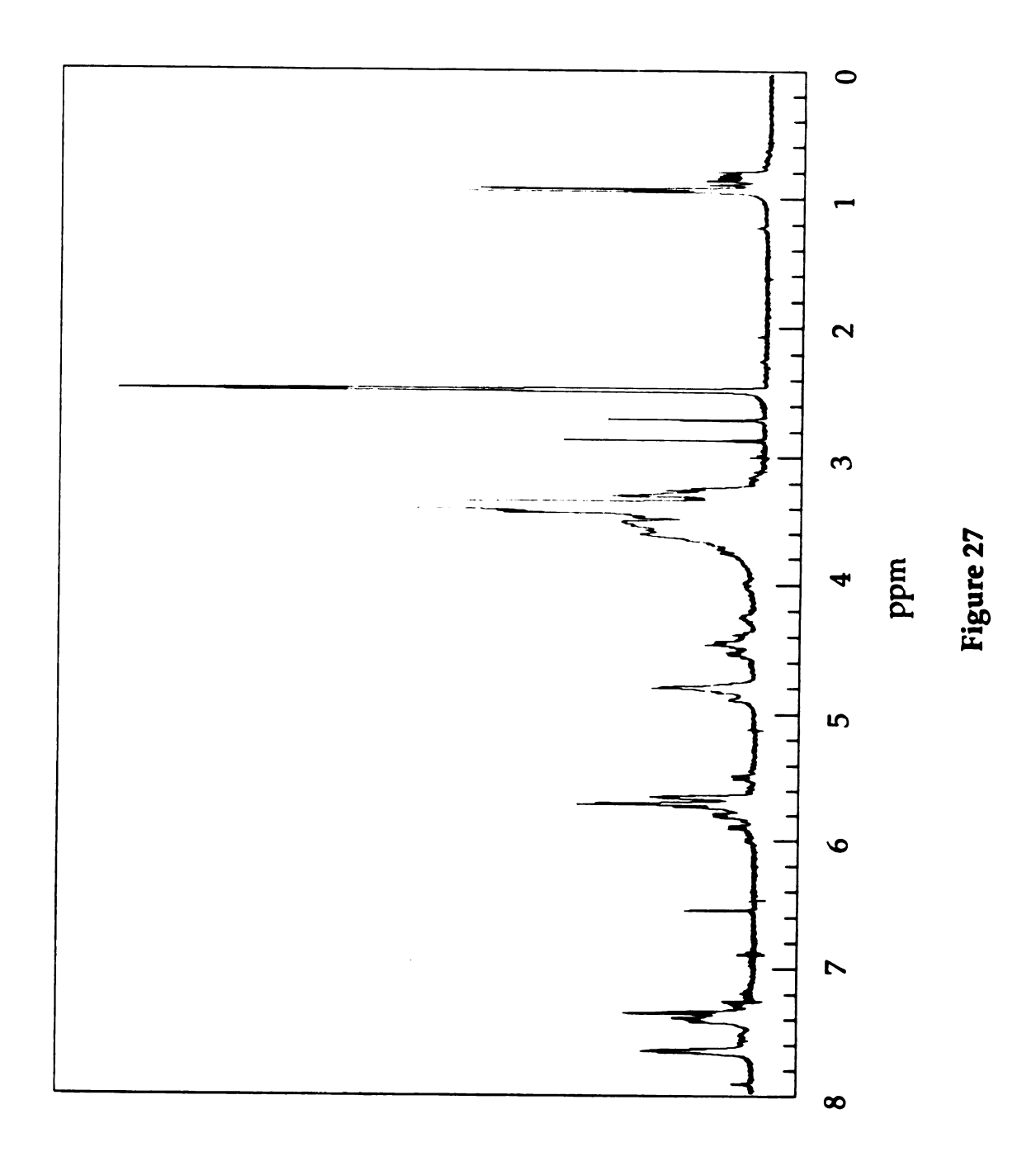
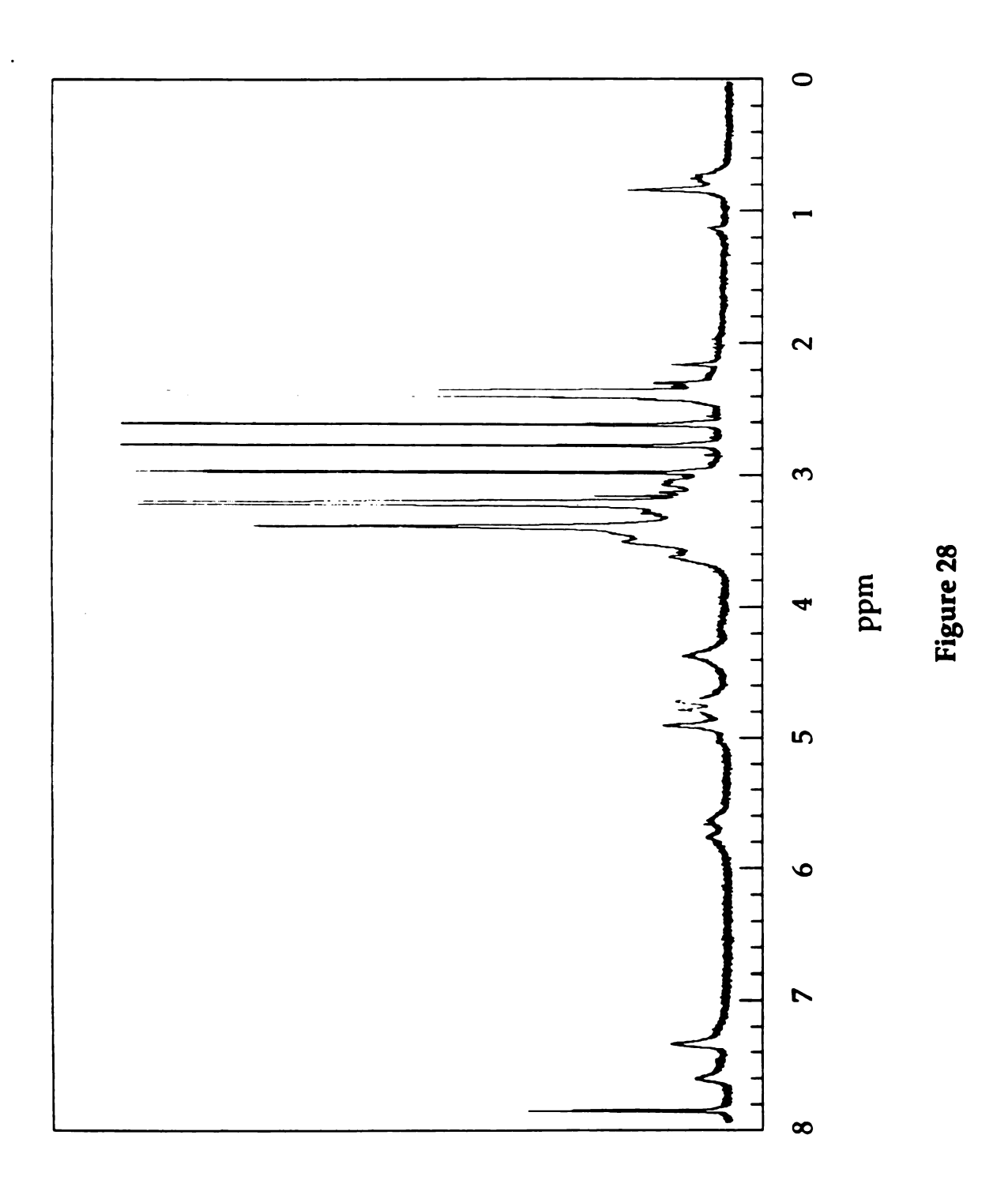


Figure 28. The 300 MHz 1 H NMR spectrum of β-CD-(OMe) $_{12}$ (OSiPh $_2$ (tert-Bu)) in d 6 -DMSO. Residual DMF peaks appear at 2.7, 2.9 and 7.9 ppm.



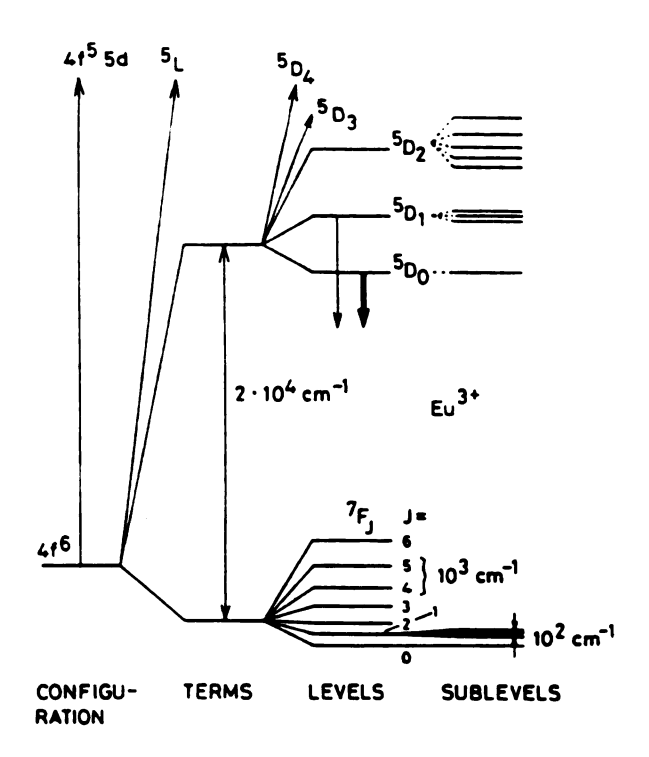
The reduced reactivity of the primary groups can be attributed to the bulkiness of our protecting group making it difficult for the methylating agent to access the hydroxyls. Complete methylation of this compound might be achieved with longer reactions times but unfortunately, we have not continued on this project.

B. Luminescence Spectroscopy

1. Background

Generally, europium(III) and terbium(III) complexes are signified by bright red and green luminescence, respectively, which originate from transitions between the lowest energy excited state, 5D_0 for Eu(III) or 5D_4 for Tb(III), to the 7F_J spin orbit manifold of the ground state. Partial energy level diagrams of Eu(III) and Tb(III) are shown in Figure 29 [40]. The $^4f^6$ and $^4f^8$ electronic configurations of Eu(III) and Tb(III) respectively give rise to terms split by electrostatic interaction (of the order of $^4D^4$ cm $^{-1}$) that are

Figure 29. Partial energy level diagrams of Eu(III) and Tb(III) emphasizing the splitting of 4f 6 and 4f 8 configurations.



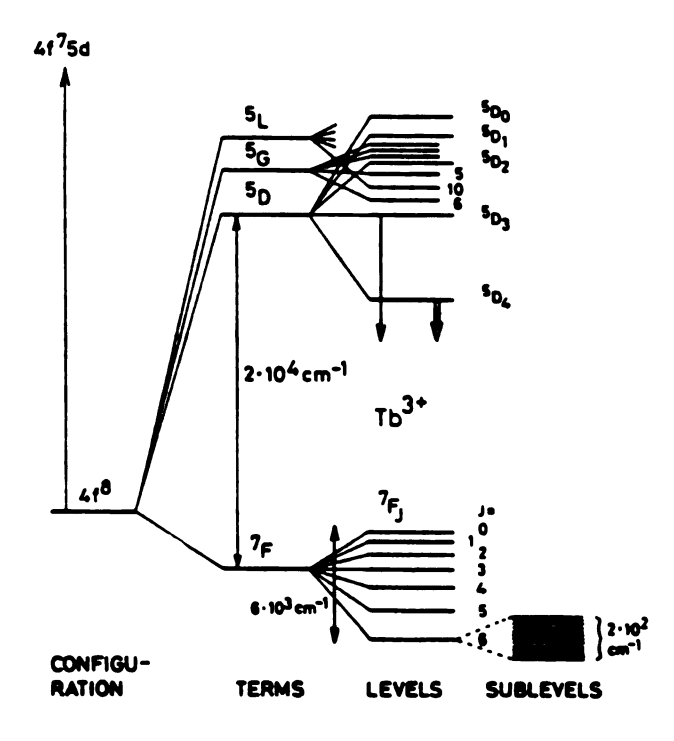


Figure 29

further split by spin orbit coupling $(10^{-3}~\text{cm}^{-1}~\text{splitting})$. The J levels are split by the ligand field to 2J+1 closely spaced components. Usually seven peaks are observed in Eu³+ luminescence spectra $(^5D_0 \rightarrow ^7F_0$ (580 nm), 7F_1 (592 nm), 7F_2 (616 nm), 7F_3 (650 nm), 7F_4 (700 nm), 7F_5 (750 nm), and 7F_6 (810 nm)), with the $^5D_0 \rightarrow ^7F_1$, 7F_2 and 7F_4 transitions accounting for over 95% of the emission intensity [89, 90, 91]. The Tb³+ emission consists of seven peaks ($^5D_4 \rightarrow ^7F_6$ (488 nm), 7F_5 (546 nm), 7F_4 (588 nm), 7F_3 (620 nm), 7F_2 (650 nm), 7F_1 (670 nm), and 7F_0 (680 nm)), with the first four transitions being the most intense [40, 89]. For a low resolution emission experiment, the splitting of the ligand field is not detected. Therefore any information as to the coordination environment of the lanthanides by emission spectroscopy is not obtained.

Excitation spectroscopy has also been used to elucidate the photophysics of lanthanide complexes [92]. Information regarding the transitions leading to the emissive excited states is revealed by scanning the absorption spectrum as a function of absorbing wavelength. Excitation spectra in europium complexes are particularly useful for revealing ligand to metal charge transfer transitions or ligand centered bands coupled to the lanthanide emissive level.

2. Results and Discussion

a. β -CD \cup 1aza \supset Eu³⁺. The spectroscopic properties of Eu³⁺ \subset aza provides the benchmark for the interpretation of the excitation spectrum of the β -CD \cup 1aza \supset Eu³⁺ supramolecular assembly [86]. Figure 30(a) displays the excitation spectrum of Eu³⁺ \subset aza obtained by monitoring the $^5D_0 \rightarrow ^7F_2$

Figure 30. Excitation spectra of (a) Eu³⁺ \subseteq aza and (b) β -CD \cup ¹aza \supset Eu³⁺ in CH₃CN monitored at λ_{em} = 616 nm.

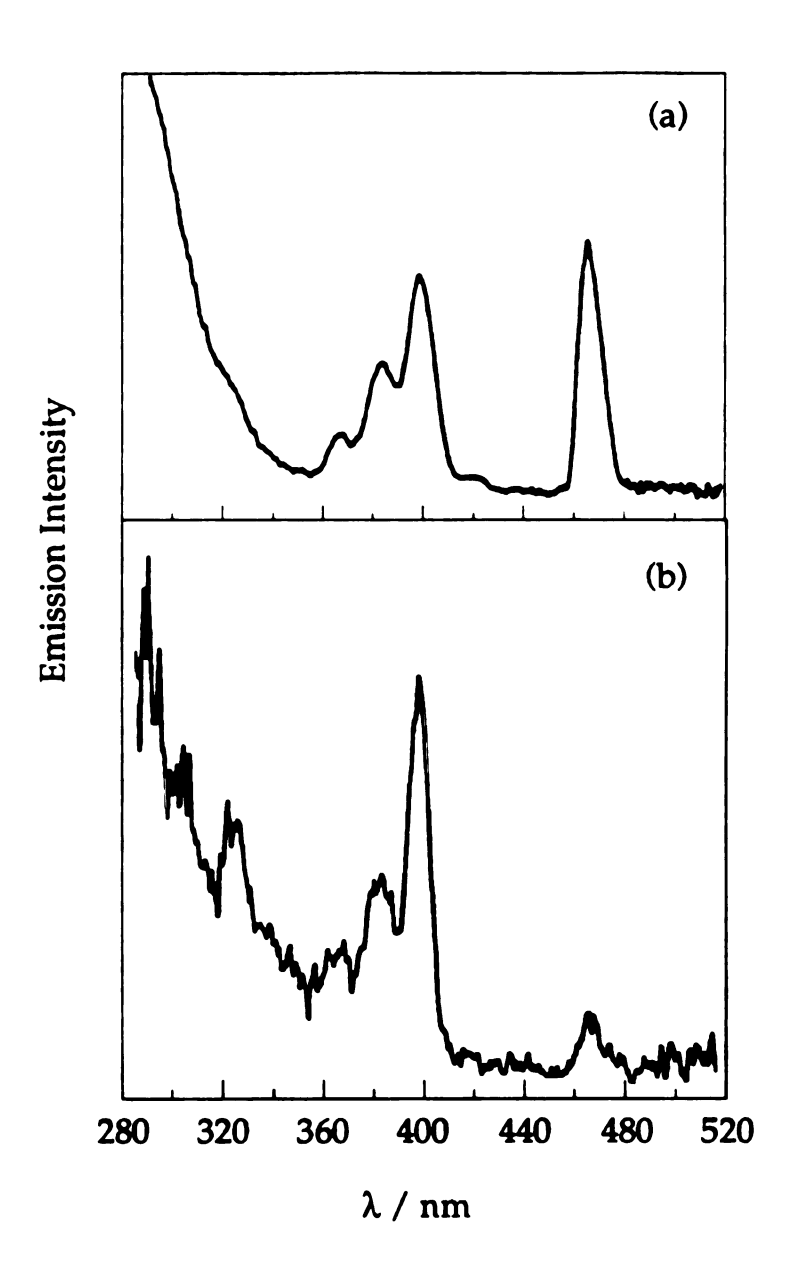


Figure 30

transition at 616 nm. The dominant ${}^5L_6 \leftarrow {}^7F_0$ and ${}^5D_2 \leftarrow {}^7F_0$ transitions, which also can be easily observed in the absorption spectra of solutions of the Eu³⁺⊂aza at modest concentrations, are in evidence at 394 and at 470 nm, respectively. Moreover the ultraviolet spectral region displays a broad and rising profile with increasing energy that is also observed in the absorption spectrum of this compound. A similar ultraviolet profile observed in the absorption and excitation spectra of Eu³⁺ \subset 2.2.1 has been assigned to a ligand-to-metal charge transfer transition from the nitrogens of the aza ligand to the Eu³⁺ center [41, 42]. Our observation of a parallel transition in Eu³⁺⊂aza is satisfying inasmuch as the skeletons of the aza and 2.2.1 ligands are comparable, with the former differing from the latter by only the absence of a diethyl ether strap. These unique spectral features in the Eu³⁺⊂aza excitation spectra are preserved in the spectrum of the product obtained from the reaction of Eu³⁺ with β -CD \cup 1aza. As shown in Figure 30(b), the ${}^5L_6 \leftarrow {}^7F_0$ and ${}^5D_2 \leftarrow {}^7F_0$ transitions of the Eu³⁺ ion and the LMCT excitation profile in the ultraviolet are both clearly apparent.

Red luminescence is observed from acetonitrile solutions of $Eu^{3+} \subset aza$ and $\beta - CD \cup {}^{1}aza \supset Eu^{3+}$ when excited at wavelengths coincident with the ${}^{5}L_{6} \leftarrow {}^{7}F_{0}$ transition ($\lambda_{exc} = 394$ nm). Steady-state luminescence spectra reveal the characteristic ${}^{5}D_{0} \rightarrow {}^{7}F_{J}$ pattern of Eu^{3+} compounds (Figure 31). Excitation into the LMCT transition at 313 nm shows the same emission pattern, which is consistent with observations of energy transfer from the ligand to the ${}^{5}D_{0}$ state of the lanthanide ion for compounds in solution and the solid state [41c].

Figure 31. Emission spectrum of Eu(NO₃)₃ in CH₃CN (λ_{exc} = 394 nm).

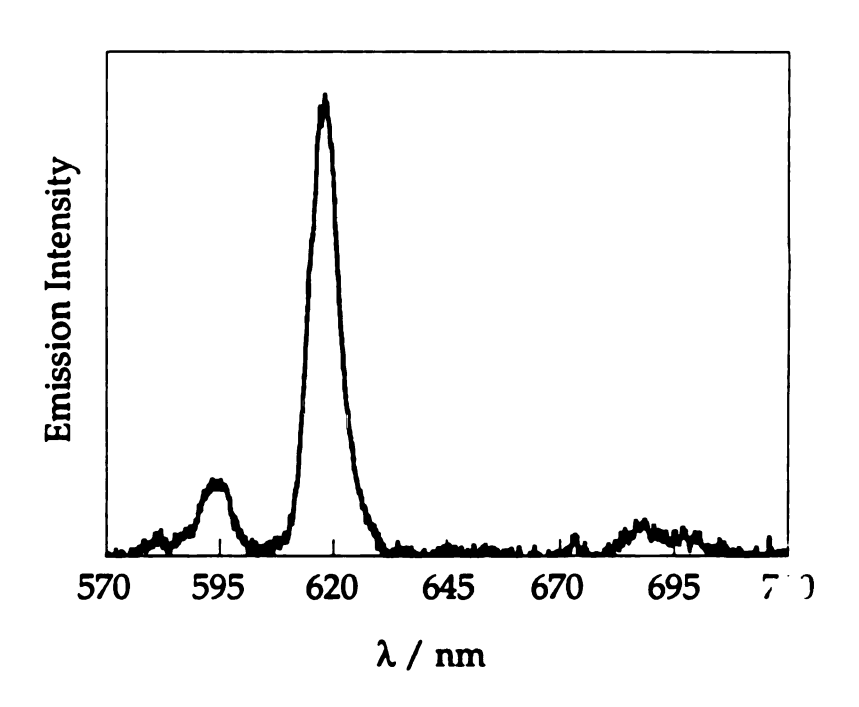


Figure 31

- b. β-CD \cup ¹aza \supset Tb³⁺. The ligand to metal charge transfer transition of this complex is not observable in the excitation spectrum at low energies because Tb³⁺ is very difficult to reduce (E⁰(Tb^{3+/2+}) = -3.7 V vs NHE for the aquo ion) whereas for Eu³⁺ this is not the case (E⁰(Eu^{3+/2+}) = -0.38 V for the aquo ion) [89]. Since the coordination properties of the two ions are very similar, we expect that the incorporation of Tb³⁺ in the aza crown moiety takes place. This is supported by the emission spectrum of the complex, which shows the characteristic Tb³⁺ luminescence pattern (Figure 32). Furthermore, evidence of coordination is demonstrated by the energy transfer experiments described later in this Chapter.
- Amine Complexes with Eu³⁺. The excitation spectra of Eu³⁺(triamine)₂(NO₃)₃ and Eu³⁺(tetraamine)₂(NO₃)₃ reveal a strong peak at 270 nm (Figure 33). We attribute this band to the expected charge transfer from the amine groups to the Eu³⁺. This is in agreement with the charge transfer transition assignment, from tertiary nitrogens to Eu³⁺, in the cryptate complexes [41]. Moreover the same band is shown in the excitation spectrum of the β -CD \cup ¹triamine complex with Eu(III) thereby excluding any coordination of the hydroxyl groups to the ion, which would contribute to a blue-shifted charge transfer band. We do not know the stoichiometry of the complex (one or two modified CDs per ion) since we do not have elemental analysis results. However, there is good possibility that Eu(III) is coordinated by two amine branches. A complex of two diethyl amine functionalized CDs with one Cu(II) ion has also been reported by Matsui [93]. All experiments of the Eu(III) CD-amines were performed in acetonitrile since their high basicity causes hydrolysis of the

Figure 32. Emission spectrum of TbCl₃ in CH₃CN (λ_{exc} = 313 nm).

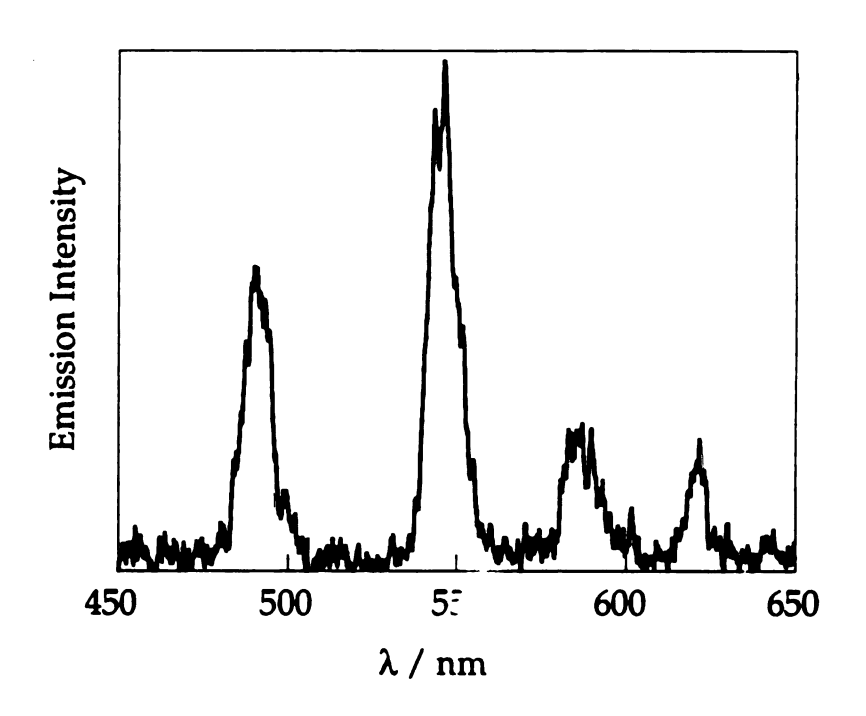


Figure 32

Figure 33. Excitation spectrum of $Eu^{3+}(triamine)_2(NO_3)_3$ in CH_3CN monitored at $\lambda_{em} = 616$ nm, representative for the Eu(III) amine complexes.

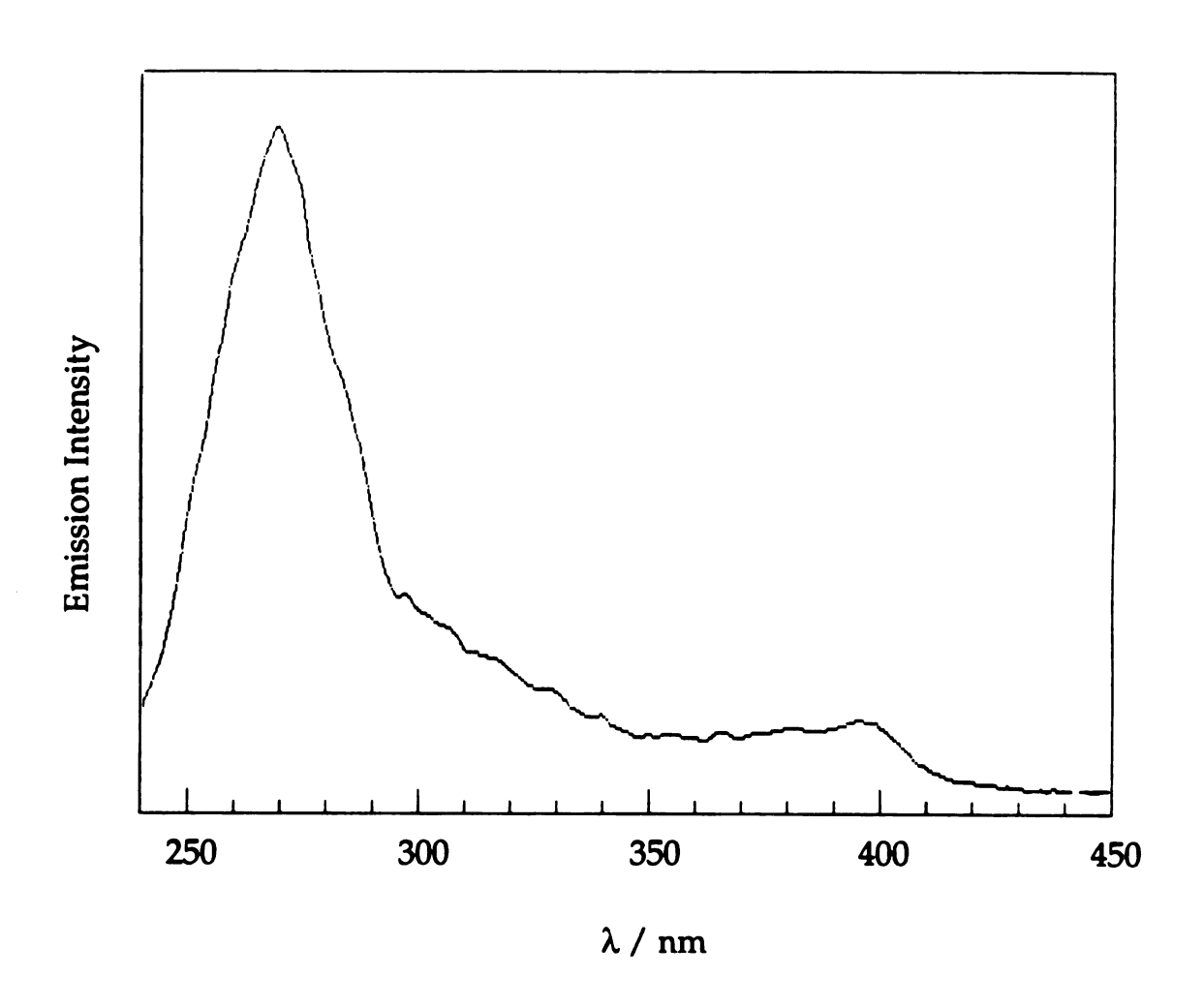


Figure 33

ion to hydroxides. Any attempt to protonate the amines and dissolve the compounds in water was unsuccessful thus eliminating energy transfer experiments.

C. Inclusion Complexes of β -CD \cup ¹aza \supset Ln³⁺

1. Background

The swing CDs provide a hydrophobic microenvironment for aromatic guest association and the ionophoric moiety for lanthanide binding thus juxtaposing an energy donor and acceptor. To this end, their design is ideal for the study of absorption-energy transfer-emission (AETE) mechanism within a supramolecular structure. The energy donor can be chosen with only the requirement that it should be a light-harvester and should incorporate in the CD cavity. In the following studies, we selected two types of light harvesting guests: those only recognized by the CD cavity and those recognized by the cavity and the lanthanide center. As we show, the lanthanide luminescence is affected by the association strength of the different guests in the supramolecular structure, and the electronic characteristics of the guests.

These studies greatly expand investigations of energy transfer within CD assemblies. Energy transfer within a modified cyclodextrin was first reported by Tabushi [54e]. A benzophenone rigidly capped modified CD was the energy donor and the included guest, 1-bromonaphthalene, the energy acceptor. Organic systems developed later were concerned mainly with excimer formation within the CD as discussed in Chapter I.

2. Results and Discussion

Association of Guests. The association constants of 1,8-ANS a. and various light-harvesting guests (LHGs) with β -CD and the β - $CD \cup {}^{1}aza \supset Y^{3+}(NO_{3})_{3}$ are shown in Table 1. They were determined by monitoring the fluorescence of 1,8-ANS (which is a competitor guest for LHGs binding), employing Benesi – Hilderbrand method as described in Chapter II. In order to avoid the complications of fluorescence quenching of 1,8-ANS by Eu³⁺, association constants of the supramolecular assembly were measured by using β -CD \cup ¹aza \supset Y³⁺. The Y³⁺ ion is similar size and has the same charge as Eu³⁺, but it is redox inactive and does not possess low energy excited states; thus electron or energy transfer quenching of 1,8-ANS is not observed, thereby simplifying competition fluorescence measurements. Inasmuch as 1,8-ANS and Bz can not directly interact with the metal ion (sulfonates are poor ligands of metal ions), differences in their binding to the unmodified and modified β -CDs are attributed to the proximity of the metal cation to the hydrophobic binding site of the cup. The more polar environment created by the introduction of the ionic metal-aza crown at the bottom of the CD cup presumably assists in the binding of the polar 1,8-ANS, as opposed to the apolar benzene, which exhibits a lower binding constant than observed for β -CD.

Whereas the binding constants of Bz in β -CD and the swing β -CD are comparable, BzA and PcA show much higher association with the β -CD supramolecule. Of course for these latter guests, molecular recognition does not occur only by hydrophobic binding within the CD cup, but is further assisted by the propensity of the carboxylate functionality to ligate

Table 1. Association constants (M^{-1}) of various light–harvesting guests with β -CD and β -CD \cup ¹aza \supset Y³⁺ hosts

Guest	K _a (β-CD)	$K_a(\beta\text{-}CD\cup^1 aza\supset Y^{3+})$
1,8-ANS	24ª	170
Benzene (Bz)	196 ^b	117
Pyridine (Py)	-	1,047
Benzoic Acid (BzA)	546 ^{c,d} , 36 ^{c,e}	36,000
Picolinic Acid (PcA)	1,370 ^d	43,000
2-Naphthoic Acid (2-NA)	-	52,570
2-Naphthyl Acetic Acid (2-CH ₂ NA)	_	83,345

^aref [60]. ^bHoshino M.; Imamura M.; Ikehara K.; Hama V. J. Phys. Chem.

1981, 85, 1820. ^cGelb R.; Schwartz L. M. J. Incl. Phenom. Mol. Recog. 1989, 7,

465. ^dprotonated. ^e deprotonated.

metal ions. Enhanced molecular recognition of anionic guests by modified CDs featuring a metal ion juxtaposed to the CD's hydrophobic cup has been observed previously [5b, 57, 60]. It is noteworthy that PcA binds β - $CD \cup {}^{1}aza \supset Y^{3+}$ more strongly than BA. The increased binding might be a result of the nitrogen coordinating to the lanthanide ion or an effect due to a stronger metal-carboxylate interaction of the more basic PcA (pKa for PcA is 5.4 towards 4.5 for BzA) [94]. The latter seems more reasonable in light of our results for pyridine binding. Pyridine (Py) binds the swing CD stronger than benzene as expected from the polarity of nitrogen, which also confers orientation to pyridine within the CD cup [48b]. Moreover, we measured the binding constants of 2-naphthoic acid (2-NA) and 2naphthylacetic acid (2-CH₂NA). Their association is of the same order of magnitude and greater than pyridine, which is attributed to the increased basicity of the carboxylate. In addition the naphthyl ring is expected to have a tighter fit in the CD cavity, thus contributing to higher binding constants than benzene or pyridine rings. In addition for the polar guests, Ueno and Toda's explanation of the higher association constants in charged-modified cyclodextrin [95] may be operative. When cyclodextrin is functionalized with a positive charge on the primary side, the electrostatic potential gradient inside the cavity is enlarged resulting in a stronger polar interaction with the polar guest.

b. AETE Studies for Various LHGs.

i. Benzene. Figure 34 displays the dependence of the integrated emission intensity from D_2O solutions of $Eu^{3+} \subset aza$ and β - $CD \cup ^1 aza \supset Eu^{3+}$ compounds on the concentration of added benzene. In the

Figure 34. Dependence of the emission intensity from D_2O solutions of Eu^{3+} caza and β -CD \cup^1 aza $\supset Eu^{3+}$ upon addition of benzene (λ_{exc} = 254 nm). Concentrations of the lumophore are 2.5×10^{-4} M.

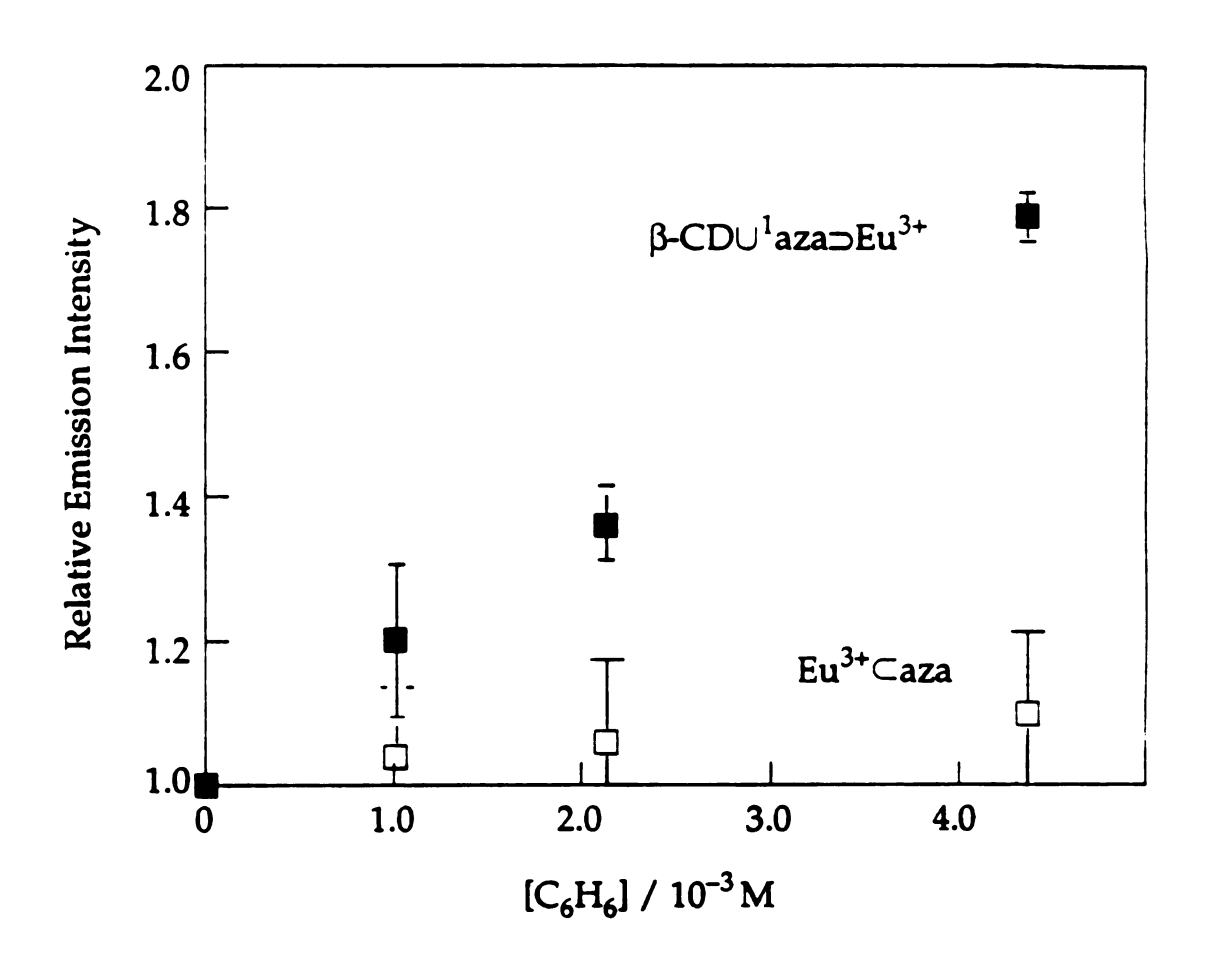


Figure 34

case of the former compound, the relative luminescence intensity increases marginally for concentrations of benzene as high as 5×10^{-3} M. Inasmuch as benzene can not ligate the Eu³⁺Caza ion, energy transfer is restricted to an inefficient bimolecular process. In comparison the relative luminescence intensity of the β -CD \cup ¹aza \supset Eu³⁺ supramolecule increases markedly over this same concentration range. In light of the affinity of benzene for the hydrophobic cavity of cyclodextrin ($K_{assoc.} = 117 \text{ M}^{-1}$), we attribute this enhancement of the emission intensity to the unimolecular AETE process involving benzene as the energy donor and Eu³⁺ ion as the energy acceptor. A noteworthy observation is that H₂O effectively quenches the luminescence of the benzene-associated supramolecular assembly. A similar result is observed for the Eu³⁺ Caza complex, which displays an emission quantum yield in D₂O that is attenuated by 75% when dissolved in H₂O. These results are not surprising inasmuch as the high frequency O-H vibrations of coordinated water molecules result in efficient nonradiative decay of lanthanide emission. Conversely, Eu³⁺ \subseteq 2.2.1 is less susceptible to quenching by H₂O ($\phi_e(H_2O)$ is 25% that of $\phi_e(D_2O)$ for 5D_0 luminescence upon 5L_6 excitation). Presumably the additional diethyl ether arm of the 2.2.1 cage as compared to aza effectively shields the ion from H₂O. For the case of the β -CD \cup ¹aza \supset Eu³⁺ assembly, if the aza ligand was cradled below the cup, then its conformation would be akin to the Eu³⁺ \subset 2.2.1 complex inasmuch as the CD cup will cover the open face of the Eu³⁺ ion in place of the diethyl ether arm of 2.2.1. Thus we believe that the β -CD \cup ¹aza \supset Eu³⁺ compound would be only marginally affected by H₂O in a conformation with the aza

tethered below the cup. However this is not the case and indeed the H_2O quenching effect of β -CD \cup 1aza \supset Eu³⁺ parallels that of Eu³⁺ \subset aza. These results suggest that the aza ligand is swung away from the base of the CD cup. In such a swing conformation, the Eu³⁺ ion is accessible to coordination by H_2O , and therefore its emission will be quenched.

ii. Benzoic and Picolinic Acids. Figure 35 displays the dependence of the integrated emission intensity from D_2O solutions of the β-CD U^1 azaDEu U^3 + supramolecule on the concentration of light-harvesting guest. For comparison the relative luminescence intensity for Bz is also shown. The range of concentration is 10^2 less for BzA and PcA when they trigger comparable Eu U^3 + luminescence. This increase in the detection limit parallels the increase in the association constant of the carboxylates with the CD supramolecule. Moreover, as discussed above, the unimolecular AETE process takes place from benzene to an azaDEu U^3 + that is swung away from the base of the CD cup. Such a swing conformation is undesirable to AETE because the distance for energy transfer is not optimally short (energy transfer exhibits a $1/r^6$ (Förster) or U^3 (Dexter) distance dependence). For the cases of BzA and PcA, the coordination of guest to the Eu U^3 + ion will shorten the distance for energy transfer leading to increased emission enhancements.

A characteristic of the plots in Figure 35 is a saturation plateau. This limit is clearly shown in the acids case but not in benzene due to the low signal/noise ratio. These results contrast with the Eu³+⊂aza case which shows only a linear dependence of the luminescence intensity on the concentration of light-harvester. This is attributed to a binding constant

Figure 35. Relative emission intensity from D_2O solutions of β- $CD\cup^1$ aza $\supset Eu^{3+}$ upon addition of light harvesting guests (λ_{exc} = 254 nm for PcA, Bz and 280 nm for BzA). Please note abscissa discontinuity. Concentrations of the lumophore are 5.8×10^{-4} M for BzA and PcA and 2.5×10^{-4} M for Bz.

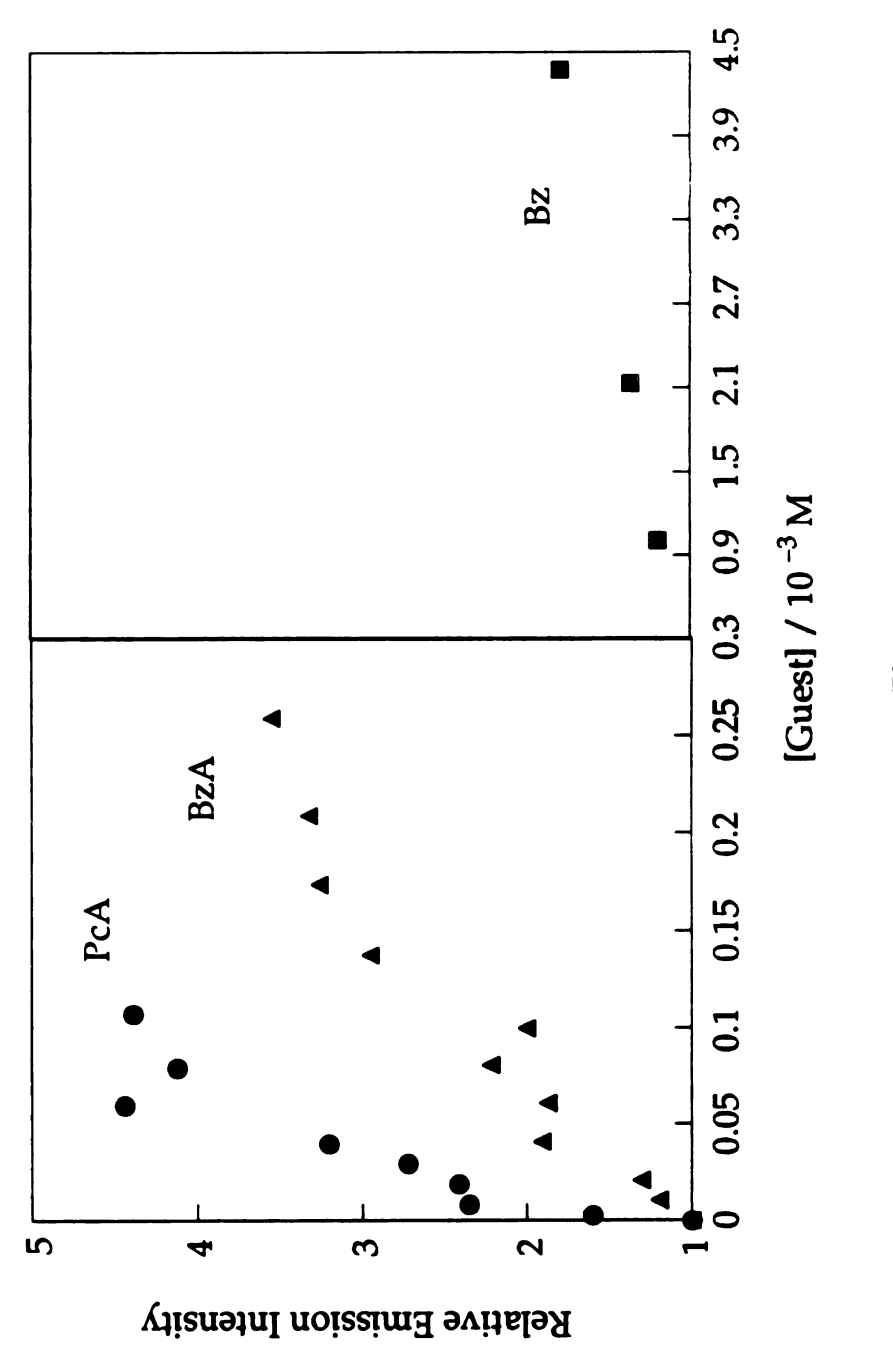


Figure 35

effect. The expected small association constants for binding of the acid to the crown do not permit high complex concentrations to be formed whereas for CD supramolecules they are easily achieved in slight excess of the guest thus allowing observation of the saturation of the complex property studied. These results are in agreement with the result of a recent study on intramolecular electron transfer within a cyclodextrin [96]. Stern-Volmer plots also show saturation when the intramolecular transfer occurs from the appended donor to the acceptor guest, but they are linear when the acceptor does not bind in the CD and electron transfer is limited to the bimolecular component. Finally, in some cases the intensity increases upon further addition of acid. This is observed when BzA is added to β - $CD \cup {}^{1}aza \supset Tb^{3+}$ (Figure 36). This can be attributed to the binding of a second molecule of BzA to the Tb³⁺, most probably from the outside of the swing. The possibility for excimer formation is excluded, since no fluorescence attributed to BzA excimer is detected. The excitation spectrum of β -CD \cup ¹aza \supset Tb³⁺ including BzA (Figure 37) reveals the characteristic benzoic acid absorption thus demonstrating the energy transfer from the acid to Tb³⁺ ion.

It is interesting that the terbium complex exhibits higher luminescence as compared with the europium, even though both assemblies exhibit the same association constant for BzA. This is consistent with lanthanide photophysics. Europium compounds have additional deactivation mechanisms owing to low energy charge transfer states, which siphon the energy from the donor before it is channeled to the emissive level.

Figure 36. Dependence of the emission intensity from D_2O solutions of β- $CD\cup^1$ aza $\supset Tb^{3+}$ upon addition of benzoic acid ($\lambda_{exc}=280$ nm). Concentration of the lumophore is 5.4×10^{-4} M.

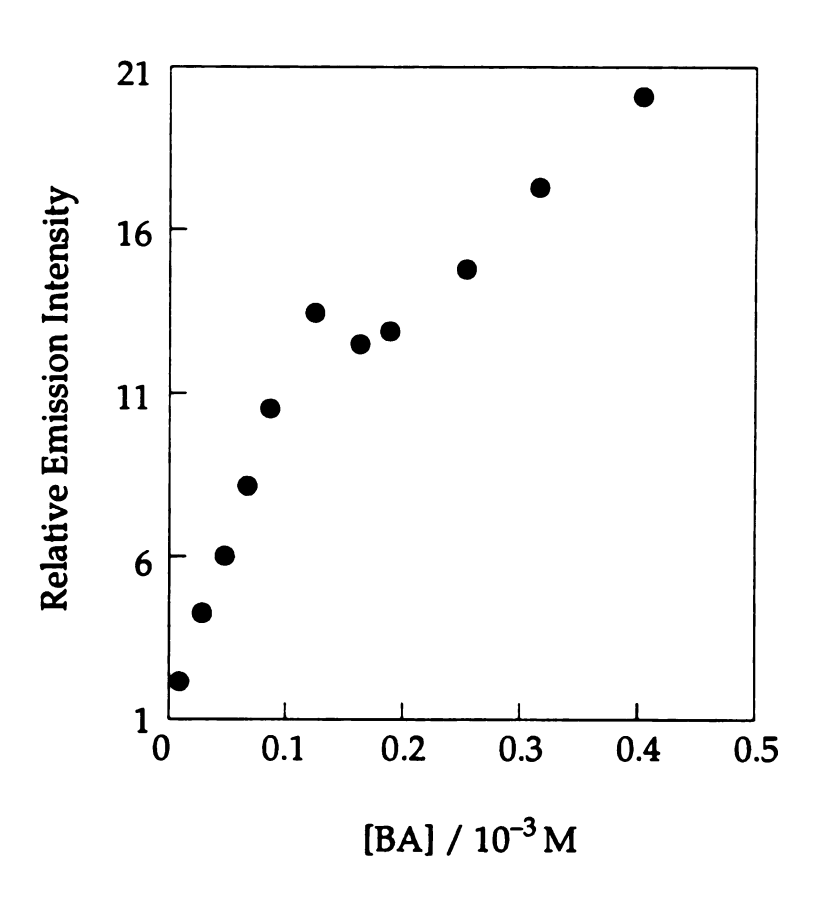


Figure 36

Figure 37. Excitation spectrum of β -CD \cup 1aza \supset Tb³⁺ including benzoic acid monitored at λ_{em} = 546 nm.

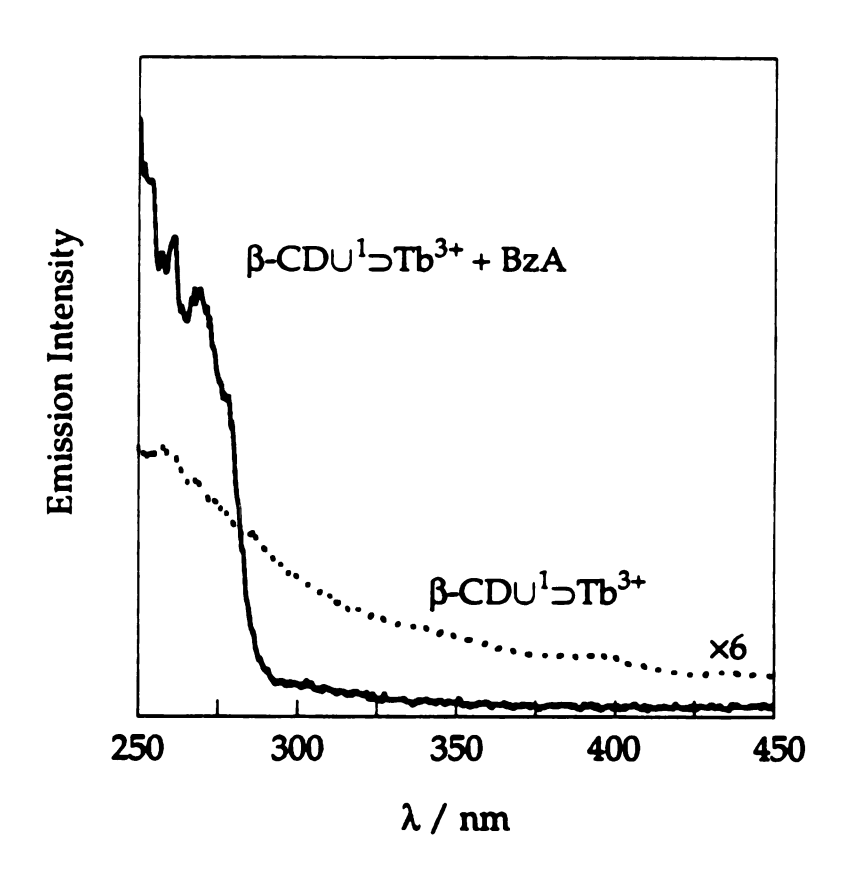


Figure 37

iii. Other Guests. Consistent with benzene, only a small increase of the luminescence intensity of β -CD \cup ¹aza \supset Eu³⁺ is observed upon pyridine addition (Figure 38). This confirms our suspicion that pyridine does not coordinate strongly to the lanthanide ion. If it did, we would expect a shortened distance for energy transfer and luminescent intensities comparable to the carboxylates.

Figure 39 shows the effect of 2-NA and 2-CH₂NA in β -CD \cup 1aza \supset Eu³⁺ luminescence. In order to evaluate the effect of the methylene spacer we performed the same experiment with Eu(NO₃)₃ as the acceptor (Figure 40). The latter case shows a significant decrease with the addition of a methylene bridge as expected from an exponential dependence of the distance (a factor of four on the exponential term when one more C–C bond is considered). For the swing CD the 2-NA triggers higher luminescence from the Eu(III) ion but the distance effect is not observed to be as great due to a higher association constant of 2-CH₂NA. This finding suggests that an appropriate choice of LHG may induce unexpected photophysical behavior as a result of better binding properties.

Finally, more efficient energy transfer appears from a solution of 10 % CH₃CN in D₂O in place of neat D₂O (Figure 41). The enhancement of Eu(III) luminescence in β -CD \cup ¹aza \supset Eu³⁺ with BzA as the light harvester can be attributed to a higher binding constant of the assembly formed with acetonitrile and BzA included in the cavity.

Summarizing, we observed that inclusion of guests within the cup triggers luminescence from the Ln³⁺ center by AETE. The most efficient AETE process results when hydrophobic recognition of the guest by the

Figure 38. Relative emission intensity from D_2O solutions of β - $CD\cup^1$ aza $\supset Eu^{3+}$ upon addition of pyridine ($\lambda_{exc}=313$ nm). Concentration of the lumophore is 3.0×10^{-4} M.

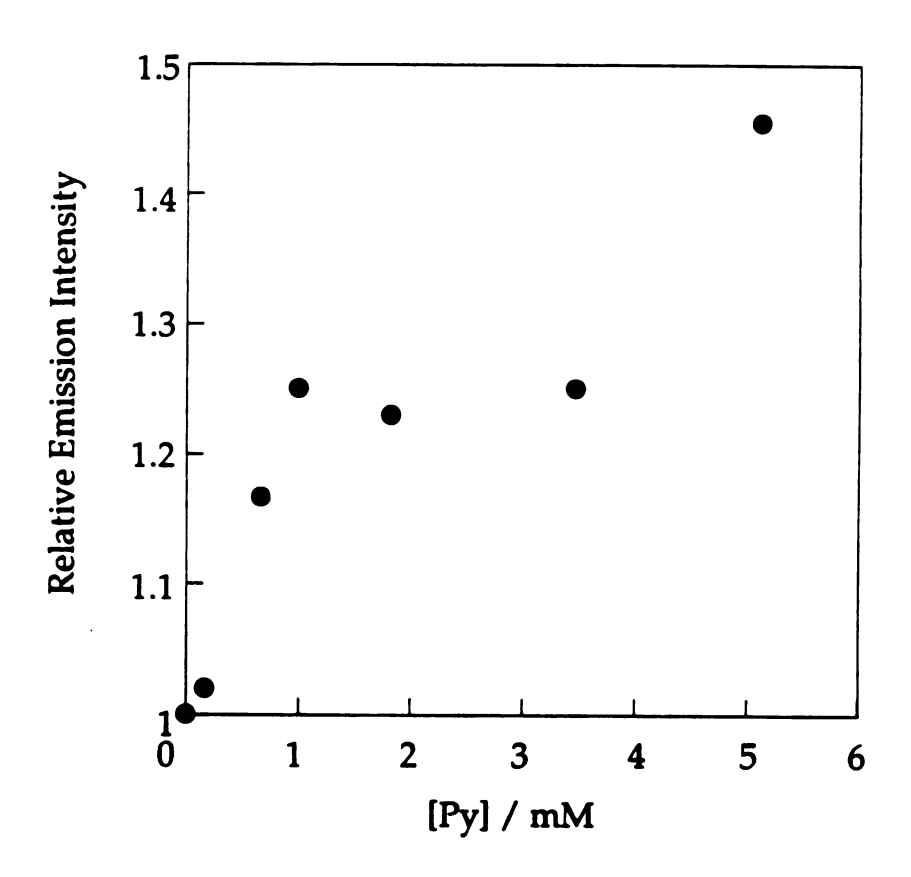


Figure 38

Figure 39. Dependence of the emission intensity from D₂O solutions of β -CD \cup 1aza \supset Eu³⁺ upon addition of naphthoic acids as LHGs (λ_{exc} = 280 nm). Concentrations of the lumophore are 4.95×10⁻⁴ M.

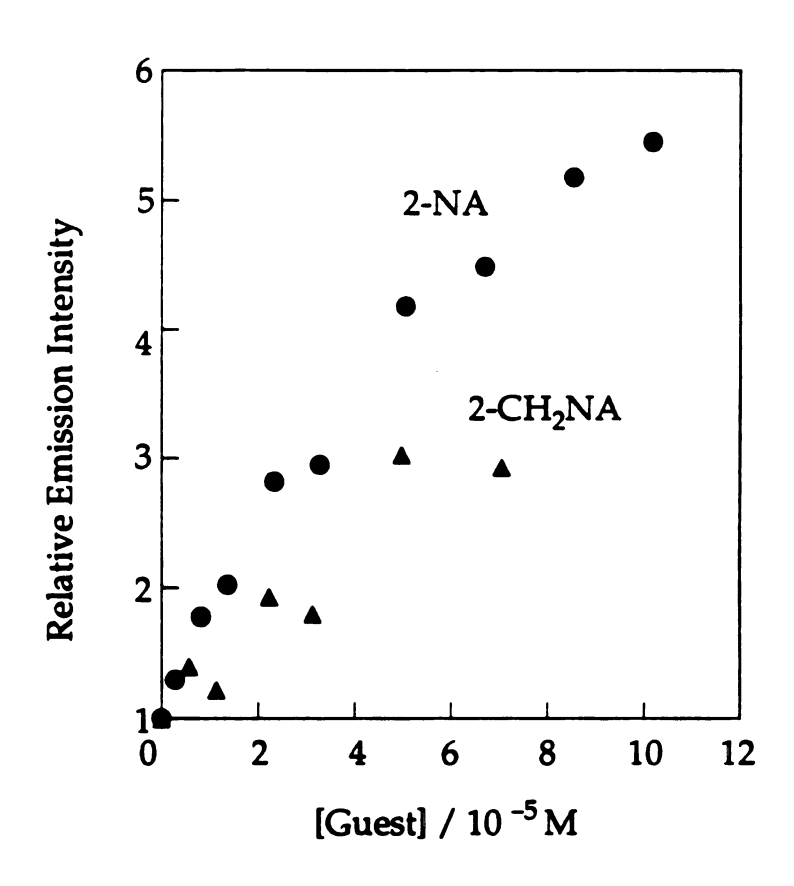


Figure 39

Figure 40. Dependence of the emission intensity from D_2O solutions of $Eu(NO_3)_3$ upon addition of naphthoic acids as LHCs (λ_{exc} = 280 nm). Concentrations of the lumophore are 4.5×10^{-4} M.

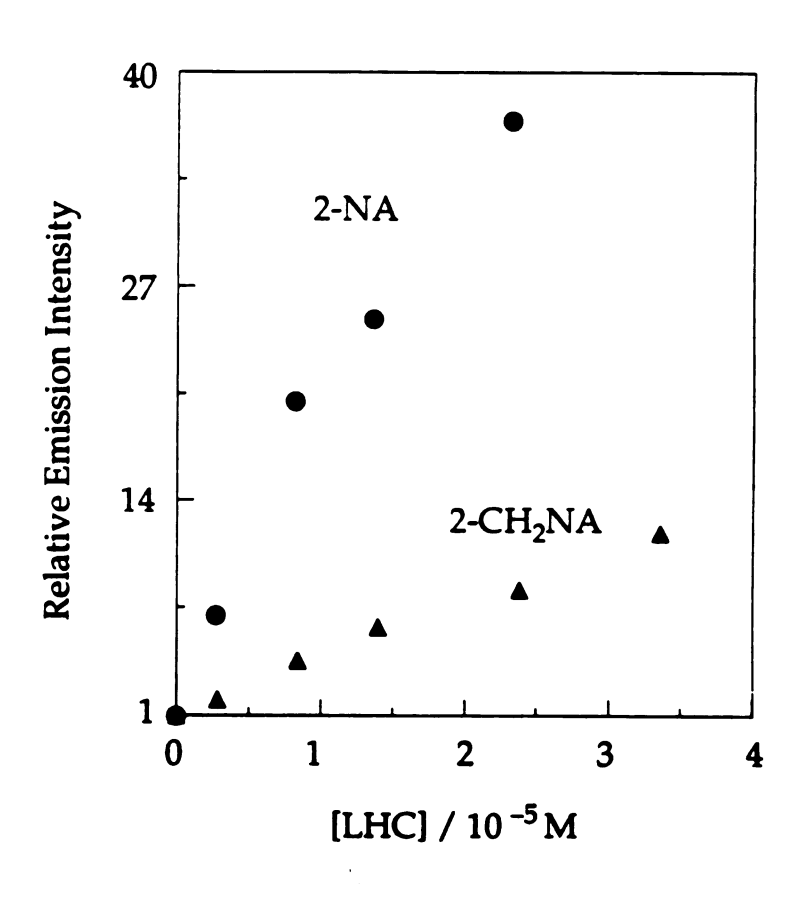


Figure 40

Figure 41. Relative emission intensity from D_2O (\triangle) and 10% CH_3CN/D_2O (\triangle) solutions of β - $CD\cup^1$ aza $\supset Eu^{3+}$ upon addition of benzoic acid (λ_{exc} = 280 nm). Concentrations of the lumophore are 6.4×10^{-4} M.

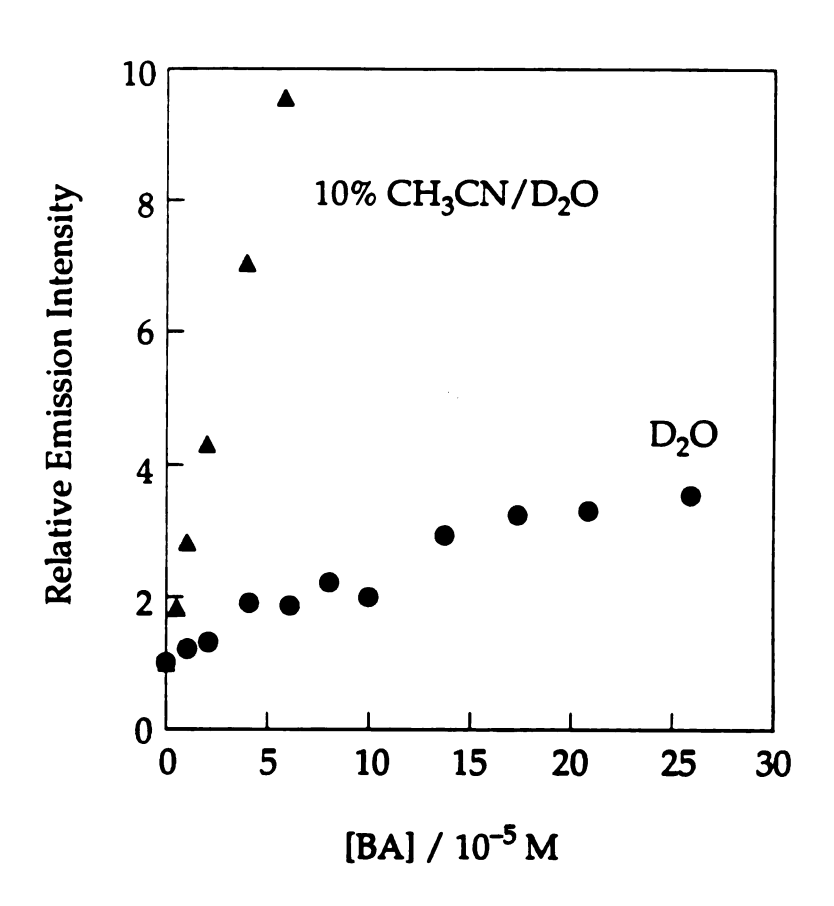


Figure 41

CD cup is cooperative with metal-guest recognition. This bifunctional recognition of anionic guests by the CD supramolecule serves to increase the association of the guest with the modified CD and shortens the donor/acceptor distance for energy transfer.

CHAPTER IV

CRADLE CYCLODEXTRINS

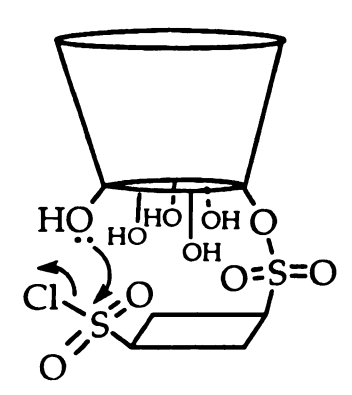
A. Synthesis and Characterization

1. Background

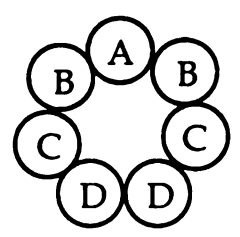
The energy transfer studies for the swing CD, reported in Chapter III, indicated that the most efficient luminescence will occur for a supramolecular assembly featuring the aza receptor site rigidly situated at the base of the CD cup, and not as a swing. This inspired the synthesis of a cradle CD where the aza crown ether is tethered to the primary side of the CD cup via both of its nitrogens.

The development of regiospecific bifunctionalized cyclodextrins was driven by the design of active artificial enzymes since sophisticated model enzymes use more than one functional group for single catalysis. Tabushi's group developed modifying reagents with rigid skeletal structures that regiospecifically functionalize two primary sides of the cyclodextrin [66, 67]. The covalent attachment of the capping reagent to

one side of the cyclodextrin rim forces it to come into proximity with the rim and react with a second primary hydroxyl group with specificity. The approach relies on the rigidity of the backbone of the modifying agent. This mechanism is called Looper's walk and is shown below for aromatic bisulfonates as the modifying reagents [97]:



Rigid capping reagents give different isomers according to the aromatic backbone size [97]. For β -CD the seven primary hydroxyl groups result in three possible isomers A,B, A,C and A,D where the cyclodextrin primary rim is represented as,



The introduction of sulfonate groups to the capped cyclodextrin provides the potential for substitution reactions to yield symmetrical or unsymmetrical derivatives, depending on whether the functional groups are the same or not. Nucleophilic substitution by amines yielding bifunctionalized CDs has been employed mainly with imidazole and histidine groups for artificial enzyme applications [98].

In the same synthetic context for substitution by amines we have tethered an aza crown ether to the primary side of the CD cup via its two nitrogens providing a double-strapped (or cradled) CD. The characterization of the compound was completed with NMR techniques. Specifically, homonuclear total correlation spectroscopy (TOCSY) [99] proved to give more information than COSY spectroscopy. Recently, the former has been very popular in carbohydrate identification due to the possibility of structural elucidation of the connectivities of building blocks and stronger signals due to through–bond magnetization transfer [100].

2. Results and Discussion

The synthesis of the cradle CD with the aza attached to the (A,D) positions of the β -CD cup [101] is summarized as follows,

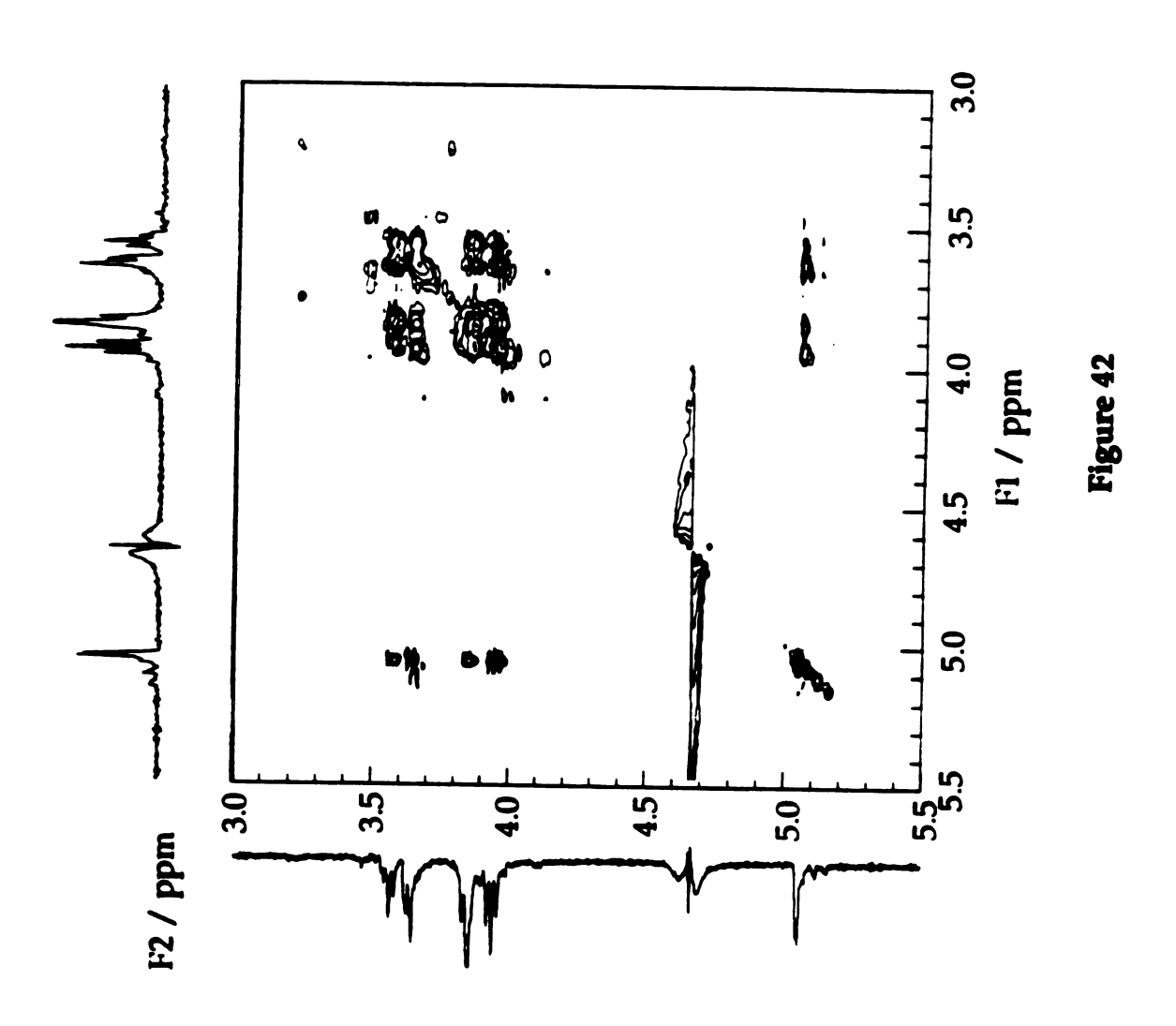
Energy minimized calculations reveal that the (A, D) attachment is the least sterically constrained. As elaborated by Tabushi, reaction of the β -CD with biphenyl-4,4'-disulfonyl chloride yields a cyclodextrin rigidly capped with the biphenyl sulfonate spanning the (A,D) glucosyl subunits. Signature of the substitution in the 1 H NMR spectrum (Figure A13) is the splitting of the anomeric protons due to both ring currents on the substituted glucose rings and dissymetry of the molecule. Subsequent reaction with KI produces the diiodo-substituted CD, which is susceptible to nucleophilic attack by amines. The aromatic peaks disappear in the 1 H NMR of the (Figure A14) indicating complete substitution and the absence of any sulfonate salt. The advantage of using the diiodo- β -CD as the intermediate before the nucleophilic substitution by amines is that treatment with tetrachloroethylene is employed in this step to effectively eliminate the sulfonate salts. The reaction with the aza crown provides only one derivatized CD and unreacted crown.

Fast atom bombardment mass spectrometry (FABMS) of the product in an acidified glycerol matrix shows a molecular ion cluster centered at 1367 mass units (M + 7H⁺), which is consistent with the derivatization of one β -CD with a single aza crown; typical matrix adduct fragments appear at +92 mass units (Figure A15). This cluster at 1367 amu is significant because it is 18 mass units less than that observed by us for the swing CD, where the aza is attached to the CD cup via one nitrogen. This difference corresponds to the mass of one hydroxyl group and a proton, which are removed upon condensation of a the second aza nitrogen to the β -CD cup. Another difference between the FABMS obtained from the double

substitution and β -CD \cup ¹aza is that the former appears to be more robust under FABMS conditions. As opposed to the facile loss of the entire aza swing in β -CD \cup ¹aza, the FABMS pattern of the compound prepared here is consistent with fragmentation of the aza crown followed by fragmentation of the CD ring; the aza crown is not observed to depart as a unit. From these FABMS data we infer that the aza crown is attached to the CD molecule at both its nitrogens and we formulate the compound as β -CD \cup ²aza.

The compound was further characterized by NMR. The ¹H NMR spectrum of the β -CD \cup ²aza in D₂O shows a more complicated pattern than that of β -CD \cup ¹aza. Specifically, the resonances associated with the β -CD exhibit higher multiplicity for the cradle CD as compared to the CD swing compound. Therefore elucidation of the compound's structure by NMR was undertaken with {1H,1H} total correlation spectroscopy (TOCSY). For the β -CD \cup 1 aza compound, NMR spectra show a single doublet in the anomeric proton region (5.0-5.2 ppm), as is observed for other monosubstituted cyclodextrins [102]. In contrast, four distinct doublets are distinguished in the TOCSY spectrum of the doubly strapped CD shown in Figure 42. This indicates a symmetry perturbation at the (A,D) sites of β -CD \cup ²aza induced by the presence of the aza moiety. These anomeric protons show relevant cross peaks with the remaining glucosyl protons at 3.8-4.0 ppm $(H_{3,5,6})$ and at 3.5-3.7 ppm $(H_{2,4})$. The islands at 3.8 and 3.7 ppm, which we attribute to the aza crown methylenes adjacent to oxygen, correlate to the 3.2 and 3.5 resonances respectively. The 3.2 and 3.5 ppm peaks are consistent with assignment to aza

Figure 42. The 500 MHz 1 H TOCSY spectrum of β -CD \cup 2 aza in D₂O at 30°C. The mixing time was 120 ms. The HDO signal is suppressed by presaturation.

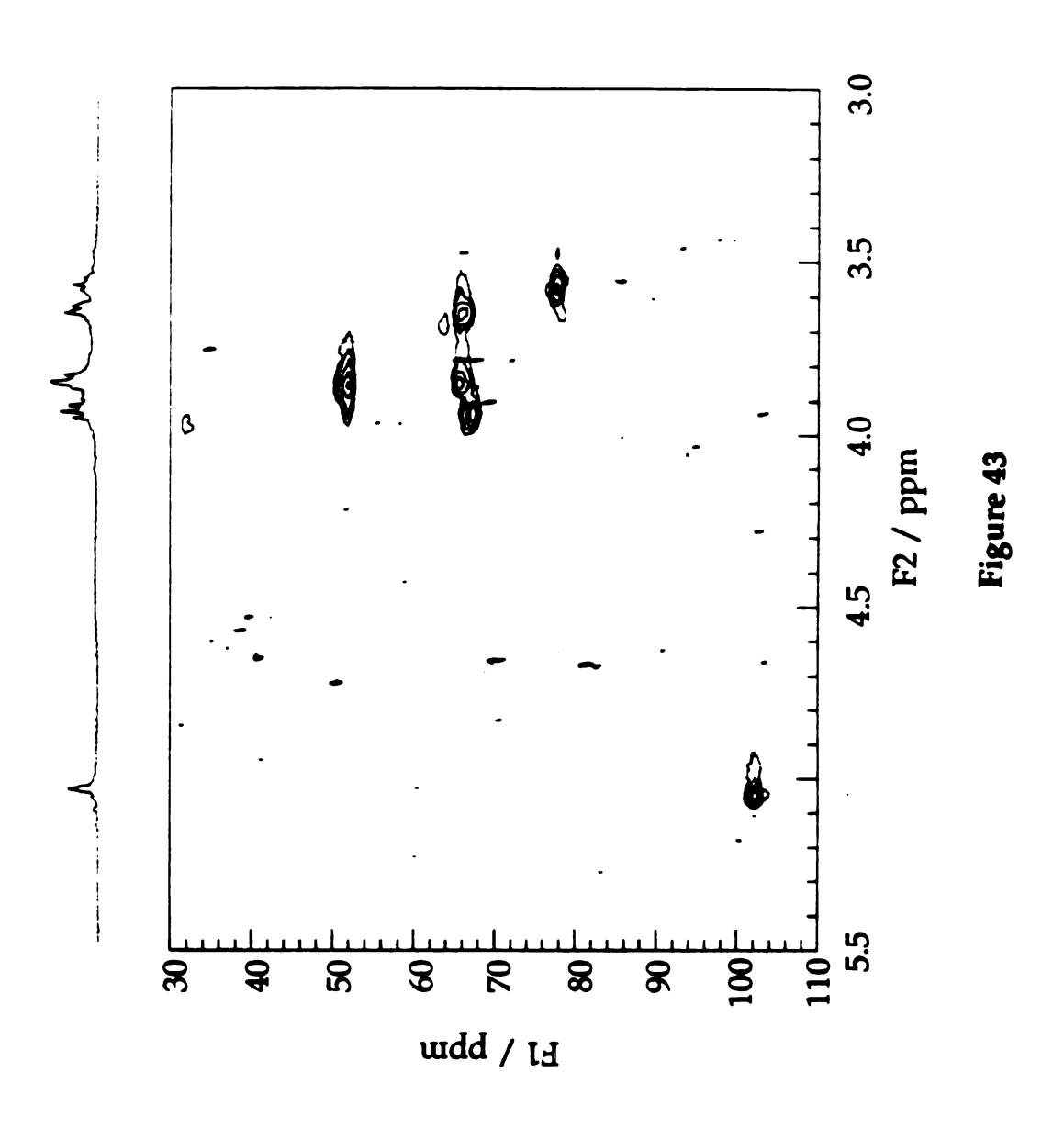


methylene protons next to nitrogen and the CD's C_6 protons of the substituted glucose residues. It is noteworthy that the 3.5 ppm peak correlates with the remaining protons of the glucosyl subunit. In addition, the peak at 4.1 ppm correlates to the $(H_{3,5,6})$ at 4.0 ppm as well as to the island at 3.7 ppm. This peak at 4.1 ppm appears to be attributed, as in other cases [98a], to the H_4 proton of the substituted glucose rings.

The correlations between carbons and protons are identified from heteronuclear multiple-quantum coherence measurements. The CD proton resonances correlate to the relevant carbons as follows: $H_{2,4}$ at 3.5-3.7 to C_2 at 68 ppm and to C_4 at 79 ppm; $H_{3,5,6}$ at 3.8-4.0 to $C_{3,5,6}$ at 67, 68 ppm; and H_1 at 5.1 to C_1 at 102 ppm (Figure 43). The protons of the methylenes adjacent to nitrogen, as well as the C_6 protons of the glucosyl units where aza substitution occurs, cannot be assigned because of the spectral congestion. However, the aza methylenes adjacent to oxygen show proton resonances at 3.7 ppm, which correlate to the carbon signal at 64 ppm.

In accordance with attachment of both nitrogens to the CD is an indirect NMR experiment that indicates the absence of a secondary nitrogen in the cradle CD. The protons on the nitrogen exchange fast and they are not usually observable by NMR. Protonation of the nitrogens shifts the adjacent methylenes downfield and according to the number of protons, the methylenes are split characteristically. Trifluoroacetic acid has been used as protonating agent in order to distinguish among primary, secondary and tertiary amines from the splitting of the methylene units [103]. We used this method to exclude the presence of secondary amine

Figure 43. The 500 MHz 1 H $^{-13}$ C HMQC spectrum of β-CD $^{-2}$ aza in D $_{2}$ O.



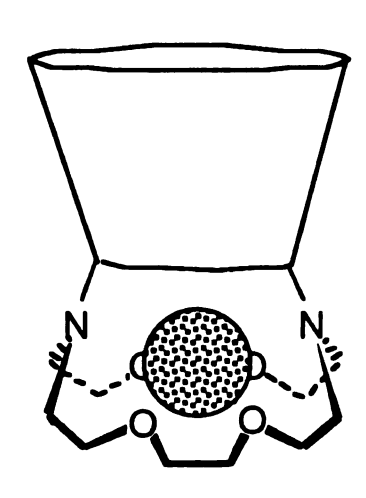
when both the nitrogens are secondary, as in free aza, the protonation further splits the methylenes to a quintet observed at 3.2 ppm. The multiplicity is a result of the splitting of the triplet from two protons. For the swing CD we observe a quintet at 3.20 ppm and a combination of two doublets at 3.40–3.48 ppm. In the case of cradle CD, only the latter peak is shown, indicating the presence of tertiary nitrogens only.

The incorporation of Eu³⁺ in the aza crown was performed with the same methodologies as for swing CD and was confirmed by luminescence spectroscopy.

B. Luminescence Spectroscopy

1. Results and Discussion

Excitation spectroscopy was employed to confirm the incorporation of Eu^{3+} in β -CD \cup ²aza \supset Eu³⁺.



 β -CD \cup ²aza \supset Eu³⁺

The charge transfer band of the nitrogens to Eu^{3+} is observed, and as described in detail in Chapter III for the swing CD confirms the identity of the Eu^{3+} ion in the aza cradle. Because of the low concentration, it was not possible to extract more information (e.g. splitting of the bands) from the excitation spectrum. Steady-state luminescence spectra of acetonitrile solutions of β -CD \cup 2aza \supset Eu³⁺ do however reveal the characteristic $^5D_0 \rightarrow$ 7F_J pattern of Eu^{3+} ion resulting from transitions from the lowest energy 5D_0 excited state to the 7F_J spin orbit manifold of the ground state when excited at λ_{exc} = 394 nm, coincident with the $^5L_6 \leftarrow ^7F_0$ transition. The small signal/noise ratio compared to that for the same concentration of the swing CD indicates that the hydroxyl group environment on the primary rim may be quenching the Eu^{3+} luminescence. This notion is supported by the modeling studies, which indicate some coordination of hydroxyl groups. The lifetime of the 5D_0 excited state of β -CD \cup 2aza \supset Eu³⁺ is 835 μ s.

C. Inclusion Complexes of β -CD \cup ²aza \supset Eu³⁺

1. Results and Discussion

a. Association of Guests. The association constants of different light-harvesting guests with β -CD \cup 2aza are shown in Table 2. The surprising result was that the binding of benzene in the CD cavity was too small to be measured. Apparently, the 3+ charge of the appended Eu³⁺Caza cradle at the bottom of the CD cup decreases the hydrophobicity of the aromatic hydrocarbon binding site thereby attenuating the association of benzene. The polar pyridine enters the cup with a smaller

157 **Table 2.** Association constants (M $^{-1}$) of light–harvesting guests with β - $CD \cup ^2 aza \supset Y^{3+}$

Guest	K₄(β-CD∪²aza⊃Y³+)
Benzene (Bz)	<10
Pyridine (Py)	348
Benzoic Acid (BzA)	_
Picolinic Acid (PcA)	7.3×10 ⁵

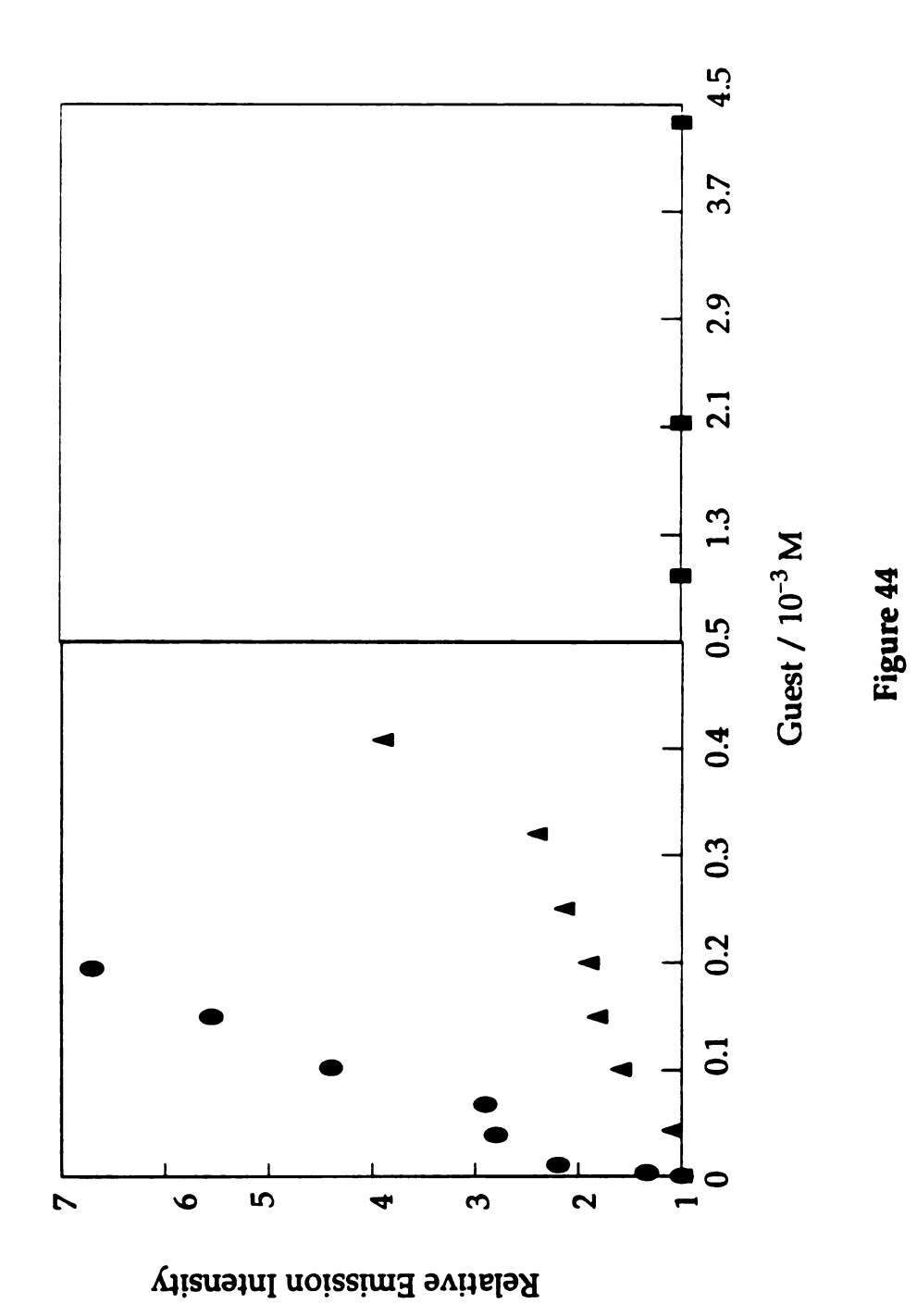
association constant than observed for the swing $K_{assoc} = 1047 \,\mathrm{M}^{-1}$. This is not the case though for picolinic acid which is polar enough to strongly bind the cradle CD. The association constant for the latter was an order of magnitude higher than for the swing. This enhancement in binding may be due to increased association of polar substances when a positive charge is appended at the primary side of the CD, described in Section 2.a in Chapter III. For the cradle CD, the results are more pronounced since the charge is rigidly situated at the bottom of the cup. This cradle provides a compliment to the biphenylsulfonyl CDs, which are rigidly capped CDs with hydrophobic moieties that enhance binding of non polar substrates [97].

b. AETE Studies for Various LHGs. Energy transfer from the light-harvesting guests to the lanthanide has been demonstrated with emission and excitation spectroscopy. In all cases, the latter reveals the respective LHG absorption profile when the lanthanide luminescence is detected thereby verifying the presence of an AETE process.

The addition of benzene in solutions of β -CD \cup ²aza \supset Eu³⁺ did not show any appreciable enhancement in Eu³⁺ luminescence (Figure 44). This is expected of the very low association constant limiting the energy transfer only to a bimolecular component of benzene binding from the outside. As we have shown in Chapter III the latter contribution is almost negligible.

However, an increase of Eu³⁺ luminescence upon association of the acids is observed as illustrated in Figure 44. The strong emission is attributed to the increased association of the polar LHGs coupled to

Figure 44. Relative emission intensity from D_2O solutions of β- $CD\cup^2$ aza $\supset Eu^{3+}$ upon addition of light harvesting guests ($\lambda_{exc}=280$ nm for BzA, PcA and 254 nm for Bz). Concentrations of the lumophore are 2.4×10^{-4} M for BzA and 2.6×10^{-4} M for PcA and Bz.



shorter AETE distances. A comparison of absolute intensities for the swing and cradle CDs including LHG-acids is not clear at this point because the conformation of the appended crown is different in the swing even if it is pulled beneath the cup owing to carboxylate binding. The swing and cradle Ln^{3+} -CDs exhibit similar intensity versus concentration plots for the acids with a rapid increase, plateau due to saturation binding and then a further increase due presumably to the binding of a second LHG on the external side of the aza. A comparison of the linear part of the plot for Eu^{3+} emission enhancement in the aza and cradle CD complex upon addition of picolinic acid suggests that the binding of the one picolinic acid molecule to one Eu^{3+} -aza is much stronger than the association of the second exogenous molecule in the CD case.

Pyridine proved to be an ideal guest to compare the results of luminescence enhancement between the swing and the cradle. The relative emission increase of Eu³⁺ luminescence in the cradle CD upon pyridine addition is shown in Figure 45. The respective enhancement of the swing is also shown for comparison. The striking result is that even though pyridine binds more weakly than in the cradle, the enhancement of emission is higher for the latter at equivalent pyridine additions. On the basis of binding constant data, the concentration of the inclusion complexes are 1.9×10^{-4} M for the swing and 1.2×10^{-4} M for the cradle for 2×10^{-3} M added pyridine ([CD] = 3.0×10^{-4} M). The only factor for more efficient AETE in the cradle CD is the shorter distance imposed by the cradle geometry for AETE process between Eu³⁺ and pyridine.

Figure 45. Comparison of the dependence of the emission intensity from D₂O solutions of β -CD \cup ²aza \supset Eu³⁺ (cradle) and β -CD \cup ¹aza \supset Eu³⁺ (swing) upon addition of pyridine (λ_{exc} = 313 nm). Concentrations of the lumophores are 3.1×10⁻⁴ M.

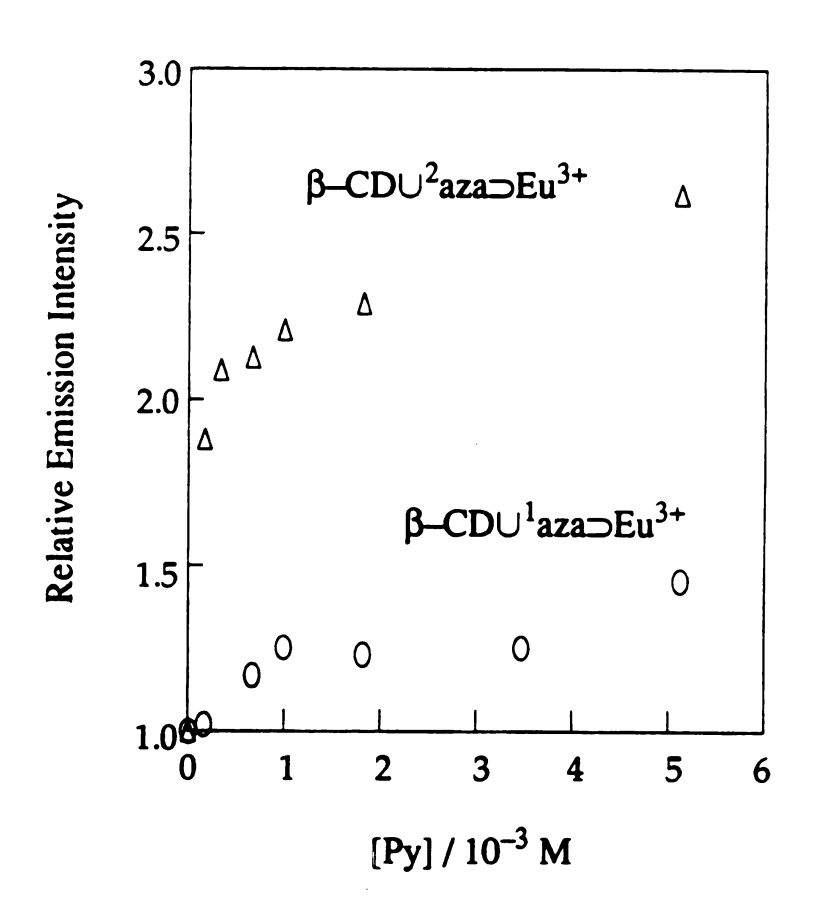


Figure 45

As an interesting side, intense pyridine fluorescence is also observed from the cradle CD. Figure 46 shows the pyridine emission upon UV excitation from β -CD \cup 2aza \supset Eu³⁺ and β -CD \cup 1aza \supset Eu³⁺ solutions at the same conditions. Neat pyridine exhibits fluoresce only in the vapor phase due to quenching mechanisms of the (n, π^*) excited state [104]. Here, quenching processes by water and oxygen are minimized due to the capping of the primary rim of the CD by the aza cradle that makes this site unaccessible to these molecules. This is not the case for the swing that is flexibly hanging away from the CD thereby leaving the primary site open. Similar pyridine fluorescence behavior was obtained for the swing and cradle CDs without the Ln³⁺ ion residing in the aza site, thus eliminating any binding effect on the pyridine luminescence properties.

In conclusion, shorter distances between the LHG and the Ln³⁺ imposed by the cradle CD are manifested in more efficient AETE processes. The high binding constants observed for only polar LHGs by the cradle enhance the luminescence properties of the assembly and permit detection of LHGs by lanthanide luminescence in small concentrations. Non-polar guests though do not associate strongly and they are eliminated as LHG-templates for AETE studies within the cradle.

Figure 46. Fluorescence of pyridine in D_2O solutions of β-CD \cup ²aza \supset Eu³⁺ (cradle) and β-CD \cup ¹aza \supset Eu³⁺ (swing) (λ_{exc} = 313 nm).

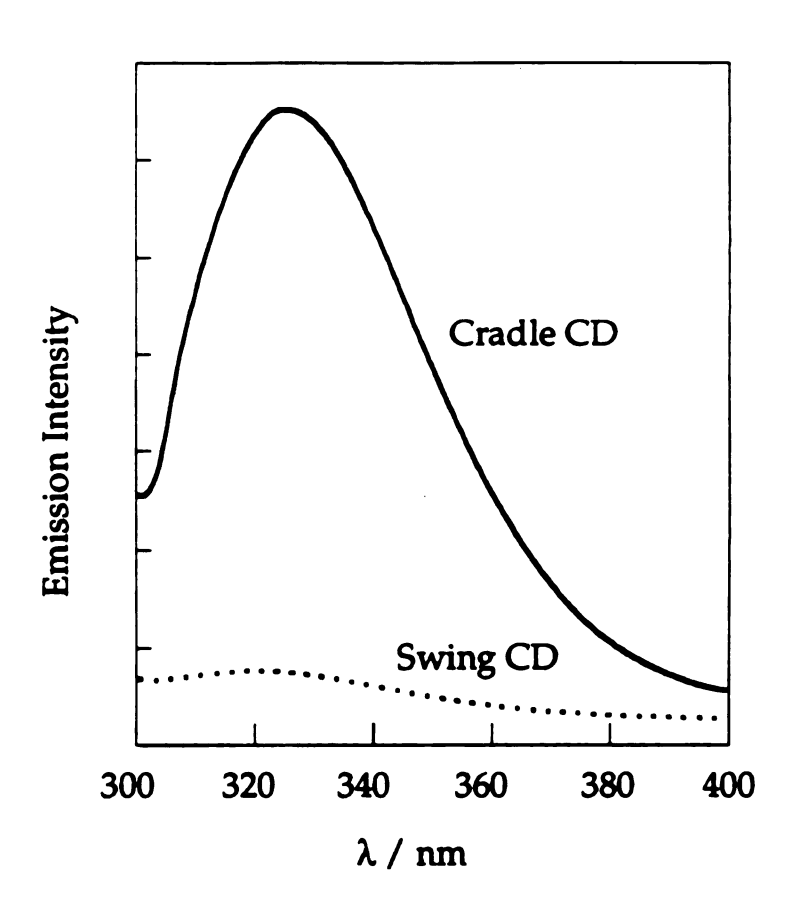


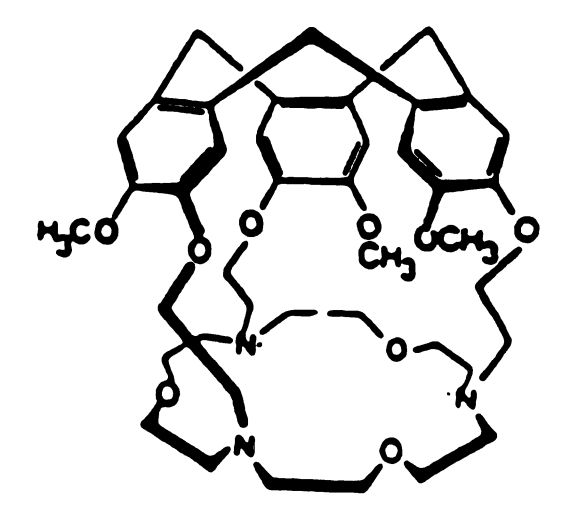
Figure 46

CHAPTER V

CONCLUDING REMARKS

The successful syntheses of crowned, swing, and cradle cyclodextrins afford new supramolecular templates for the study of unimolecular AETE process. They incorporate many of the structural features of other supramolecules displaying a crown subunit shown in Figure 47. Spealand (top) [3] and calixarene (bottom) [22] receptors functionalized with crowns provide a hydrophobic aromatic pocket for substrate binding and a polar moiety for ion binding. But these compounds have limited application as photoactive supramolecules because the hydrophobic binding pocket is itself composed of chromophores. The cyclodextrin cup of the swing and cradle CDs is transparent to UV and visible irradiation thereby allowing photoinduced energy and electron schemes to be established. The potential of studying photophysical processes and developing photochemical devices is therefore high because it is dictated by only the light–harvesting guest and the photoluminescent center.

Figure 47. Examples of receptors with structural characteristics similar to crowned cyclodextrins.



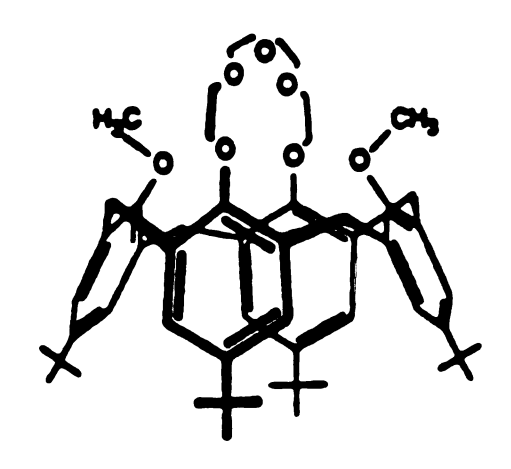


Figure 47

The recognition of poor- or non- coordinating LHGs, pyridine and benzene, respectively, by the hydrophobic cavity of the swing CD results in a triggered luminescence response not observable by a bimolecular energy transfer event. When benzoic and picolinic acids are employed as LHGs, the Ln³+ luminescence enhancement is increased relative to benzene and pyridine cases. This effect may be attributed to two reasons: (1) bifunctional recognition of the guest resulting from the hydrophobic interaction of the aromatic ring which is cooperative with the Ln³+ carboxylate moiety binding that leads to high association constants, (2) the unimolecular AETE process occurs from benzene or pyridine to a Ln³+ \subset aza that is swung away from the rim of the CD cup. In the case of the acids, the binding of the carboxylate to the Ln³+ center pulls the swing under the cup and shortens the donor/acceptor distance for energy transfer. These conformations of the aza are supported by molecular modeling and are illustratively shown in Figure 48.

The cradle CD was designed so that the Ln³+⊂aza site would be nestled under the CD cup. Although this supramolecule offers an ideal conformation for AETE, low association constants of benzene and pyridine result in poor intensity enhancements upon molecular recognition. Apparently, the 3+ charge of the appended Eu³+⊂aza cradle at the bottom of the CD cup decreases the hydrophobicity of the aromatic hydrocarbon, thereby attenuating the association constant especially in the case of benzene. The effect of the cradle conformation, in comparison with the swing, is established by the higher luminescence enhancement when pyridine is the LHG. Since the binding constant of pyridine in the cradle is

Figure 48. Conformations of the appended aza \supset Eu³⁺ moiety in the swing CD (β -CD \cup ¹aza \supset Eu³⁺) in the presence of benzene and benzoic acid guests.

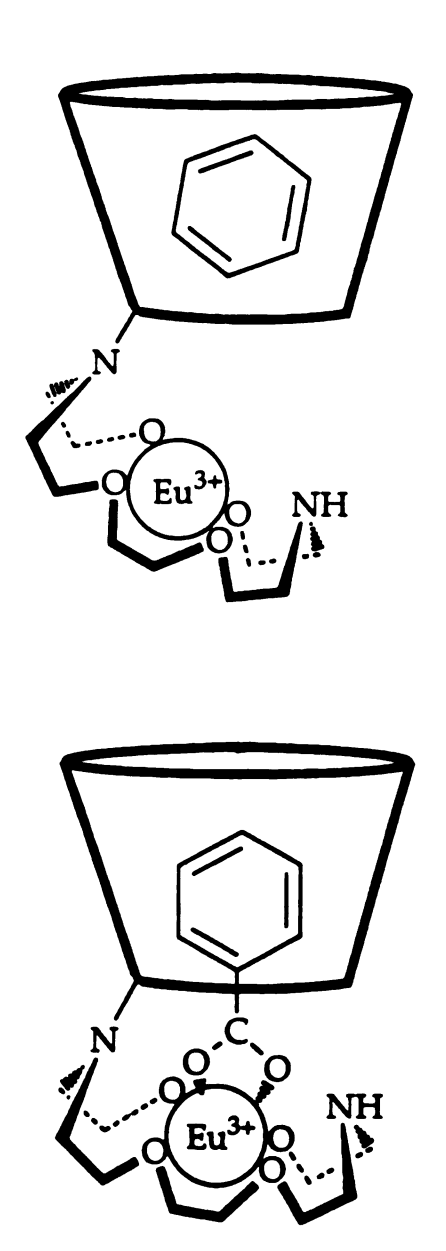
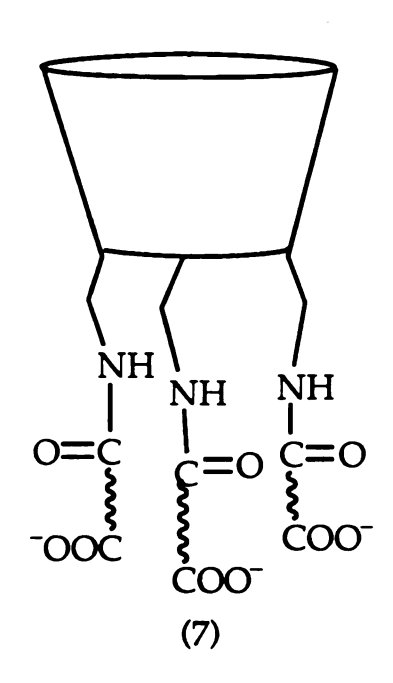


Figure 48

smaller than that of the swing, more intense luminescence observed from β -CD \cup 2aza \supset Eu³+ may be attributed to a more efficient AETE process owing to the shorter distances imposed by the cradle geometry (Figure 49). As might be expected the AETE between the acids and β -CD \cup 2aza \supset Eu³+ does not show large differences from β -CD \cup 1aza \supset Eu³+ since similar conformations of the appended Eu³+ \subset aza are achieved.

Our AETE results with the cradle CD, generally indicate an attenuated luminescence response by decreased association of the LHGs to the CD cup. A different approach is needed to overcome the binding limitation. It may be realized by the syntheses of new complexes in which the Eu³⁺ recognition site is a trianion group. A promising example is shown below with carboxylate functionalities on the primary rim of the CD,



In this case, the Eu³⁺ charge will be neutralized thereby preserving the hydrophobic environment at the bottom of the CD cup. AETE processes

Figure 49. Comparison of pyridine residing in the swing and cradle CD.

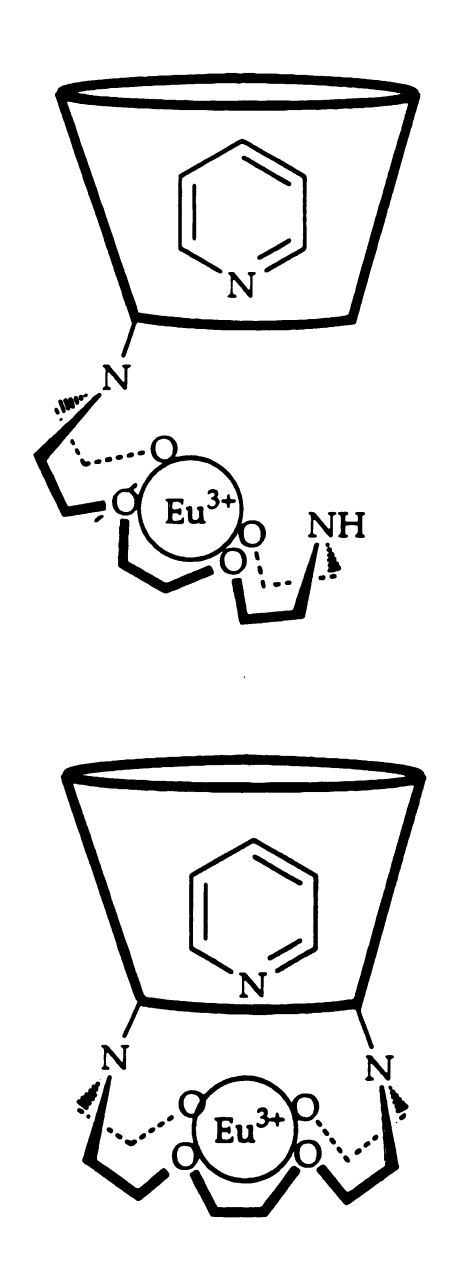


Figure 49

may also be realized between antennas appended on the CD rim and energy trap guests. Appropriate functionalization on the CD may also permit metal complex binding, expanding the application area of this class of compounds.

Practically, the AETE within cyclodextrins represents a triggered optical response that may lead to a generalized design of optical sensors. The low concentration detection limits of the aforementioned LHGs studies support this contention. Moreover, the supramolecular approach is powerful for sensor design. The high selectivity achieved by the molecular recognition of the analyte and the control of its communication with the photoluminescent center are functions of the supramolecular structural design, nature of the binding pocket, number of recognition sites, and distance between analyte and luminescent center.

Different photophysical schemes may also be studied within an architecture of a modified cyclodextrin relying only on the imagination of the chemist to appropriately design the structure.

Since the burst of supramolecular chemistry gave control over molecules, supramolecules and materials for expressing desired properties, we need to develop and benefit as people did, using the fire brought by Prometheus!

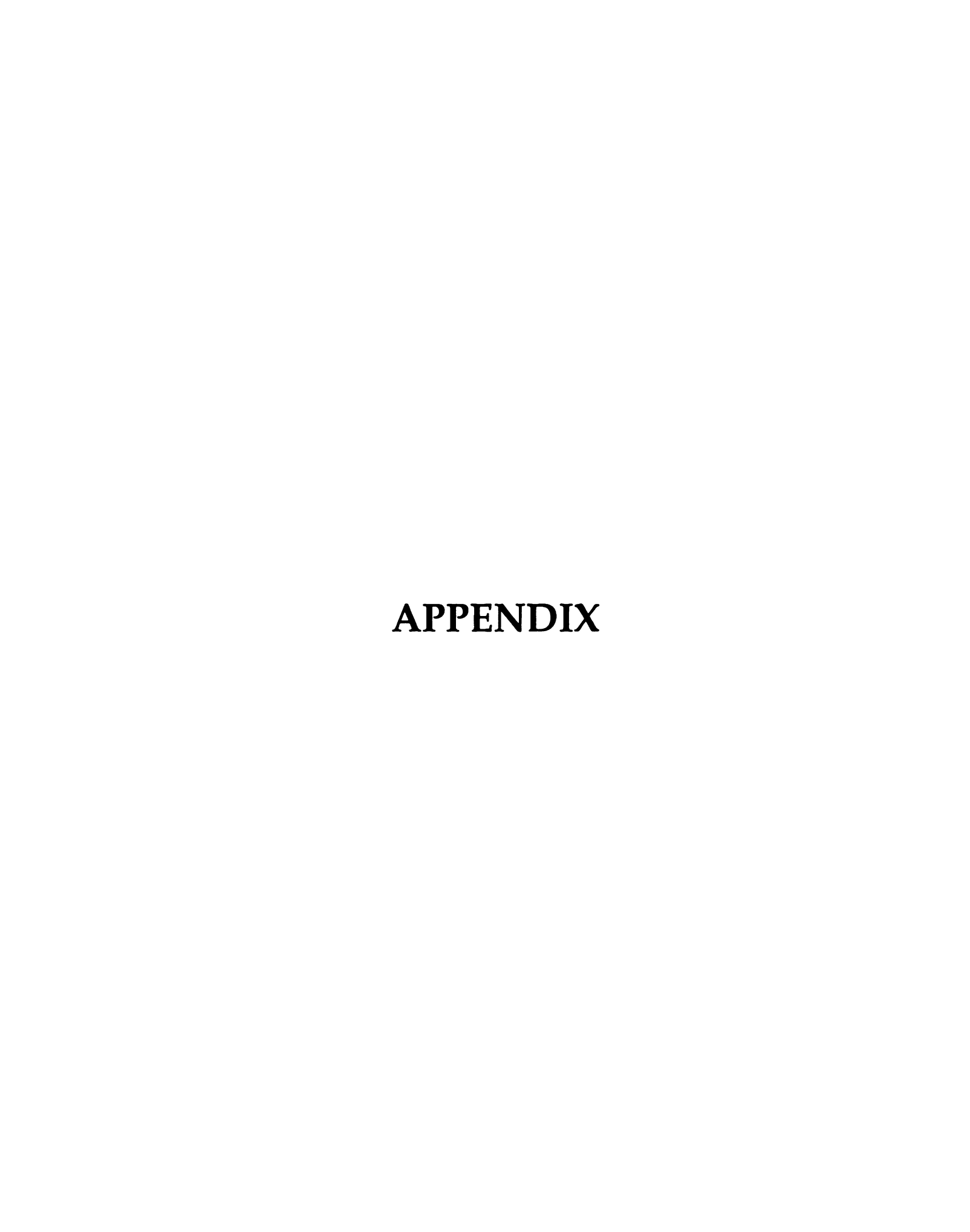


Figure A1. The 300 MHz 1 H NMR spectrum of β -CD in d 6 -DMSO.

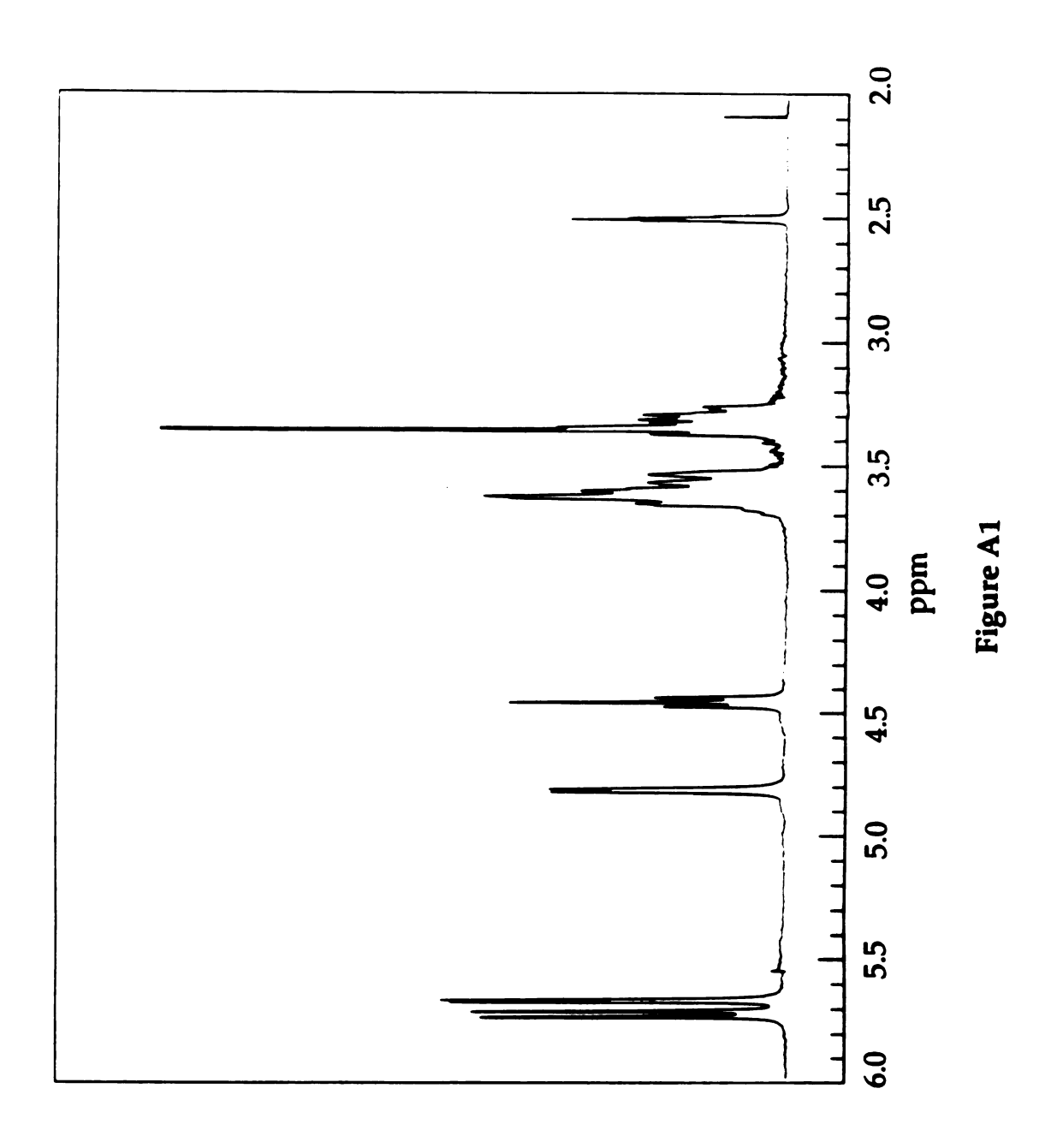


Figure A2. The 75 MHz 13 C NMR spectrum of β -CD in d^6 -DMSO.

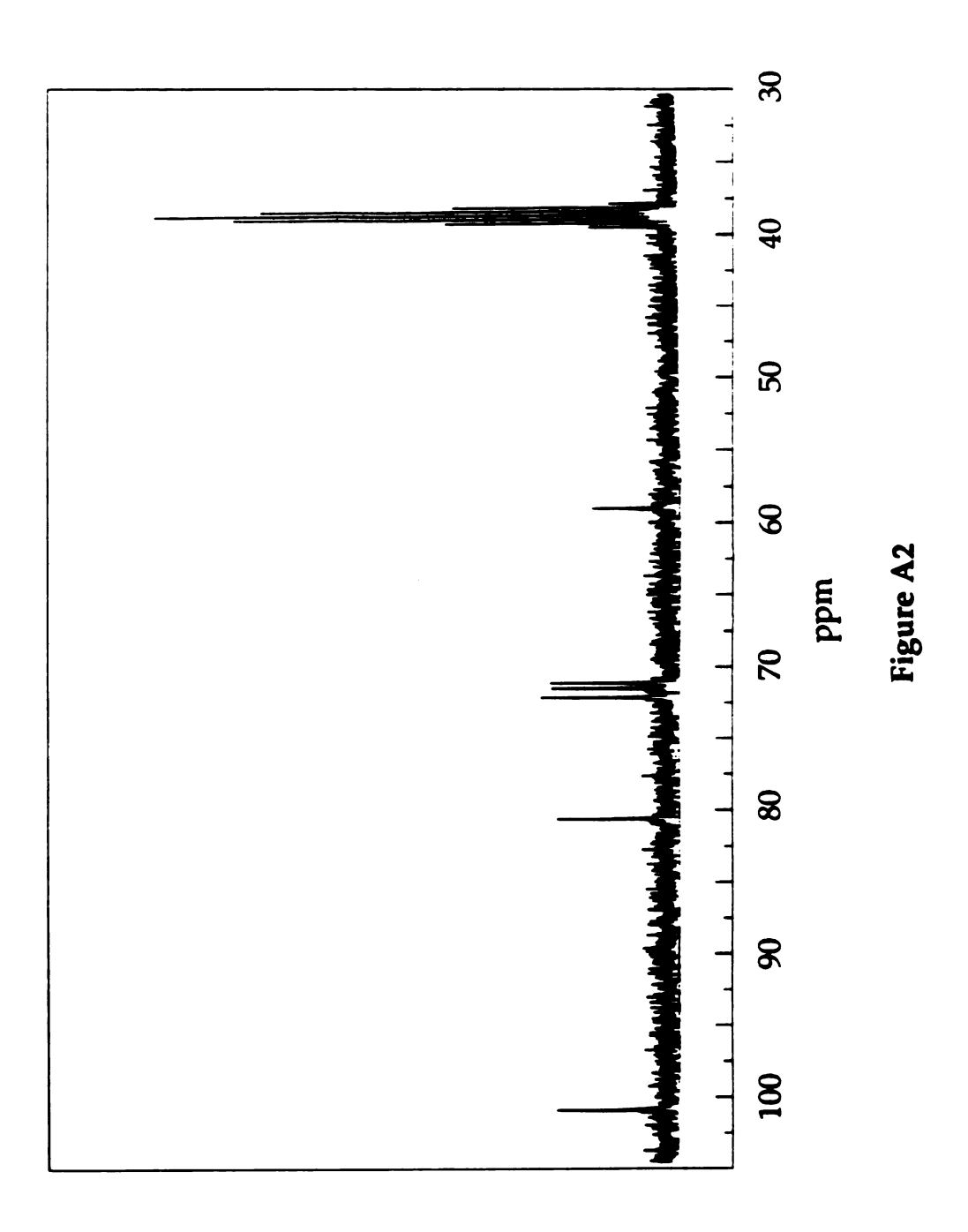


Figure A3. The 500 MHz 1 H NMR spectrum of β -CDO–Ts in d^6 -DMSO.

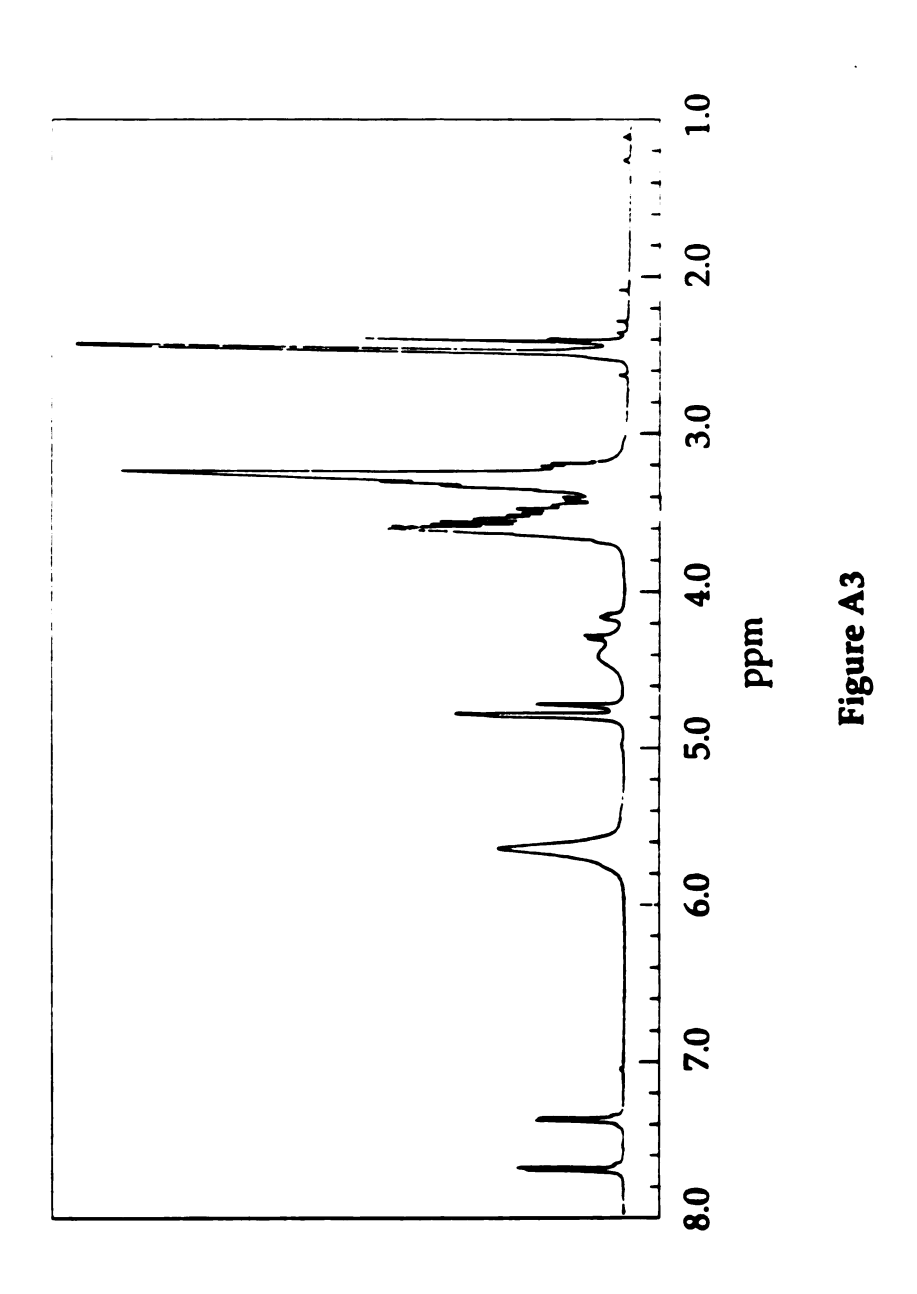


Figure A4. The 75 MHz 13 C NMR spectrum of β -CDO–Ts in d^6 -DMSO.

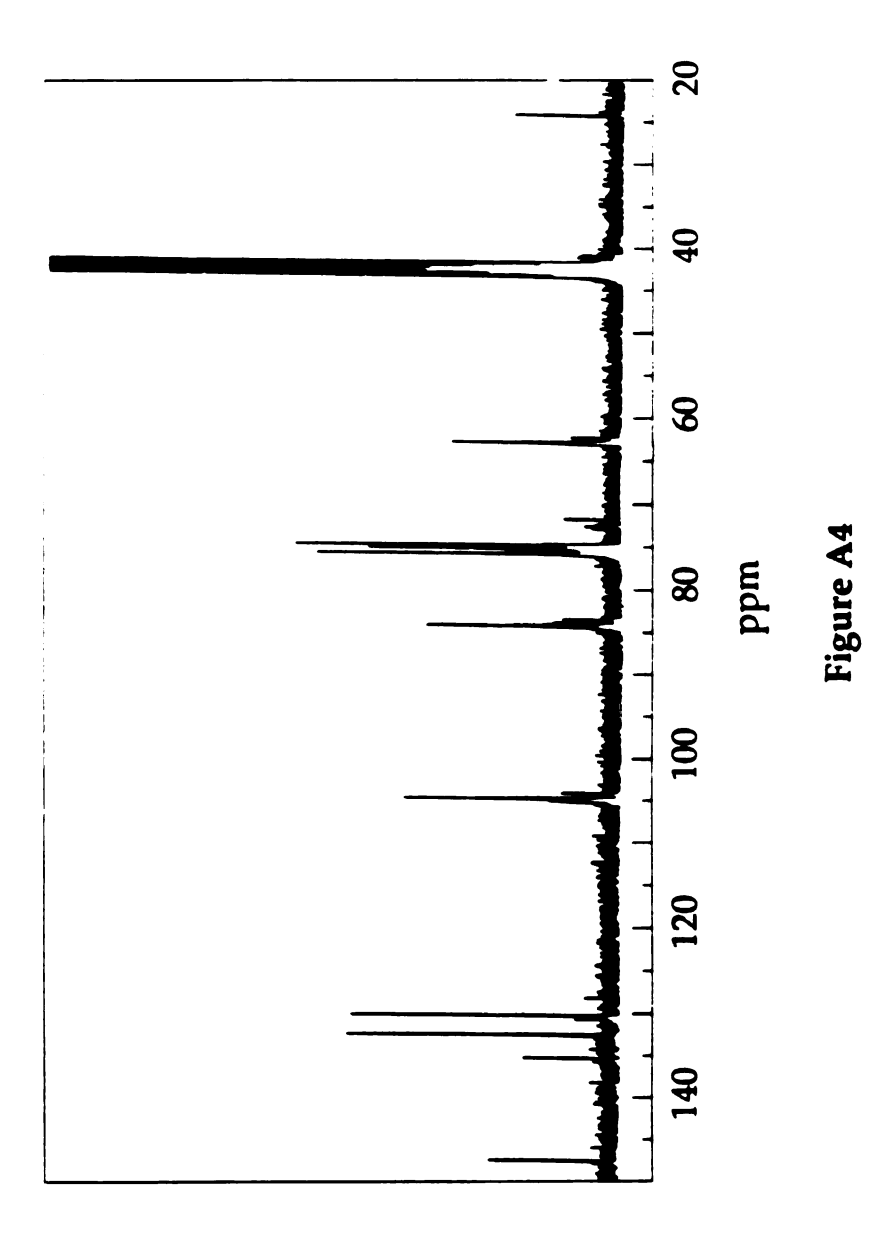


Figure A5. The 300 MHz 1 H NMR spectrum of aza in d 6 -DMSO.

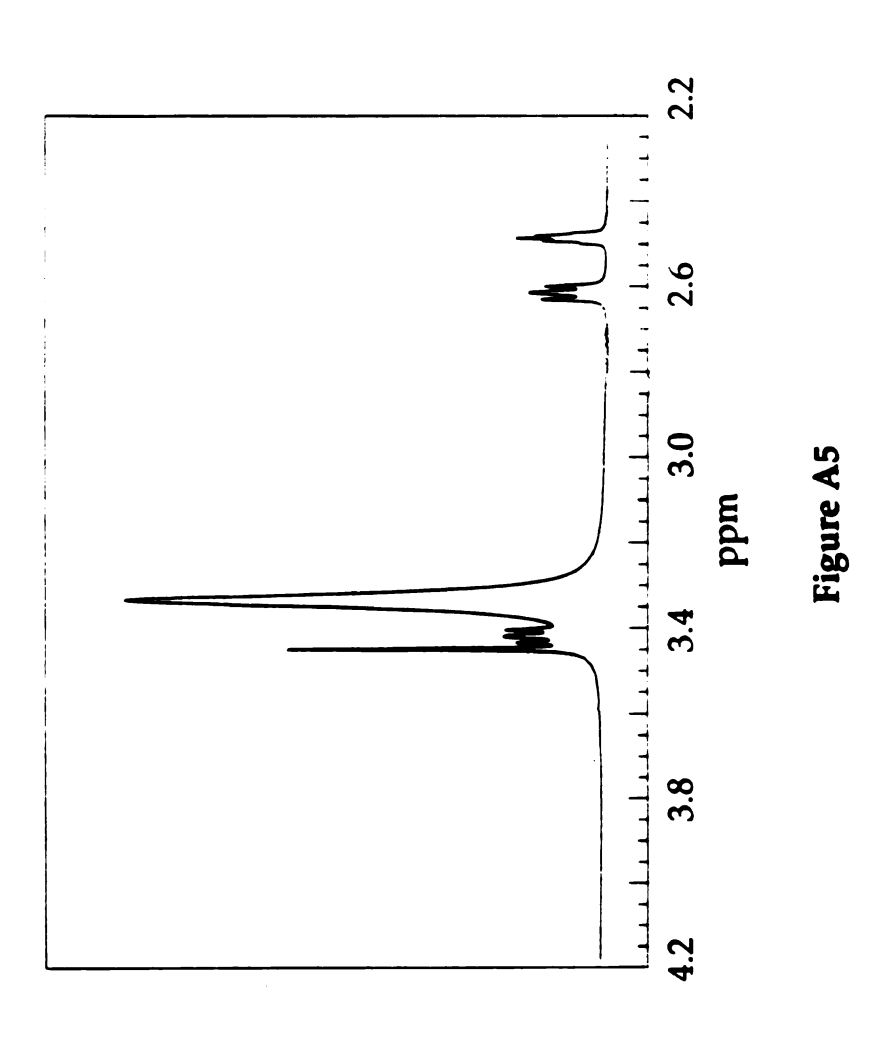


Figure A6. The 75 MHz 13 C NMR spectrum of aza in d⁶-DMSO.

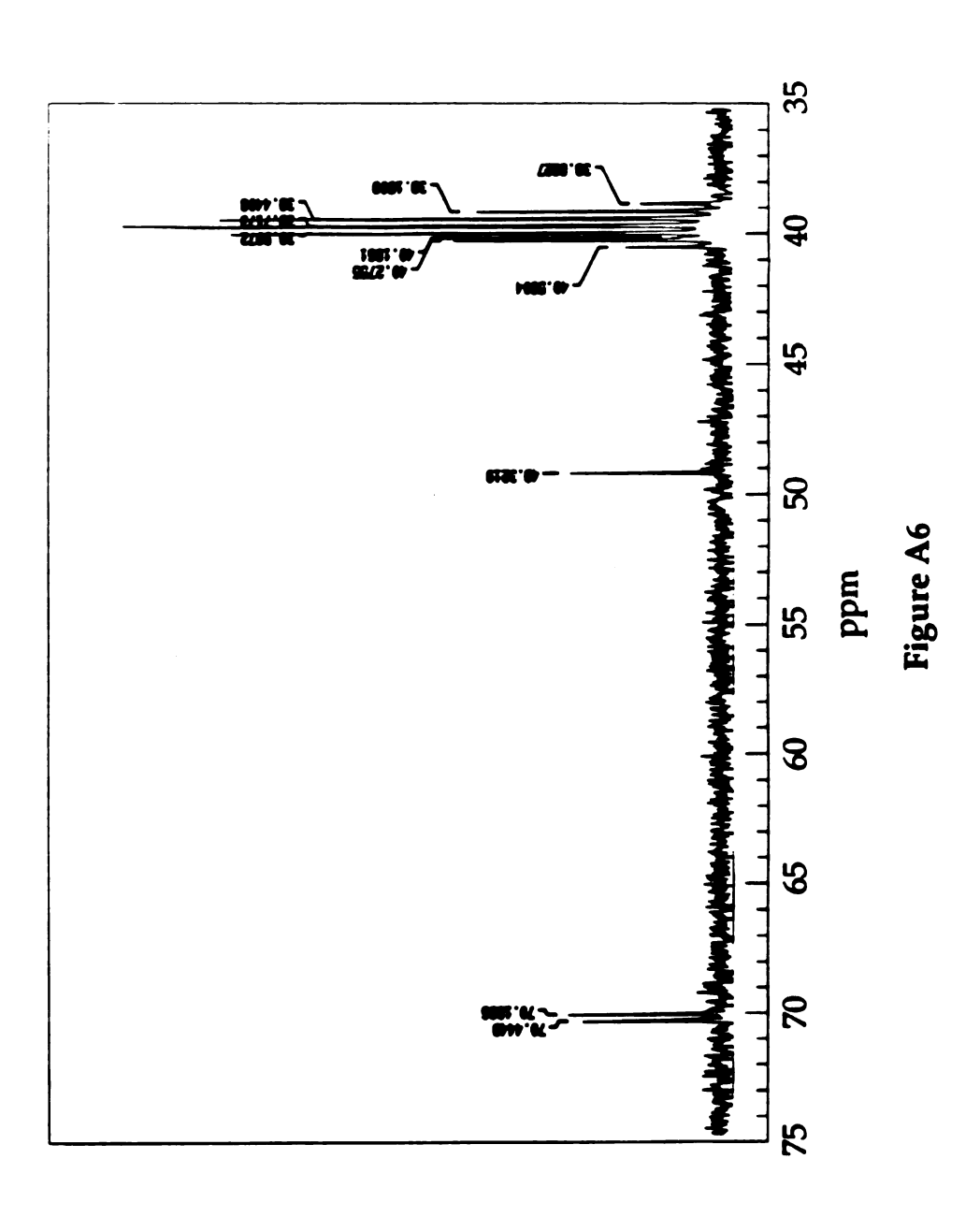


Figure A7. The positive ion FABMS spectrum of β -CD 1 aza with glycerol as matrix. The molecular ion peak is shown at 1379.8 amu and the fragment corresponding to the matrix adduct with a loss of the azaCH $_2$ —group is at 1105.7 amu. The peak at 1381.7 amu corresponds to an adduct of the matrix upon the fragmentation therefore it shows as a doublet comparing with the molecular ion peak. A higher fragment corresponds to a usual presence of sodium which tends to form complexes with carbohydrates.

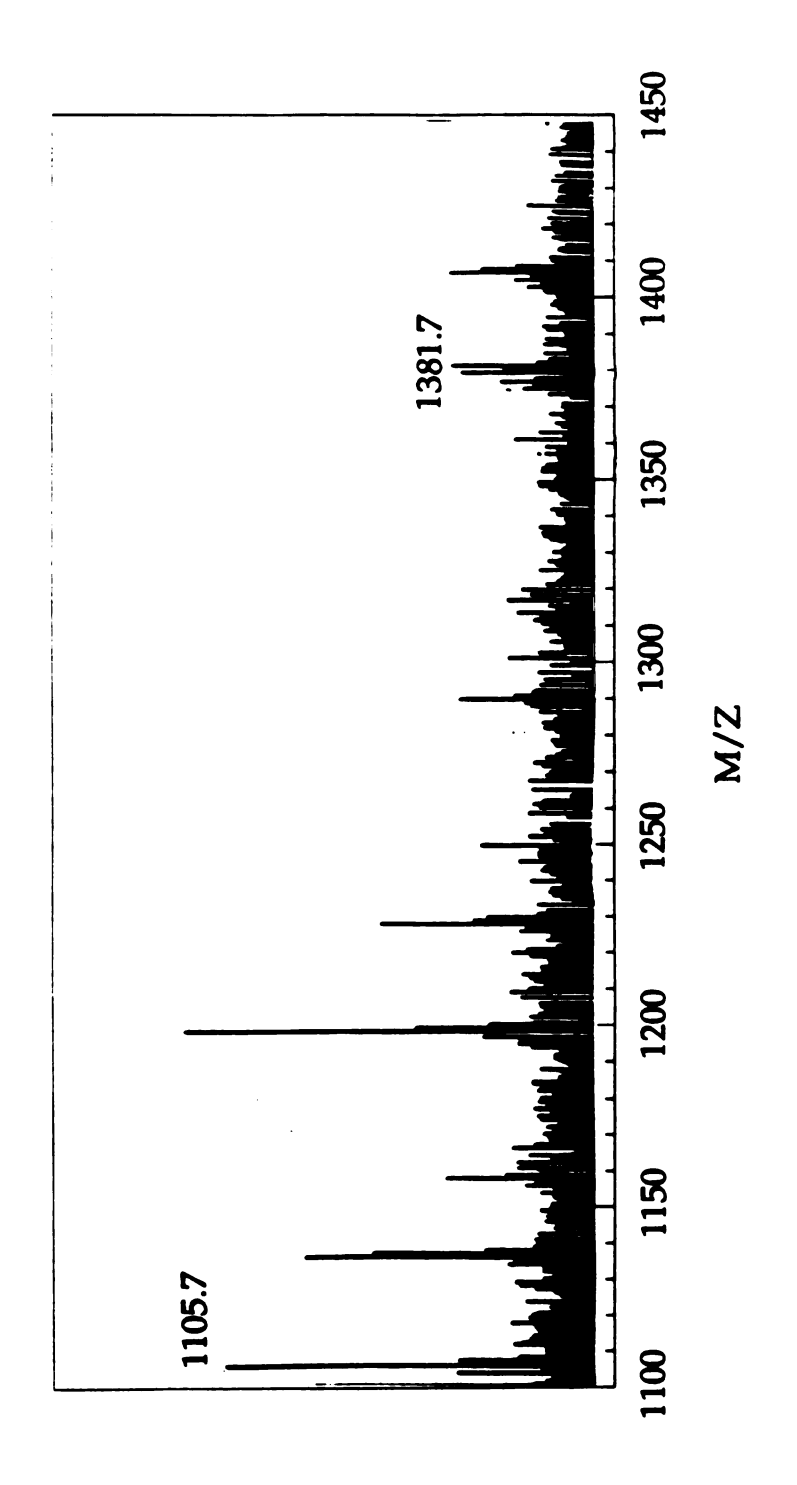


Figure A7

Figure A8. The 500 MHz 1 H TOCSY spectrum of β -CD \cup 1 aza in D $_2$ O at 30°C. The mixing time was 120 ms. The HDO signal is suppressed by presaturation.

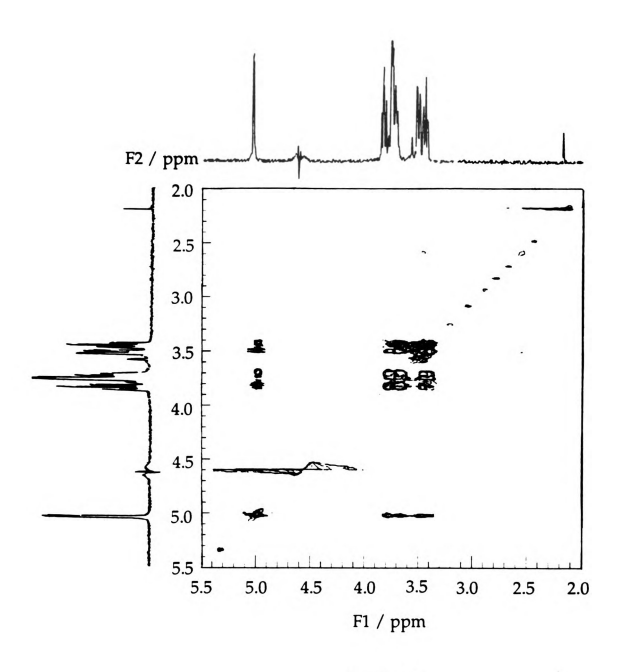


Figure A8

Figure A9. The 75 MHz 13 C NMR spectrum of β -CD \cup 1 aza in d 6 -DMSO.

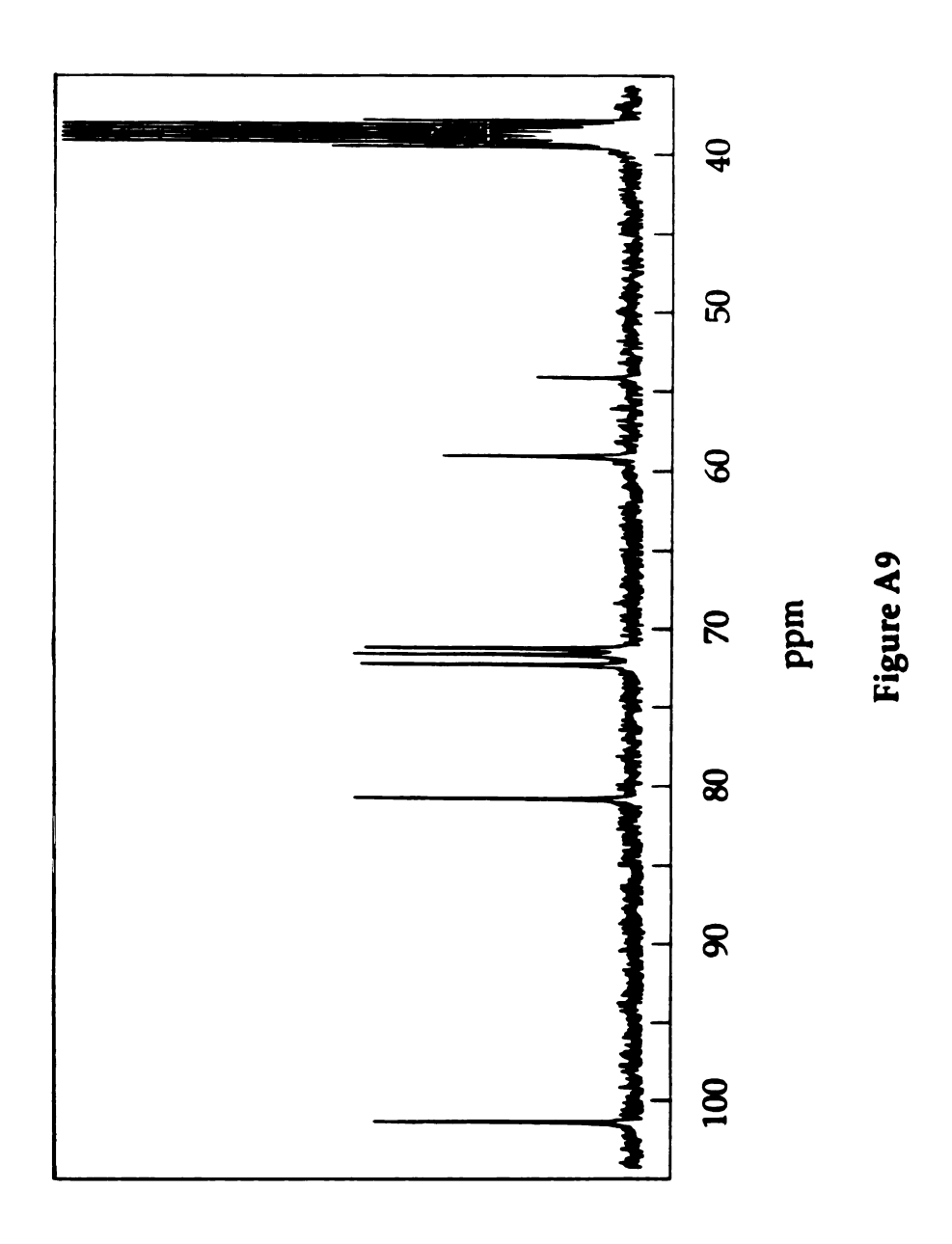


Figure A10. The 300 MHz 1 H NMR spectrum of Eu $^{3+}$ Caza in d 3 -nitromethane.

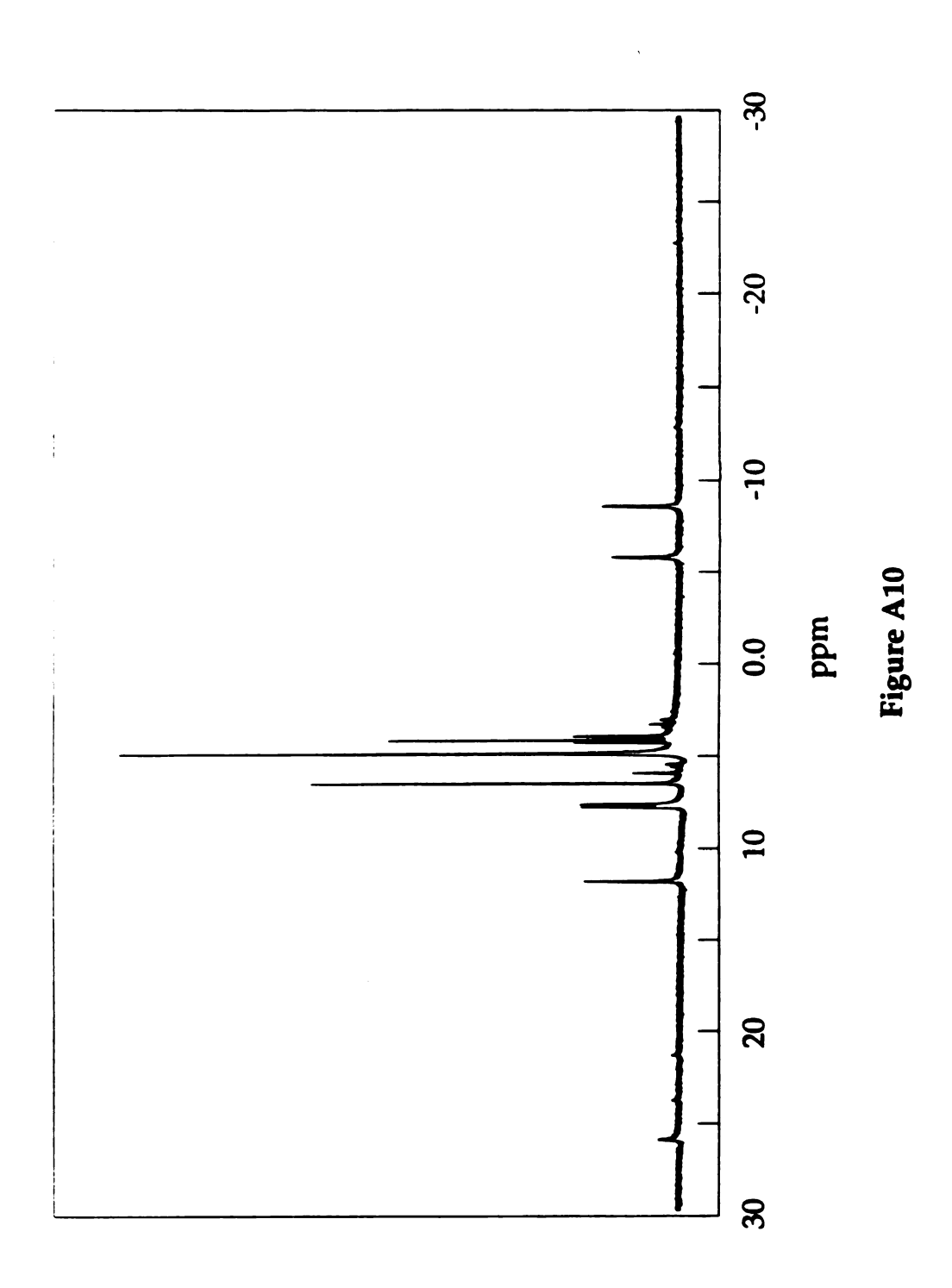


Figure A11. The 300 MHz 1 H NMR spectrum of triamine in D_2O .

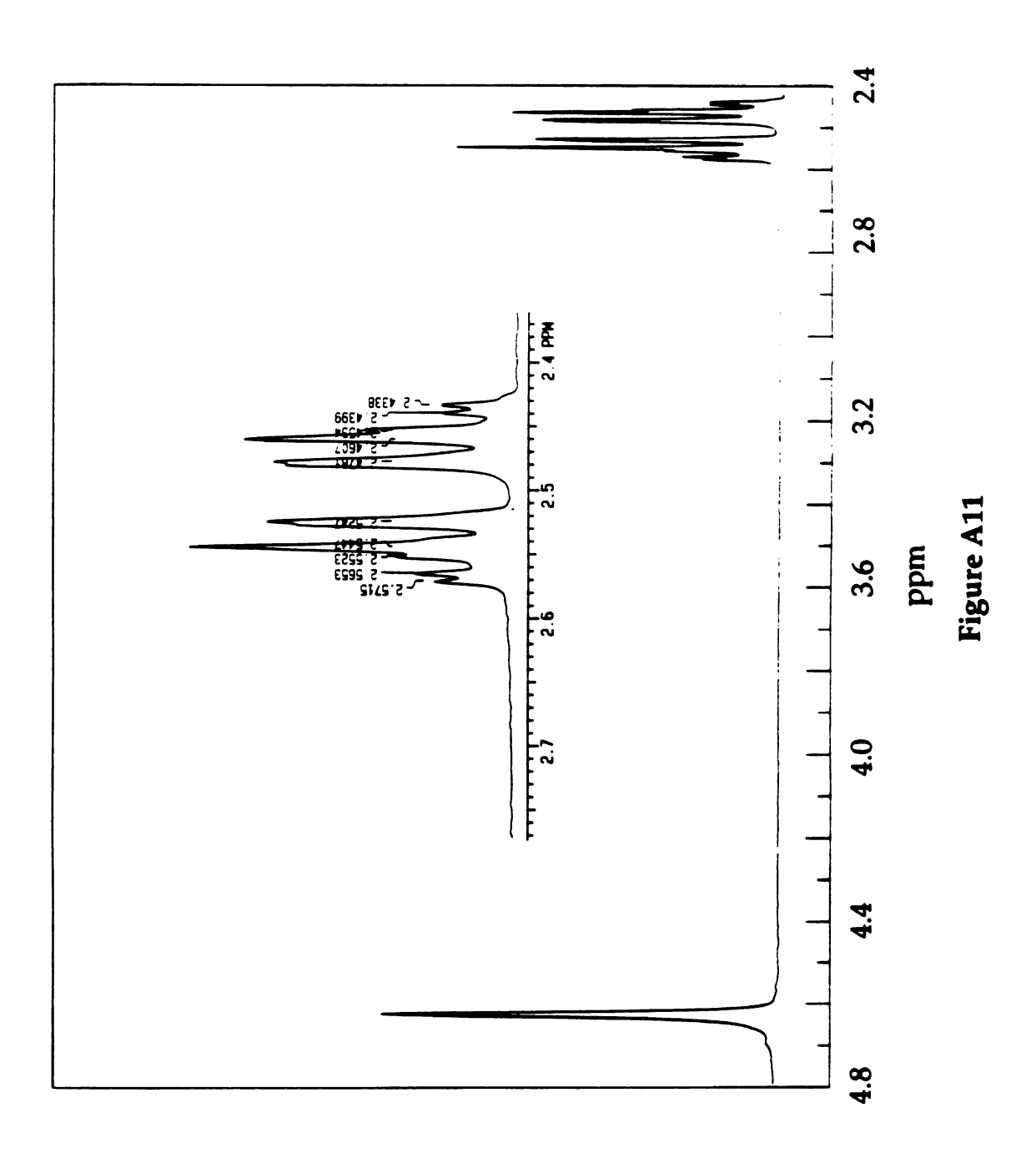


Figure A12. The 75 MHz ^{13}C NMR spectrum of $\beta\text{-CDO-SiPh}_2(\text{tert-Bu})$ in d⁶-DMSO.

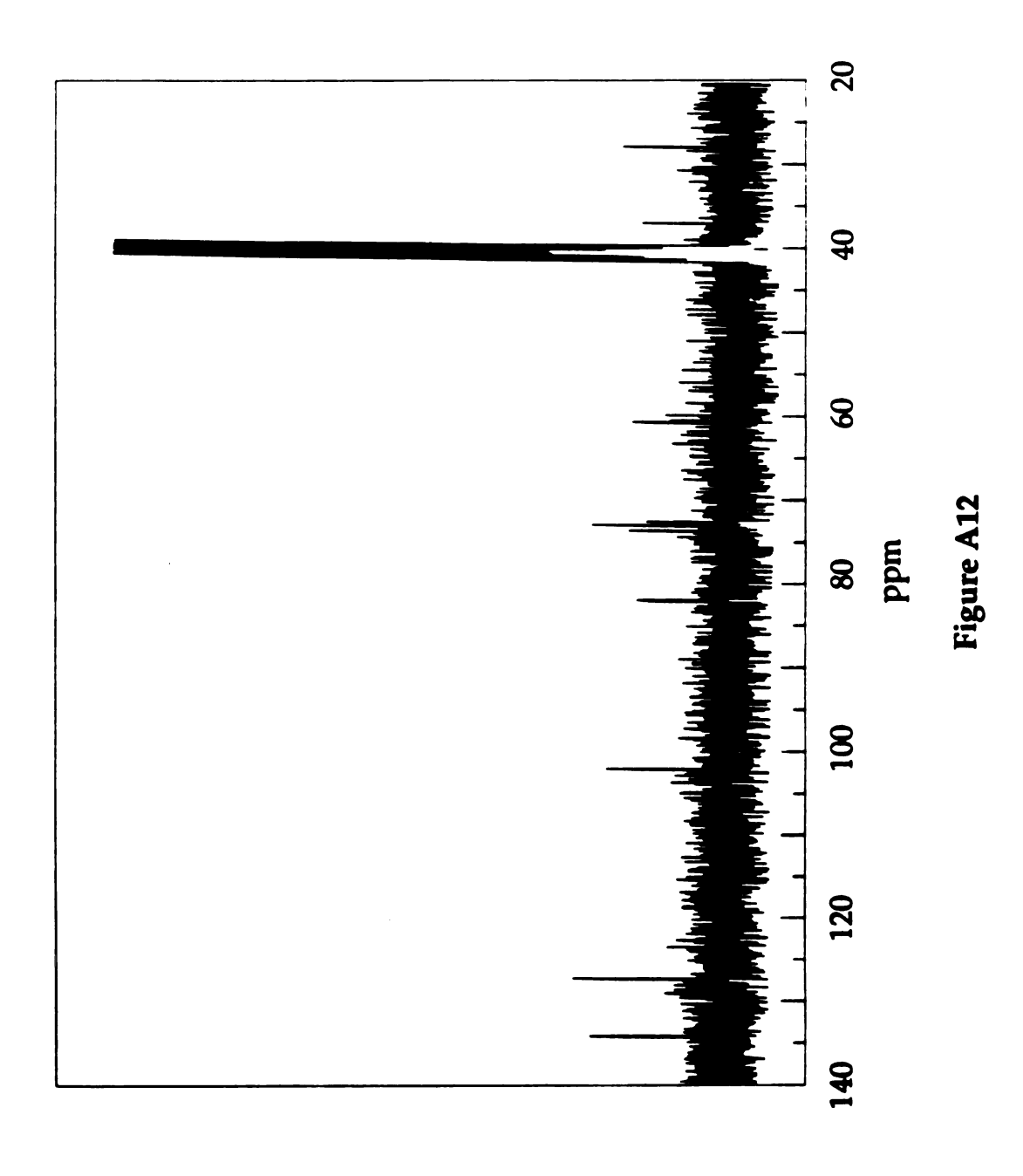


Figure A13. The 300 MHz 1 H NMR spectrum of biphenyl-4,4′-disulfonyl-A,D-capped β -CD in d^6 -DMSO.

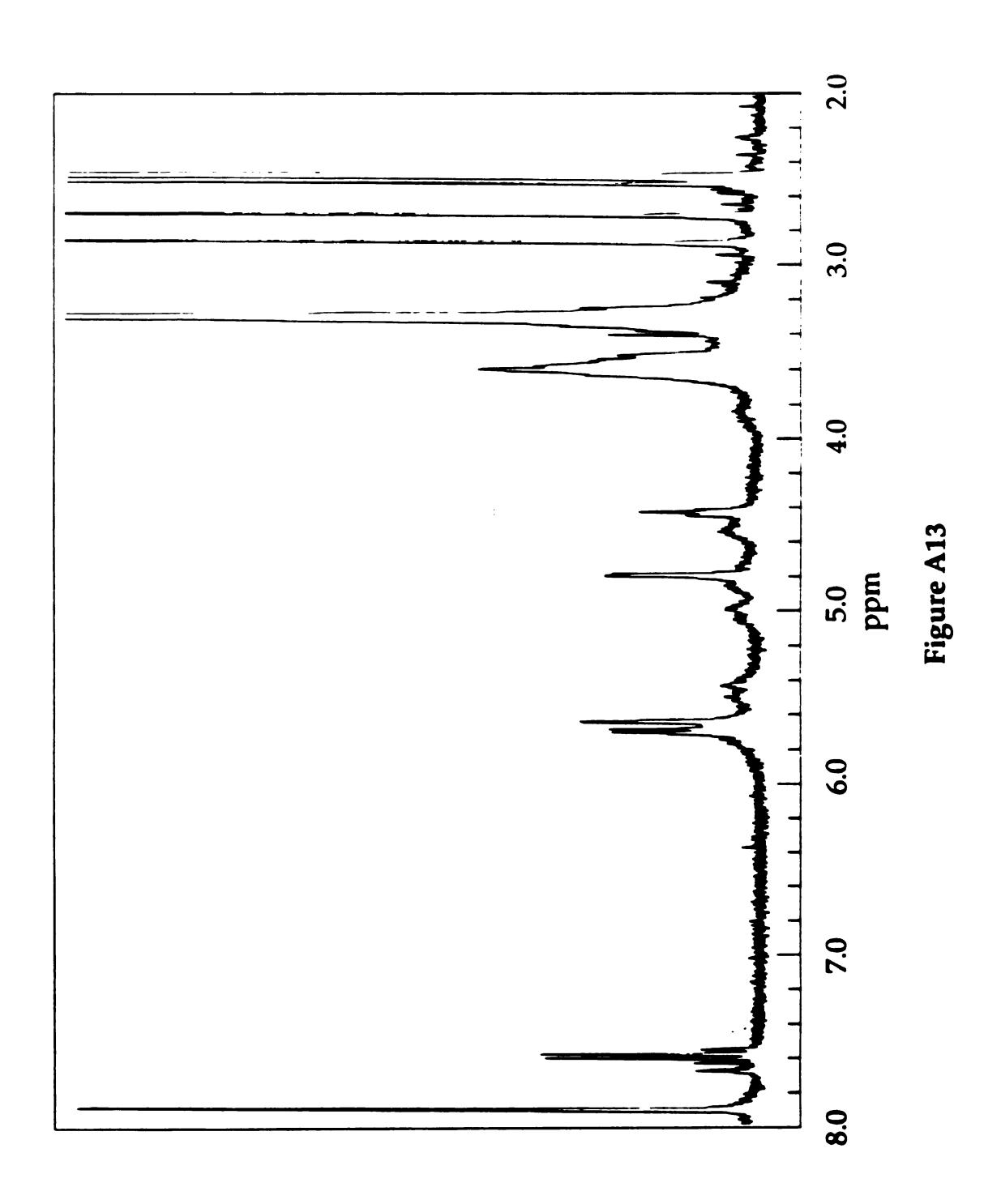


Figure A14. The 300 MHz 1 H NMR spectrum of diiodo- β -CD in d 6 -DMSO.

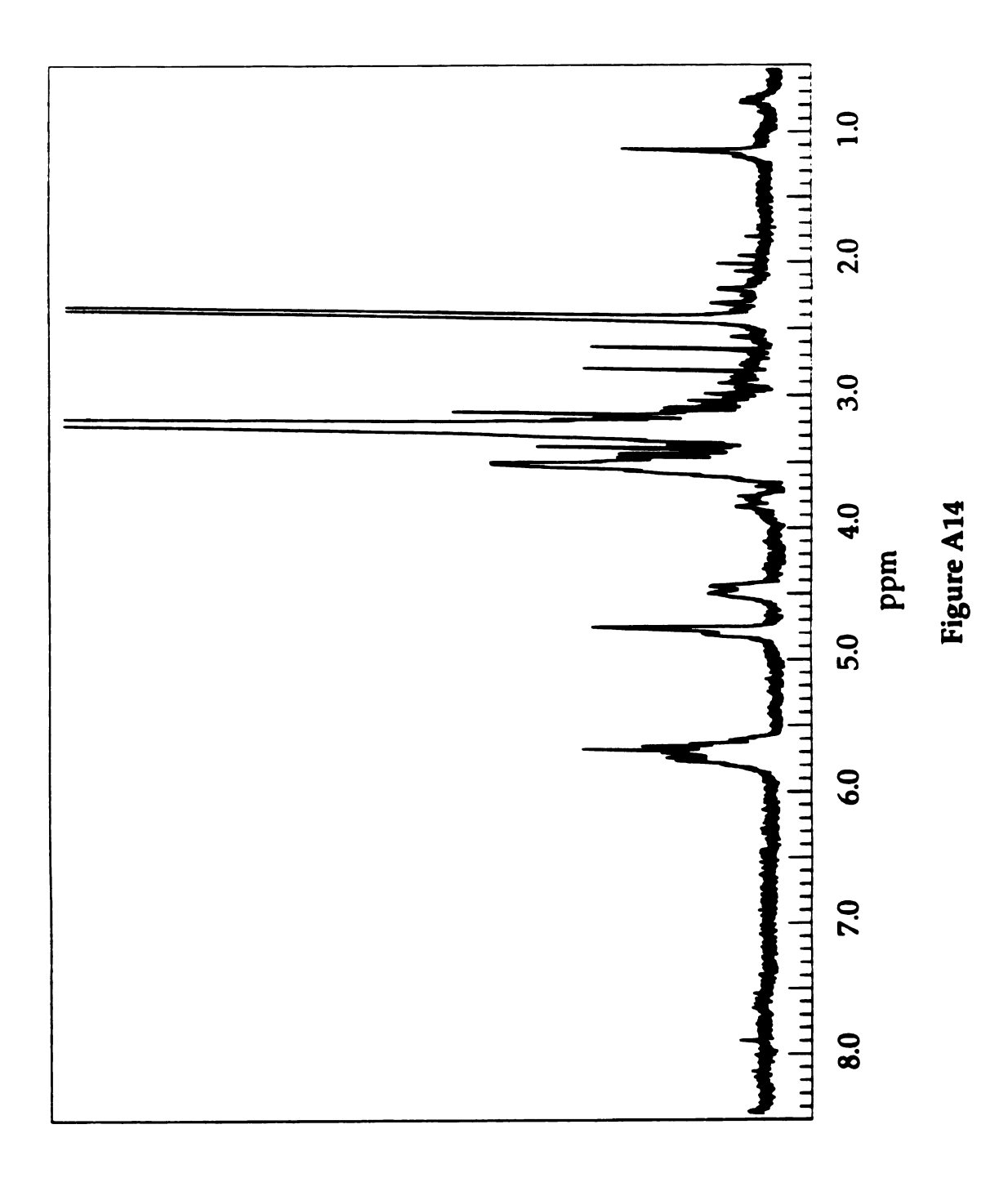
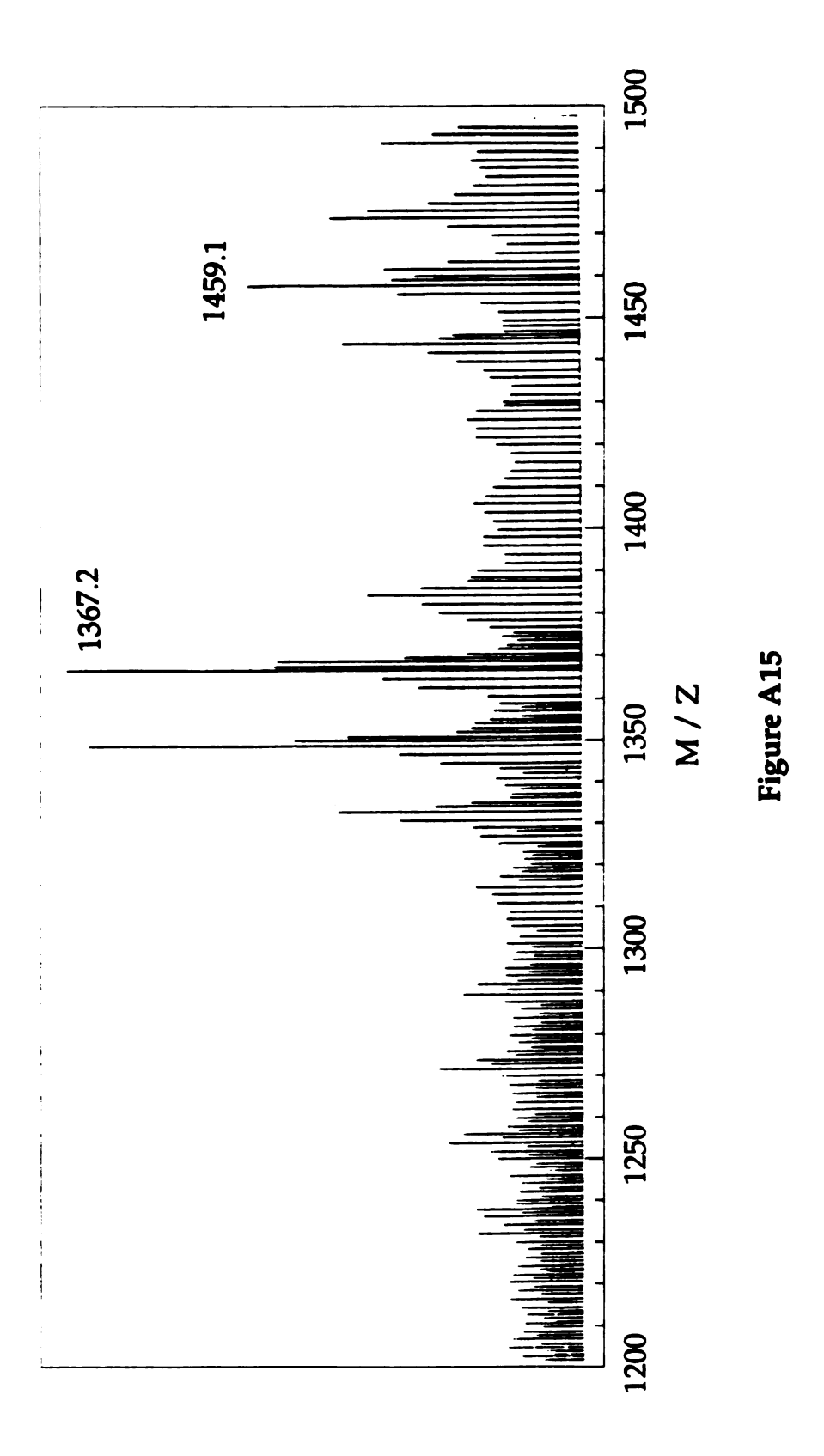
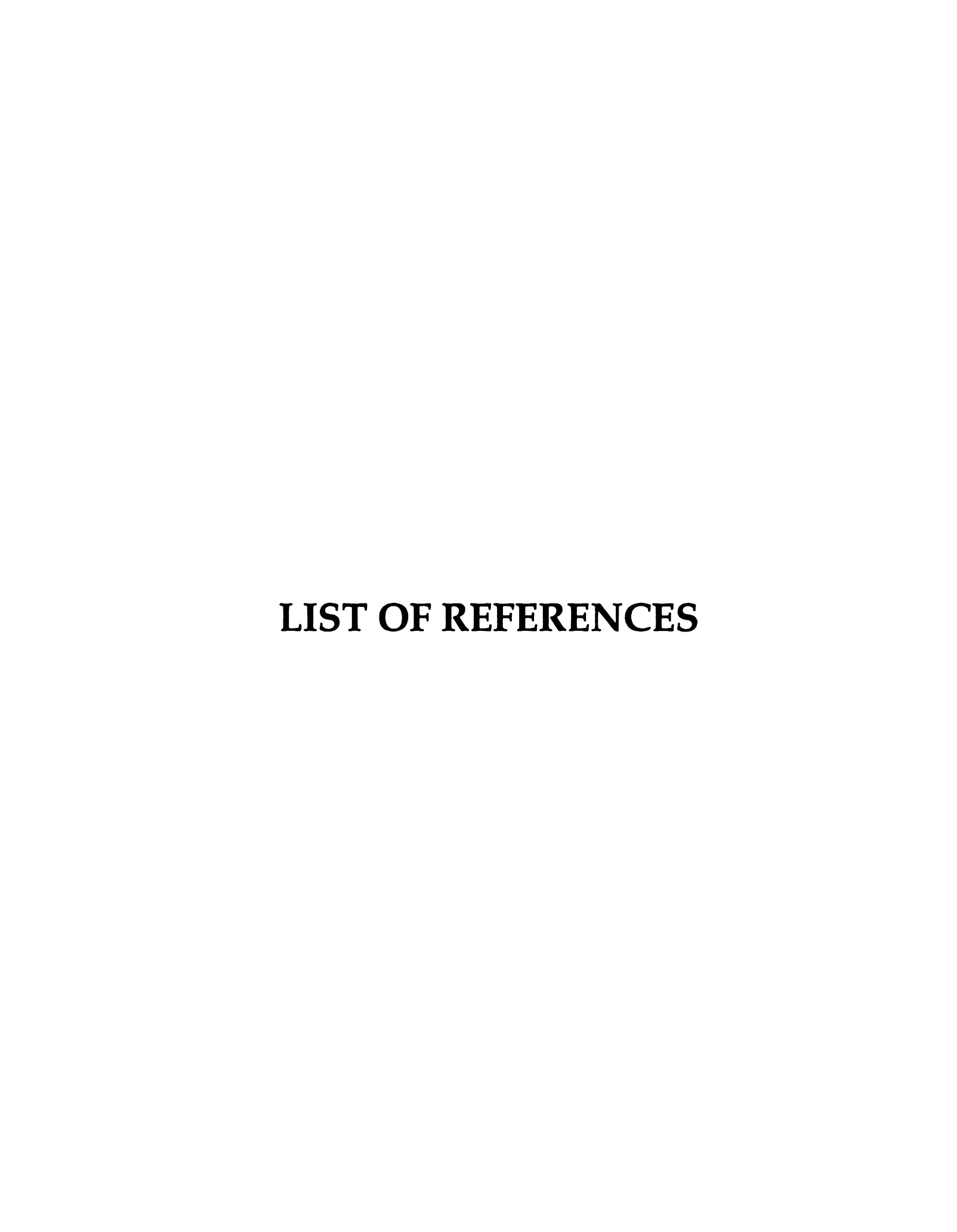


Figure A15. The positive ion FABMS spectrum of protonated β-CD U^2 aza with glycerol as matrix. The $(M + 5H^+)$ is shown at 1367.2 amu and the fragment corresponding to the matrix adduct is shown at 1459.1 amu. The loss of the azaCH $_2$ — group is at 1071 amu not shown at this scale. Higher fragments correspond to presence of sodium and water molecules.





LIST OF REFERENCES

- Lehn, J.-M. Angew. Chem. Int. Ed. Engl. 1988, 100, 91; Angew. Chem. Int. Ed. Engl. 1988, 27, 89; Science (Washington D. C.) 1985, 227, 849; Pure Appl. Chem. 1978, 50, 871.
- (a) Baxter, P; Lehn, J.-M.; De Cian, A.; Fischer, J. Angew. Chem. Int. Ed. Engl.. 1993, 32, 69. (b) Lehn, J.-M. Angew. Chem. Int. Ed. Engl.. 1990, 29, 1304. (c) Lehn, J.-M.; Rigault, A.; Siegel, J.; Harrowfield, J.; Chevrier, B.; Moras, D. Proc. Natl. Acad. Sci. USA 1987, 84, 2565.
- 3. (a) Popov, A. I.; Lehn, J.-M In Coordination Chemistry of Macrocyclic Compounds, Melson, G. A., Ed.; Plenum: New York, 1979; p 537. (b) Lehn, J.-M. In Supramolecular Photochemistry, Balzani, V., Ed.; Reidel: Dordrecht, The Netherlands, 1987; p 29. (c) Vögtle, F., Ed. Supramolecular Chemistry; John Wiley & Sons: West Sussex, England, 1991. (d) An, H.; Bradshaw, J. S.; Izatt, R. M. Chem. Rev. 1992, 92, 543. (e) Seel, C.; Vögtle, F. Angew. Chem. Int. Ed. Engl.. 1992, 31, 528.
- (a) Pedersen, C. J. Angew. Chem. Int. Ed. Engl. 1988, 27, 1021; J. Am. Chem. Soc. 1967, 89, 2495, 7017.
 (b) Pedersen, C. J.; Frensdorff, H. K. Angew. Chem. Int. Ed. Engl. 1972, 84, 16; Angew. Chem. Int. Ed. Engl. 1972, 11, 16.
- (a) Dietrich, B.; Lehn, J.-M.; Sauvage, J.-P. Tetrahedron Lett. 1969, 2885, 2889 (b) Dietrich, B.; Lehn, J.-M.; Sauvage, J.-P.; Blanzat, J. Tetrahedron 1973, 29, 1629. (c) Lehn, J.-M. Acc. Chem. Res. 1978, 11, 49. (d) Lehn, J.-M. Pure Appl. Chem. 1978, 50, 871.

- 6. Cram, D. J. Angew. Chem. Int. Ed. Engl. 1986, 98, 1041; Angew. Chem. Int. Ed. Engl. 1986, 25, 1039; Angew. Chem. Int. Ed. Engl. 1988, 27, 1009.
- 7. (a) Bradshaw, J. S.; Hui, J. Y. K. J. Heterocycl. Chem. 1974, 11, 649. (b) Gokel, G. W.; Dishong, D. M.; Schultz, R. A.; Gatto, V. J. Synthesis 1982, 997.
- 8. For a review see Izatt, R. M.; Pawlak, K.; Bradshaw, J. S. *Chem. Rev.* **1991**, *91*, 1721.
- 9. (a) Pressman, B. C.; Harris, H. J.; Jagger, W. S.; Johnson, J. H. Proc. Natl. Acad. Sci. USA 1967, 58, 1948. (b) Moore, C.; Pressman, B. C. Biochem. Biophys. Res. Commun. 1964, 15, 562. (c) Brockmann, H.; Geeren, H. Justus Liebigs Ann. Chem. 1957, 603, 217.
- (a) Gokel, G. Crown Ethers and Cryptands, Stoddart, J. F., Ed.; Royal Society of Chemistry Series in Monographs in Supramolecular Chemistry: Cambridge, England, 1991. (b) Gokel, G.; Korzeniowski, S. H Macropolycyclic Polyether Synthesis, Hafner, S., Rees, C. W., Trost, B. M., Lehn, J.-M., von Rague Schleyer P., Zahnradnik, R., Eds.; Springer-Verlag Series in Reactivity and Structure Concepts in Organic Chemistry: New York, 1982.
- (a) Dye, J. L.; Ceraco, J. M.; Lok, M. T.; Barnett, B. L.; Tehan, F. J. J. Am. Chem. Soc. 1974, 96, 608. (b) Tehan, F. J.; Barnett, B. L.; Dye, J. L. J. Am. Chem. Soc. 1974, 96, 7203.
- 12. Ellaboudy, S. A.; Dye, J. L.; Smith, P. B. J. Am. Chem. Soc. 1983, 105, 6490.
- 13. (a) Kiggen, W.; Vögtle, F. Angew. Chem. Int. Ed. Engl. 1984, 23, 714. (b) Stutte, P.; Kiggen, W.; Vögtle, F. Tetrahedron 1987, 43, 2065.
- 14. Diederich, F. *Cyclophanes* Stoddart, J. F., Ed.; Royal Society of Chemistry Series in Monographs in Supramolecular Chemistry: Cambridge, England, 1991.

- 15. (a) Jullien, L.; Lehn, J.-M. Wasserman, E. J. Incl. Phenom. Mol. Recog. Chem. 1992, 12, 55. (b) Pregel, M. J.; Jullien, L.; Lehn, J.-M. Angew. Chem. Int. Ed. Engl. 1992, 31, 1637.
- 16. (a) Wasserman, E. . Am. Chem. Soc. 1960, 82, 4433. (b) Frisch, H. L.; Wasserman, E. J. Am. Chem. Soc. 1961, 83, 3789.
- 17. (a) Walba, D. M. *Tetrahedron* **1985**, 41, 3161. (b) Walba, D. M.; Richards, R. M.; Hermsmeier, M.; Haltiwanger, R. C. *J. Am. Chem. Soc.* **1987**, 109, 7081.
- (a) Dietrich-Buchecker, C. O.; Marnot, P. A.; Sauvage, J.-P.; Kirchhoff, D. R.; McMillin, D. R. J. Chem. Soc., Chem. Commun. 1983, 513. (b) Dietrich, C. O.; Sauvage, J.-P.; Kern, J. M. J. Am. Chem. Soc. 1984, 106, 3043. (c) Dietrich, C. O.; Sauvage, J.-P. Chem. Rev. 1987, 87, 795. (d) Dietrich, C. O.; Sauvage, J.-P. Angew. Chem. Int. Ed. 1989, 28, 189. (e) Sauvage, J.-P. Acc. Chem. Res. 1990, 23, 319. (f) Chambron, J. C.; Mitchell, D. K.; Sauvage, J.-P. J. Am. Chem. Soc. 1992, 114, 4625.
- (a) Alwood, B. L.; Spencer, N.; Shahriari-Zavareh, H.; Stoddart, J. F.; Williams, D. J. J. Chem. Soc., Chem. Commun. 1987, 1061. (b) Anelli, P. L.; Ashton, P. R.; Ballardini, R.; Balzani, V.; Delgado, M.; Gandolfi, M. T.; Goodnow, T. T.; Kaifer, A. E.; Philp, D.; Pietraszkiewicz, M.; Prodi, L.; Reddinghton, M. V.; Slawin, A. M. Z.; Spencer, N.; Stoddart, J. F.; Vicent, C.; Williams, D. J. J. Am. Chem. Soc. 1992, 114, 193.
- 20. (a) Gutsche, C. D. Calixarenes Stoddart, J. F., Ed.; Royal Society of Chemistry Series in Monographs in Supramolecular Chemistry: Cambridge, England, 1989. (b) Vicens, J., Böhmer, V., Eds., Calixarenes A Versatile Class of Macrocyclic Compounds; Kluwer Academic Topics in Inclusion Science: Dordrecht, The Netherlands, 1991.
- (a) Ungaro, R.; Pochini, A. J. Incl. Phenom. Mol. Recog. Chem. 1984, 2, 199. (b) Gutsche, C. D.; Iqbal, M.; Nam, K. C.; See, K. A.; Alam, I. Pure Appl. Chem. 1988, 60, 483. (c) Ghidini, E.; Ugozolli, F.; Ungaro, R.; Harkema, S.; El-Fadl, A. A.; Reinhoudt, D. N. J. Am. Chem. Soc. 1990, 112, 6979. (d) Asfari, Z.; Abidi, R.; Arnaud, F.; Vicens, J. J. Incl.

- Phenom. Mol. Recog. Chem. 1992, 13, 163. (e) Asfari, Z.; Vicens, J.; Weiss, J. Tetrahedron Lett. 1993, 34, 627.
- (a) Sabbatini, N.; Guardigli, M.; Mecati, A.; Balzani, V.; Ungaro, R.; Ghidini, E.; Casnati, A.; Pochini, A. J. Chem. Soc., Chem. Commun. 1990, 878.
 (b) Pappalardo, S.; Bottino, F.; Giunta, L.; Pietraszkiewicz, M.; Karpiuk, J. J. Incl. Phenom. Mol. Recog. Chem. 1991, 10, 387.
 (c) Asfari, Z.; Harrowfield, J. M.; Ogden, M. I.; Vicens, J.; White, A. H. Angew. Chem. Int. Ed. 1991, 30, 854.
 (d) Aoki, I.; Sakaki, T.; Shinkai, S. J. Chem. Soc., Chem. Commun. 1992, 730.
 (e) Cacciapaglia, R.; Casnati, A.; Mandolini, L.; Ungaro, R. J. Am. Chem. Soc. 1992, 114, 10956.
- (a) Ouan, M. L. C.; Cram, D. J. J. Am. Chem. Soc. 1991, 113, 2754. (b)
 Sherman, J. C.; Knobler, C. B.; Cram, D. J. J. Am. Chem. Soc. 1991, 113, 2194. (c) Bryant, J. A.; Blanda, M. T.; Vincenti, M.; Cram, D. J. J. Am. Chem. Soc. 1991, 113, 2167.
- 24. (a) Balzani, V.; Scandola, F. Supramolecular Photochemistry Kemp, T. J., Ed.; Ellis Horwood Series in Physical Chemistry: Chichester, West Sussex, England, 1991. (b) Balzani, V.; De Cola, L.; Prodi, L.; Scandola, F. Pure & Appl. Chem. 1990, 62, 1457. (c) Balzani, V. Pure & Appl. Chem. 1990, 62, 1099. (d) Alpha, B.; Ballardini, R.; Balzani, V.; Lehn, J. M.; Perathoner, S.; Sabbatini, N. Photochem. Photobiol. 1990, 52, 299. (e) Balzani, V., Ed. Supramolecular Photochemistry; NATO ASI Series; Reidel: Dordrecht, The Netherlands, 1987.
- 25. (a) Feher, G.; Norris, J. R. Israel J. Chem. 1992, 32, 369. (b) Van Grondelle, R. Biochim. Biophys. Acta 1985, 811, 147. (c) Jean, J. M.; Chan, C.-K. Fleming, G. R. Israel J. Chem. 1988, 28, 169. (d) Allen, J. P.; Feher, G.; Yeates, T. O.; Rees, D. C.; Deisenhofer, J.; Michel, H.; Huber, R. Proc. Natl. Acad. Sci. USA 1986, 83, 8589. (e) Babcock, G. T. In New Comprehensive Biochemistry 15, Photosynthesis; Amasz, J. Ed.; Elsevier: Amsterdam, The Netherlands, 1987.
- 26. Forster, T. Discuss. Faraday Soc. 1959, 27, 7.
- 27. Dexter, D. L. J. Chem. Phys. 1953, 21, 836.

- (a) Marcus, R. A. Ann. Rev. Phys. Chem. 1964, 15, 155. (b) Hush, N. S. Electrochim. Acta 1968, 13, 1005. (c) Sutin, N. Prog. Inorg. Chem. 1983, 30, 441. (d) Marcus, R. A.; Sutin, N. Biochim. Biophys. Acta 1985, 811, 265.
- 29. Closs, G. L.; Johnson, M. D.; Miller, J. R.; Piotrowiak, P. J. Am. Chem. Soc. 1989, 111, 3751.
- 30. (a) Heiler, D.; McLendon, G. L.; Rogalskyj, P. J. Am. Chem. Soc. 1987, 109, 604. (b) Osuka, A.; Maruyama, K. Chem. Lett. 1987, 825. (c) For a review see Wasielewski, M. R. Chem. Rev. 1992, 92, 435. (d) Osuka, A.; Kobayashi, F.; Nakajima, S.; Maruyama, K.; Yamazaki, I.; Nishimura, Y. Chem. Lett. 1993, 161.
- 31. Bucks, R. R.; Boxer, S. G. J. Am. Chem. Soc. 1982, 104, 340.
- 32. (a) Helms, A.; Heiler, D.; Mc Lendon, G. L. J. Am. Chem. Soc. 1991, 113, 4325. (b) Wasielewski, M. R.; Niemczy, M. P.; Johnson, D. G.; Svec, W. A.; Minsek, D. W. Tetrahedron 1989, 45, 4785. (c) For a review see Conolly, J. S.; Bolton, J. R. In Photoinduced Electron Transfer Part D, Fox, M. A., Chanon, M., Eds.; Elsevier: Amsterdam, The Netherlands, 1988; p 303.
- (a) Gust, D.; Moore, T. A.; Moore, A. L. Acc. Chem. Res. 1993, 26, 198.
 (b) Gust, D.; Moore, T. A.; Moore, A. L.; Devadoss, C.; Liddell, P. A.; Hermant, R. A.; Nieman, R. A.; Demanche, L. J.; DeGraziano, J. M.; Gouni, I. J. Am. Chem. Soc. 1992, 114, 3590. (c) Gust, D.; Moore, T. A. Science 1989, 244, 35. (d) Bensasson, R. V.; Land, E. J.; Moore, A. L.; Crouch, R. L.; Dirks, G.; Moore, T. A.; Gust, D. Nature 1981, 290, 329.
 (e) Dirks, G.; Moore, A. L.; Moore, T. A.; Gust, D.; Photochem. Photobiol. 1980, 32, 277.
- 34. Sessler, J. L.; Capuano, V. L.; Harriman, A. J. Am. Chem. Soc. 1993, 115, 4618.
- (a) Bissell, R. A.; De Silva, P.; Gunaratne, H. Q. N.; Lynch, P. L. M.; Maguire, G. E. M.; Sandanayake,, K. R. A. S. Chem. Soc. Rev. 1992, 187.
 (b) Arrhenius, T. S.; Blanchard-Desce, M.; Dvolaitzky, M.; Lehn, J.-M. Proc. Natl. Acad. Sci. USA 1986, 83, 5355.

- (a) Bignozzi, C. A.; Bortolini, O.; Chiorboli, C.; Indelli, M. T.; Rampi, M. A.; Scandola, F. Inorg. Chem. 1992, 31, 172. (b) Kalyanasundaram, K.; Grätzel, M.; Nazeeruddin, Md. K. Inorg. Chem. 1992, 31, 5243. (c) Scandola, F.; Bignozzi, C. A. In Supramolecular Photochemistry, Balzani, V., Ed.; NATO ASI Series; Reidel: Dordrecht, The Netherlands, 1987; p 121. (d) Petersen, J. D. Coord. Chem. Rev. 1991, 111, 319.
- (a) Fox, M. A. Acc. Chem. Res. 1992, 25, 569. (b) Gould, S.; Gray, K. H.; Linton, R. W.; Meyer, T. J. Inorg. Chem. 1992, 31, 5521. (c) Younathan, J. N.; Jones, W. E.; Meyer, T. J. J. Phys. Chem. 1991, 95, 488. (d) Fox, M. A.; Britt, P. F. J. Phys. Chem. 1990, 94, 6351. (e) Meyer, T. J. Acc. Chem. Res. 1989, 22, 163.
- 38. (a) Campagna, S.; Denti, G.; Sabatino, L.; Serroni, S.; Ciano, M. Balzani, V. J. Chem. Soc., Chem. Commun. 1989, 1500. (b) Denti, G.; Campagna, G.; Sabatino, L.; Serroni, S.; Ciano, M. Balzani, V. Inorg. Chem. 1990, 29, 4750. (c) Campagna, G.; Denti, G.; Serroni, S.; Ciano, M. Balzani, V. Inorg. Chem. 1991, 30, 3728. (d) Denti, G.; Campagna, G.; Sabatino, L.; Serroni, S.; Ciano, M. Balzani, V. J. Am. Chem. Soc. 1992, 114, 2944.
- 39. Sabbatini, N.; Guardigli, M.; Mecati, A.; Balzani, V.; Ungaro, R.; Ghidini, E.; Casnati, A.; Pochini, A. J. Chem. Soc., Chem. Commun. 1990, 878.
- 40. Bünzli, J.-C. G.; Choppin, G. R. Eds. Lanthanide Probes in Life, Chemical and Earth Sciences; Elsevier: Amsterdam, The Netherlands, 1989.
- (a) Sabbatini, N.; Dellonte, S.; Ciano, M.; Bonazzi, A.; Balzani, V. Chem. Phys. Lett. 1984, 107, 212. (b) Sabbatini, N.; Dellonte, S.; Blasse, G. Chem. Phys. Lett. 1986, 129, 541. (c) Blasse, G.; Buys, M.; Sabbatini, N. Chem. Phys. Lett. 1986, 124, 538.
- 42. (a) Lehn, J. M. In Supramolecular Photochemistry, Balzani, V., Ed.; Reidel: Dordrecht, The Netherlands, 1987; p 29. (b) Sabbatini, N.; Perathoner, S.; Lattanzi, G.; Dellonte, S.; Balzani, V. J. Phys. Chem. 1987, 91, 6136.

- 43. (a) Alpha, B.; Ballardini, R.; Balzani, V.; Lehn, J. -M. Perathoner, S.; Sabbatini, N. Photochem. Photobiol. 1990, 52, 299. (b) Blasse, G.; Dirksen, G. J.; Sabbatini, N.; Perathoner, S.; Lehn, J. M.; Alpha, B. J. Phys. Chem. 1988, 92, 2419. (c) Alpha, B.; Lehn, J. M.; Mathis, G. Angew. Chem., Int. Ed. Engl. 1987, 26, 266. (d) Alpha, B.; Balzani, V.; Lehn, J. M.; Perathoner, S.; Sabbatini, N. Angew. Chem., Int. Ed. Engl. 1987, 26, 1266. (e) Rodriguez-Ubis, J. C.; Alpha, B.; Plancherel, D.; Lehn, J. M. Helv. Chim. Acta 1984, 67, 2264.
- (a) Ziessel, R.; Maestri, M.; Prodi, L.; Balzani, V.; Van Dorsselaer, A. Inorg. Chem. 1993, 32, 1237.
 (b) Mukkala, V. M.; Kankare, J. J Helv. Chim. Acta 1992, 75, 1578.
 (c) Prodi, L.; Maestri, M.; Ziessel, R.; Balzani, V. Inorg. Chem. 1991, 30, 3798.
- 45. (a) Yu, J.-a; Lessard, R. B.; Nocera, D. G. *Chem. Phys. Lett.* **1991**, *187*, 263. (b) Pikramenou, Z.; Yu, J.-a; Lessard, R. B.; Ponce, A.; Wang, P. A.; Nocera, D. G. *Coord. Chem. Rev.* submitted.
- 46. Fages, F.; Desvergne, J.-P.; Bouas-Laurent, H.; Marsau, P.; Lehn, J.-M.; Kotzyba-Hibert, F.; Albrecht-Gary, A.-M.; Al Joubbeh, M. J. Am. Chem. Soc. 1989, 111, 8672.
- 47. (a) Duchêne, D. Ed. New trends in cyclodextrins and derivatives; Editions de Santé: Paris, France, 1993. (b) Szejtli, J. Cyclodextrins and their Inclusion Complexes Akademiai Kiado: Budapest, Hungary, 1982. (c) Tabushi, I. Acc. Chem. Res. 1982, 15, 66.
- 48. (a) Matsui, Y.; Nishioka, T.; Fujita, T. Topics in Current Chemistry 1985, 128, 61. (b) Bergeron, R. In Inclusion Compounds, Atwood, J.L. Ed.; Academic: New York, 1984, p 391. (c) Saenger, W. Angew. Chem., Int. Ed. Engl 1980, 19, 344.
- 49. (a) Li, S.; Purdy, W. C. Chem. Rev. 1992, 92, 1457. (b) Sinha, H. K.; Yates, K. J. Am. Chem. Soc. 1991, 113, 6062. (c) Bright, F. V.; Catena, G. C.; Huang, J. J. Am. Chem. Soc. 1990, 112, 1343. (d) Kaluanasundaram, K. Photochemistry in Microheterogenous Systems Academic Press: New York, 1987. (e) Eaton, D. F. Tetrahedron 1987, 43, 1551. (f) Cline (III), J.

- I.; Dressick, W. J.; Demas, J. N.; DeGraff, B. A. J. Phys. Chem. 1985, 89, 94.
- 50. (a) Ponce, A.; Wong, P. A.; Way, J. J.; Nocera, D. G. J. Phys. Chem. submitted (b) Turro, N. J; Bolt, J. D.; Kuroda, Y.; Tabushi, I. Photochem. and Photobiol. 1982, 35, 69.
- 51. (a) Ueno, A.; Minato, S.; Osa, T. Anal. Chem. 1992, 64, 2562. (b) Ueno, A.; Suzuki, I.; Osa, T. J. Am. Chem. Soc. 1989, 111, 6391.
- 52. (a) Hamasaki, K.; Ueno, A.; Toda, F. J. Chem. Soc., Chem. Commun. 1993, 331. (b) Ueno, A.; Kuwabara, T.; Nakamura, A.; Toda, F. Nature 1992, 356, 136.
- (a) Brugger, N.; Deschenaux, R.; Ruch, T; Ziessel, R. Tetrahedron, Lett. 1992, 33, 3871. (b) Akkaya, E. U.; Czarnik, A. W. J. Phys. Org. Chem. 1992, 5, 540. (c) Akkaya, E. U.; Czarnik, A. W. J. Am. Chem. Soc. 1988, 110, 8553. (d) McNamara, M.; Russell, N. R. J. Incl. Phenom. Mol. Recog. Chem. 1991, 10, 485. (e) Klingert, B.; Rihs, G. J. Incl. Phenom. Mol. Recog. Chem. 1991, 10, 255. (f) Bonomo, R. P.; Cuccinotta, V.; D' Alessandro, F.; Impellizzeri, G.; Maccarrone, G.; Vecchio, G.; Rizzarelli, E. Inorg. Chem. 1991, 30, 12708. (g) Alston, D. R.; Ashton, P. R.; Lilley, T. H.; Stoddart, J. F.; Zarzyski, R. Carbohydrate Res. 1989, 192, 259.
- (a) Johnson, M. D.; Reinsborough, V. C.; Ward, S. *Inorg. Chem.* 1992, 31, 1085.
 (b) Berberan-Santos, M. N.; Canceill, J.; Brochon, J.-C.; Jullien, L.; Lehn, J.-M.; Pouguet, J.; Tauc, P.; Valeur, B. *J. Am. Chem. Soc.* 1992, 114, 6427.
 (c) Aquino, A. M.; Abelt, C. J.; Berger, K. L.; Darragh, C. M.; Kelley, S. E.; Cossette, M. V. *J. Am. Chem. Soc.* 1990, 112, 5819.
 (d) Ueno, A.; Moriwaki, F.; Tomita, Y.; Osa, T. *Chem. Lett.* 1985, 493.
 (e) Tabushi, I.; Fujita, K.; Yuan, L. C. *Tetrahedron Lett.* 1977, 2503.
- (a) Komiyama, M.; Sawata, S.; Takeshige, Y. J. Am. Chem. Soc. 1992, 114, 1070.
 (b) Impellizzeri, G.; Maccarrone, G.; Rizzarelli, E.; Vecchio, G.; Corradini, R.; Marchelli, R. Angew. Chem., Int. Ed. Engl. 1991, 30, 1348.
 (c) Krechl, J.; Castulik, P. Chimica Scripta 1989, 29, 173.
 (d)

- Tabushi, I.; Kuroda, Y. J. Am. Chem. Soc. 1984, 106, 4580. (e) Breslow, R. Science 1982, 218, 532. (f) Bender, M. L., Komiyama, M., Eds. Cyclodextrin Chemistry; Springer-Verlag: New York, 1978.
- 56. For reviews see: (a) Szejtli, J. J. Incl. Phenom. Mol. Recog. Chem. 1992, 14, 25. (b) Croft, A. P.; Bartsch, R. A. Tetrahedron 1983, 39, 1417. (c) Tabushi, I. Tetrahedron 1984, 40, 269.
- 57. (a) Willner, I.; Goren, Z. *J. Chem. Soc., Chem. Commun.* **1983**, 1469. (b) Fujii, I.; Kiyama, R.; Knematsu, K. *Bioorg. Chem.* **1989**, 17, 245.
- 58. Gordon, A. J., Ford, R. A., Eds. *The Chemist's Companion*; Wiley: New York, 1972.
- 59. Matsui, Y.; Okimoto, A. Bull. Chem. Soc. Jpn. 1978, 51, 3030.
- 60. Tabushi, I.; Shimizu, N.; Sugimoto, T.; Shiozuka, M.; Yamamura, K. *J. Am. Chem. Soc.* **1977**, *99*, 7100.
- 61. Matsui, Y.; Yokoi, T.; Mochida, K. Chem. Lett. 1976, 1037.
- 62. Szejtli, J.; Liptak, A.; Jodal, I.; Fügedi, P.; Nanasl, P.; Neszmelyl, A. *Starch* 1980, 32, 165.
- 63. Desraux, J.F.; Renard, A; Duyckaerts, G. *Inorg. Nucl. Chem.* **1977**, 39, 1587.
- 64. Pruett, J. D. Ph. D. Dissertation, Michigan State University, 1978.
- 65. Forsberg, J. H.; Moeller, T. *Inorg. Chem.* **1969**, *8*, 883.
- 66. (a) Tabushi, I.; Yamamura, K.; Nabeshima, T. J. Am. Chem. Soc. 1984, 106, 5267. (b) Tabushi, I.; Kuroda, Y.; Yokota, K.; Yuan, L. C. J. Am. Chem. Soc. 1981, 103, 711.
- 67. Tabushi, I.; Kuroda, Y. J. Am. Chem. Soc. 1984, 106, 4580.
- 68. Still, W. C.; Kahn, M.; Mitra, A. J. Org. Chem. 1978, 43, 2923.
- 69. El Khadem, H. S. Carbohydrate Chemistry Monosaccharides and Their Oligomers; Acedemic Press, 1988.

- 70. Zweig, G.; Sherma, J. Handbook of Chromatography; CRC Press: Cranwood Parkway, 1972.
- 71. Mayo, S. L.; Olafson, B. D.; Goddard III, W. A. J. Phys. Chem. 1990, 94, 8897.
- 72. Mussell, R. D.; Nocera, D. G. J. Am. Chem. Soc. 1988, 110, 2764.
- 73. Benesi, H.A.; Hilderbrand, H. J. Am. Chem. Soc. 1949, 71, 2703.
- 74. (a) Connors K. A. Binding Constants; Wiley: New York, 1987. (b) Takahashi K.; Ohtsuka Y.; Nakada S.; Hattori K.; J. Incl. Phenom. Mol. Recog. Chem. 1991, 10, 63.
- 75. (a) Catena, G. C.; Bright, F. V. Anal Chem. 1989, 61, 905. (b) Crescenzi, V.; Gamini, A.; Palleschi, A.; Rizzo, R. Gazz. Chim. Ital. 1986, 116, 435.
 (c) Cramer, F.; Saenger, W.; Spatz, H.-Ch. J. Am. Chem. Soc. 1967, 89, 14.
- 76. Newsham, M. D.; Gianellis, T. J.; Pinnavaia, T. J.; Nocera, D. G. J. Am. Chem. Soc. 1988, 110, 3885.
- 77. Boger, J.; Corcoran, R. J.; Lehn, J.-M. Helv. Chim. Acta 1978, 61, 2191.
- (a) Ashton, P. R.; Ellwood, P.; Staton, I.; Stoddart, J. F. Angew. Chem., Int. Ed. Engl. 1991, 30, 80. (b) Petter, R. C.; Salek, J. S.; Sikorski, C. T.; Kumaravel, G.; Lin, F.-T. J. Am. Chem. Soc. 1990, 112, 3860. (c) Iwakura, Y.; Uno, K.; Toda, F.; Ozonuka, S.; Hattori, K.; Bender, M. L. J. Am. Chem. Soc. 1975, 97, 4432. (d) Melton, L. D.; Slessor, K. N. Carbohydr. Res. 1971, 18, 29.
- 79. Perly, B.; Djedaïni, F.; Berthault, P. In New trends in cyclodextrins and derivatives, Duchêne, D. Ed.; Editions de Santé: Paris, France, 1993, p181.
- 80. Spencer, C. M.; Stoddart, J. F.; Zarzycki, R. J. Chem. Soc. Perkin Trans. II 1987, 1323.
- 81. Cramer, F.; Mackensen, G.; Sensse, K. Chem. Ber. 1969, 102, 494.

- 82. (a) Tanimoto, T.; Tanaka, M.; Yuno, T.; Koizumi, K. *Carbohydr. Res.* **1992**, 223, 1. (b) Ling, C.-C.; Coleman, A. W.; Miocque, M.; *Carbohydr. Res.* **1992**, 223, 287. (c) Siegel, B. *J. Inorg. Nucl. Chem.* **1979**, 41, 609.
- 83. Coleman, A. W.; Zhang. P.; Ling, C.-C.; Parrot-Lopez, H.; Galons, H. *Carbohydr. Res.* **1992**, 224, 307.
- 84. Fugedi, P. Carbohydr. Res. 1989, 192, 366.
- 85. (a) Lalonde, M.; Chan, T. H. Synthesis 1985, 817. (b) Hanessian, S.; Lavallee, P. Can J. Chem. 1975, 53, 2975.
- 86. Pikramenou Z.; Nocera D. G., *Inorg. Chem.* **1992**, *31*, 532.
- 87. Casu, B.; Regianni, M.; Gallo, G. G.; Vigevani, A. *Tetrahedron* **1966**, 22, 3061.
- 88. Wife, R. L.; Reed, D. E.; Leworthy, D. P.; Barnett, D. M.; Regan, P. D.; Volger, H. C. In *Proceedings of the First International Symposium on Cyclodextrins*, Szejtli, J., Ed.; Reidel: Budapest, Hungary, 1981; p 301.
- 89. Carnall, W. T. In *Handbook on the Physics and Chemistry of Rare Earths*, Gschneidner, K. A., Eyring, L.R., Eds.; North-Holland: Amsterdam, The Netherlands, 1979; p 171.
- 90. Brittain, H. G. In *Molecular Luminescence Spectroscopy Methods and Applications*: Part 2, Chemical Analysis Series, Schulman, S. G., Ed.; Wiley-Interscience: New York, 1988; p 401.
- 91. Haas, Y.; Stein, G. J. Phys. Chem. 1971, 75, 3668.
- 92. Horrocks, W. DeW.; Albin, M. Progr. Inorg. Chem. 1984, 31, 1.
- 93. Matsui, Y.; Yokoi, T.; Mochida, K. Chem. Lett. 1976, 1037.
- 94. Pikramenou, Z.; Nocera, D. G. In *Proceedings of the Sixth International Symposium on Cyclodextrins*; Editions de Santé, Paris, France, 1992.
- 95. Wang, Y.; Ikeda, T.; Ueno, A.; Toda, F. Tetrahedron Lett. 1993, 34, 4971.

- 96. Kuroda, Y.; Ito, M.; Sera, T.; Ogoshi, H. J. Am. Chem. Soc. 1993, 115, 7003.
- 97. (a) Tabushi, I. In *Inclusion Compounds*, Atwood, J.L. Ed.; Academic: New York, 1984, p 445. (b) Tabushi, I. *Acc.Chem. Res.* 1982, 15, 66.
- (a) Cucinotta, V.; D'Alesssandro, F.; Impellizzeri, G.; Vecchio, G. Carbohydr. Res. 1992, 224, 95. (b) Tabushi, I.; Kuroda, Y.; Mochizuki, A. J. Am. Chem. Soc. 1980, 102, 1152. (c) Breslow, R. Isr. J. Chem. 1979, 18, 187.
- 99. Ernst, R. R. Angew. Chem., Int. Ed. Engl. 1992, 31, 805.
- (a) Imagaki, F. Magn. Reson. Chem. 1992, 30, S125. (b) van Halbeek, H.;
 Poppe, L. Magn. Reson. Chem. 1992, 30, S74.
- 101. Pikramenou, Z.; Johnson, K. M.; Nocera, D. G. *Tetrahedron Lett.* **1993**, 34, 3531.
- 102. Parrot-Lopez, H.; Galons, H.; Coleman, A. W.; Mahuteau, J.; Miocque, M. *Tetrahedron Lett.* **1992**, 33, 209.
- 103. Silverstein, R. M.; Bassler, G. C.; Morril, T. C. Spectrometric Identification of Organic Compounds Sawicki, D., Stiefel, J., Eds.; Wiley: New York, 1991.
- 104. (a) Yamazaki, I.; Baba, H. J. Chem. Phys. 1977, 66, 5826. (b) Yamazaki, I.; Sushida, K.; Baba, H. J. Chem. Phys. 1979, 71, 381.

MICHIGAN STATE UNIV. LIBRARI
31293010432031